Role of serine and paraventricular nucleus-NMDA receptors in whole-body metabolism and energy homeostasis

Elena López Gonzales

Vollständiger Abdruck der von Fakultät für Medizin der Technischen Universität München zur Erlangung einer Doktorin der Naturwissenschaften (Dr. rer. nat) genehmigten Dissertation.

Vorsitz: Prof. Dr. Percy A. Knolle

Prüfer*innen der Dissertation: 1. TUM Junior Fellow Dr. Siegfried Ussar

2. Prof. Dr. Ilona Grunwald Kadow

Die Dissertation wurde am 06.12.2022 bei der Technischen Universität München eingereicht und durch die Fakultät für Medizin am 21.02.2023 angenommen.

I. List of abbreviations

1-deoxySLs	1-deoxysphingolipid
AAV	adeno-associated virus
Acaca	acetyl-CoA carboxylase
ACC	acetyl-CoA carboxylase
aCSF	artificial cerebrospinal fluid
AD	Alzheimer's Disease
ADHD	attention deficit hyperactivity
AE	aqueous extract
ALS	amyotrophic lateral sclerosis
AMPK	AMP-activated protein kinase
apMPOA	anteroventral and periventricular portions of medial preoptic area
ARC	arcuate nucleus
ASD	autism spectrum disorder
ATGL	adipose triglyceride lipase
ATP	adenosine triphosphate
BAT	brown adipose tissue
BMI	body mass index
CD	chow diet
CD68	cluster of differentiation 68
CNQX	6-Cyano-7-nitroquinoxaline-2,3-dione
CNS	central nervous system
COPD	obstructive pulmonary disease
CSF	cerebrospinal fluid
DHA/EPA	docosahexaenoic acid/eicosapentaenoic acid
DHF	dihydrofolate
DHFR	dihydrofolate reductase
DMEM	Dulbecco's Modified Eagle Medium
DMN	dorsomedial nucleus
DNA	deoxyribonucleic acid
DNL	*de novo* lipogenesis
DTT	dithiothreitol
EDTA	ethylenediaminetetraacetic acid
EE	energy expenditure
ER	endoplasmic reticulum
Fasn	fatty acid synthase
FBS	fetal bovine serum
FCCP	carbonyl cyanide-p-trifluoromethoxyphenylhydrazone
FDA	Food and Drug administration
Foxo1	forkhead box protein 1
G6Pase	glucose-6-Phosphatase

GABA	gamma-aminobutyric acid
GCN2	general control nonderepressible 2
GFP	green fluorescent protein
GLP1	glucagon-like peptide 1
GMS	glycine modulator site
GRAS	generally recognized as safe
GSH	glutathione system
GSIS	glucose-stimulated insulin secretion
GTT	Glucose tolerance test
Gys-2	glycogen synthase-2
HbA1c	glycosylated hemoglobin A1c
HDL	high-density lipoprotein
HE	Haematoxylin and Eosin
HFD	high-fat diet
HPA	hypothalamic-pituitary-adrenal
HSAN1	hereditary sensory autonomic neuropathy type 1
HSL	hormone-sensitive lipase
HTP	hypothalamic-pituitary-thyroid
IBMX	3-Isobutyl-1-methylxanthine
IL-6	interleukin 6
IR-DIC	infrared differential interference contrast
IRS2	insulin receptor substrate-2
K_{ATP}	ATP-sensitive potassium channel
LH	lateral hypothalamus
LPS	lipopolysaccharide
LTD	long–term depression
LTP	long-term potentiation
MAT	methione adenosyltransferase
MC4Rs	melanocortin 4 receptors
MGL	monoacylglycerol lipase
MND	motor neuron disease
MTBE	methyl tert-butyl ether
MTHFD2	methylenetetrahydrofolate dehydrogenase
MTHFR	methylenetetrahydrofolate reductase
NAD+	nicotinamide adenine dinucleotide
NAFLD	non-alcoholic fatty acid liver disease
NDMAR	N-methyl-D-aspartate receptor
NMR	nuclear magnetic resonance
NOD	non-obese diabetic
NPY	neuropeptide 1

NTS	nucleus tractus solitarius
OCR	oxygen consumption rate
PBS	phosphate-buffered saline
PC	phosphatidylcholine
PC	pyruvate carboxylase
PCR	polymerase chain reaction
PD	Parkinson's Disease
PE	phosphatidylethanolamine
Pepck	phosphoenolpyruvate carboxykinase
PFA	paraformaldehyde
Pgc1α	peroxisome-proliferator activated receptor gamma co-activator 1α
PGF	perigonadal fat
Pgyl	glycogen phosphorylase
PHGDH	phosphoglycerate dehydrogenase
pHSL	phosphorylated-hormone-sensitive lipase
PKA	protein kinase A
POA	pre-optic area
POMC	proopiomelanocortin
Prdm16	PR domain containing 16
PRPP	phosphoribosyl pyrophosphate
PS	phosphatidylserine
PSAT	phosphoserine transferase
PSP	phosphoserine phosphatase
PTT	Pyruvate tolerance test
PVFD	polyvinylidene difluoride
PVN	paraventricular nucleus
PVN^{CRH}	corticotrophin-releasing hormone neurons in the paraventricular nucleus
PVN^{MCR4}	melanocortin-4-receptor-expressing neurons in the paraventricular nucleus
PVN^{OXT}	oxytocin neurons in the paraventricular nucleus
PVNTH	tyrosine hydroxylase-expressing neurons in the hypothalamus
PVN^{TRH}	thyrotropin-releasing hormone neuron in the paraventricular nucleus
RER	respiratory exchange ratio
RIPA	radioimmunoprecipitation assay buffer
RMR	resting metabolic rate
RNA	ribonucleic acid
SAH	S-adenosyl-homocysteine
SAM	S-adenosyl methionine
SCF	subcutaneous fat
SCN	suprachiasmatic nucleus
SDH	serine dehydratase

SHMT	serine hydroxymethyltransferase
SHTM1	serine hydroxymethyltransferase 1
SHTM2	serine hydroxymethyltransferase 2
SOD	superoxide dismutase
SPT	serine palmitoyltransferase
SPTLC1/2	serine Palmitoyltransferase Long Chain Base Subunit 1/2
Srebp1	sterol regulatory element-binding protein 1
SRR	serine racemase
STZ	streptozotocin
SVF	stromal vascular fraction
T1D	type 1 diabetes
T2D	type 2 diabetes
T3	3,3',5'-Triiodo-L-thyronine
TG	triglyceride
THF	tetrahydrofolate
TNFα	tumor necrosis factor *α*
UCP1	uncoupled protein 1
VMN	ventromedial nucleus
WAT	white adipose tissue
α-MSH	α-melanocyte stimulating hormone

II. List of figures

III. List of tables

IV. Abstract

Obesity is a major concern to society due to its high and growing prevalence. In addition, it precedes the development of type 2 diabetes as well as other co-morbidities. Both obesity and type 2 diabetes emerge from an imbalance in energy homeostasis, driven by multiple lifestyle, environmental and genetic factors, which make them difficult to tackle. Thus, it is essential to explore alternatives to prevent or treat these diseases and to understand the underlying mechanisms. In this regard, we studied the metabolic effects of L-serine supplementation as well as the role of NMDARs in the paraventricular nucleus of the hypothalamus in the regulation of insulin secretion and whole-body metabolism in mice. L-serine is obtained from the diet, but also synthesized *de novo*, and participates in important metabolic pathways involved in glucose metabolism, antioxidant defense, one-carbon metabolism, nucleotide production and neurotransmission. Supplementation with L-serine has beneficial effects on food intake, insulin secretion and β-cell function in mice. Additionally, in humans, L-serine is associated with improved glucose and insulin metabolism and decreased obesity risk. NMDAR is an ionotropic glutamate receptor involved in neurotransmission and synaptic plasticity, which is co-activated by D-serine, the enantiomer of L-serine. In this thesis, it is shown that L-serine supplementation in mice decreased body weight regain after fasting by increasing BAT thermogenesis and an involvement of NMDARs in the paraventricular nucleus of the hypothalamus in energy balance regulation through BAT activity. These findings suggest L-serine supplementation as a potential approach to prevent and/or treat obesity and provide compelling data on the role of NMDARs in the hypothalamus in the regulation of energy homeostasis.

V. Zusammenfassung

Adipositas stellt aufgrund ihrer hohen und wachsenden Prävalenz ein großes Problem für die Gesellschaft dar. Darüber hinaus geht sie der Entwicklung von Typ-2-Diabetes sowie anderen Komorbiditäten voraus. Sowohl Fettleibigkeit als auch Typ-2-Diabetes entstehen aus einem Ungleichgewicht in der Energiehomöostase, welches durch ein komplexes Zusammenspiel aus Lebensstil-, Umwelt- und genetische Faktoren verursacht wird, was die Bekämpfung zusätzlich erschwert. Daher ist es unerlässlich, Alternativen zur Vorbeugung oder Behandlung dieser Krankheiten zu erforschen und die zugrunde liegenden Mechanismen zu verstehen. In diesem Zusammenhang untersuchte ich die metabolischen Wirkungen einer L-Serin-Supplementierung sowie die Rolle von NMDARs im paraventrikulären Kern des Hypothalamus in der Regulation der Insulinsekretion und des Ganzkörperstoffwechsels bei Mäusen. L-Serin wird aus der Nahrung gewonnen, aber auch *de novo* synthetisiert und ist an wichtigen Stoffwechselwegen beteiligt, die am Glukosestoffwechsel, der Abwehr von Antioxidantien, dem Ein-Kohlenstoff-Stoffwechsel, der Nukleotidproduktion und der Neurotransmission beteiligt sind. Die Supplementierung mit L-Serin hat positive Auswirkungen auf die Nahrungsaufnahme, die Insulinsekretion und die β-Zellfunktion bei Mäusen. Darüber hinaus wird L-Serin beim Menschen mit einem verbesserten Glukose- und Insulinstoffwechsel und einem verringerten Fettleibigkeitsrisiko in Verbindung gebracht. NMDAR ist ein inotroper Glutamatrezeptor, der an der Neurotransmission und synaptischen Plastizität beteiligt ist und durch D-Serin, das Enantiomer von L-Serin, koaktiviert wird. In dieser Arbeit wird gezeigt, dass eine L-Serin-Supplementierung bei Mäusen die Körpergewichtszunahme nach Fasten durch eine Erhöhung der BAT-Thermogenese und eine Beteiligung von NMDARs im paraventrikulären Kern des Hypothalamus an der Regulierung des Energiegleichgewichts durch BAT-Aktivität verringerte. Diese Ergebnisse deuten auf eine L-Serin-Supplementierung als potenziellen Ansatz zur Vorbeugung und/oder Behandlung von Fettleibigkeit hin und liefern überzeugende Daten zur Rolle von NMDARs im Hypothalamus bei der Regulierung der Energiehomöostase.

Table of contents

1. Introduction

1.1. Obesity: a worldwide health concern

Over the past decades, obesity prevalence has increased exponentially in women and men around the world. More strikingly, obesity prevalence has risen 6% in children from 1975 to 2016 (Blüher, 2019). By continuing this trend, a larger part of the adult population will be obese in the near future. The large number of obese subjects is concerning, but the most alarming fact is that these subjects are prone to develop co-morbidities that may cost them their lives. Obesity is a metabolic disease defined as an excessive fat accumulation impairing health or as a body mass index (BMI)≥ 30 kg/m^2 (Blüher, 2019; Roden and Shulman, 2019). As mentioned before, obesity is a risk factor for the development of other diseases such as type 2 diabetes mellitus (T2D), cardiovascular diseases, hypertension and some cancers (Loos and Yeo, 2022). As in many diseases, prevention and early diagnosis of obesity is essential. The complexity of obesity etiology lies not only in the environment and lifestyle (nutrition and physical exercise), but also in genetics. Furthermore, scientific evidence shows how hard-wired our bodies are to resist weight loss. Despite that, there is still the disbelief that we are fully in control of our bodies and, thus, obesity is a choice. This disbelief also leads to weight stigma in the healthcare system (Batterham, 2022). Weight stigma has detrimental effects on the health of individuals. Subjects of weigh stigma might suffer from eating and sleeping disorders, increased energy intake by eating energy-dense foods, depression, anxiety and substance abuse (Wu and Berry, 2018; Rubino *et al.*, 2020; Batterham, 2022). To overcome this additional problem, we should also raise awareness of the social impact of being overweight and obese and educate the population including healthcare professionals. Overall, the key points to tackle the obesity pandemic and its co-morbidities are the identification of individuals prone to develop obesity as well as the detrimental environmental and social factors, to promote healthy lifestyle, educate the population and investigate mechanisms underlying obesity as well as new treatment strategies.

1.1.1. Type 2 Diabetes mellitus

Obese individuals have a higher risk for developing T2D. T2D displays hyperglycemia due to a deficient insulin secretion by pancreatic β-cell and insulin resistance (Roden and Shulman, 2019). As well as obesity, T2D etiology is heterogeneous and has started to emerge in obese children and young adults (<40 years) (Arslanian *et al.*, 2018; Roden and Shulman, 2019; Magliano *et al.*, 2020). Compared to the late-onset-T2D, prevention and diagnosis are especially important in children and young adults since an earlier onset of T2D leads to a faster β-cell decline and a

greater risk for complications. To this end, predictors have been identified such as low birthweight, genetics, ethnicity, high triglycerides, hypertension and low HDL (Magliano *et al.*, 2020). Besides the traditional co-morbidities of T2D involving macrovascular conditions such as kidney disease, retinopathy, neuropathy, peripheral vascular diseases, coronary heart disease and heart failure, a broad spectrum of complications is emerging. These complications comprise several types of cancers, liver disease, infections and neurological diseases from depression, anxiety, eating disorders to dementia and Alzheimer's disease (Tomic, Shaw and Magliano, 2022). Controlling blood glucose levels is the main target of T2D management (Perreault, Skyler and Rosenstock, 2021). However, diet and physical exercise for body weight loss also contribute to T2D and obesity remissions (Magkos, Hjorth and Astrup, 2020). Nevertheless, all current approaches tend to be more individualized, towards precision medicine (Ashley, 2016; Perreault, Skyler and Rosenstock, 2021).

1.2. Body weight loss strategies

There are countless weight loss diets (e.g.: high-protein diets), diet regimes (e.g.: intermittent fasting) and exercise programs. Although these methods could be effective in the short term, they might not be effective in the long term or may even be harmful if unsupervised by health professionals (Jebeile *et al.*, 2021; Colombarolli Stivaleti, Oliveira and Cordás, 2022).

1.2.1. Bariatric surgery intervention and intragastric balloons

Surgical interventions such as bariatric surgery or intragastric balloons are also alternatives to decrease body weight. Bariatric surgery is very effective but not accessible to all the patients. It is expensive and only for those patients meeting specific characteristics, as a high BMI or co-morbidities (Gomez and Stanford, 2018; Müller *et al.*, 2022). The most common types of bariatric surgical interventions are the vertical sleeve gastrectomy and the Roux-en-Y gastric bypass. Both methods show similar weight loss and improvements in adipose tissue health in obese and diabetic patients (Docherty and le Roux, 2020). The intragastric balloon is a less invasive non-surgical option for body weight loss in overweight and obese individuals and more effective than lifestyle changes alone (Mohammadpour *et al.*, 2020). These balloons are placed endoscopically or swallowed restricting the capacity of the stomach and delaying gastric emptying (Chow *et al.*, 2022). Both methods improve overall health, but there is always a potential post-surgery body weight regain.

1.2.2. Fasting strategies

Fasting or intermittent fasting aim to reduce energy intake as an alternative to reduce body weight. There are several types of intermittent fasting which may be followed along with physical exercise (Nowosad and Sujka, 2021). There is complete alternate fasting or alternate days fasting in which patients do not eat high-energy food and drinks or consume only 20-25% of their energy demands, respectively. Additionally, there is the time-restricted fasting in which eating occurs only during a window of time of 8 h while fasting 16 h every day (Nowosad and Sujka, 2021). Most studies on intermittent fasting in diabetic and obese adults resulted in not only body weight loss (Nowosad and Sujka, 2021; Domaszewski *et al.*, 2022; Ostendorf *et al.*, 2022; Varady *et al.*, 2022), but also in improvements in fasting glucose and insulin sensitivity, HbA1c levels (Nowosad and Sujka, 2021), body composition and visceral fat (Domaszewski *et al.*, 2022).

1.2.3. Pharmacological treatment

Several drugs are approved for body weight loss. For short-term use: phentermine, diethylpropion, phendimetraxine and benzphetamine; and for long-term use: orlistat, phentermine/topiramate, bupropion/naltrexone, liraglutide (Gomez and Stanford, 2018) and semaglutide (Müller *et al.*, 2022). However, the adverse effects do not outweigh their benefits in some cases (Cheung, Cheung and Samaranayake, 2013) and they might not be covered by the health insurances (Hinney, Körner and Fischer-Posovszky, 2022). Nevertheless, there have been substantial advances. Some promising drugs such as metrelepin or setmelanotide for the treatment of specific types of obesity are also available. Furthermore, innovative strategies such as unimolecular pharmacology, which is a combination of therapies to potentiate metabolic improvements, are available for particular conditions. For instance, tirzepatide (a glucose-dependent insulinotropic polypeptide and glucagon-like peptide 1 (GLP1) agonist) a drug approved for overweight or obese patients with T2D, which efficiently reduces body weight (Hinney, Körner and Fischer-Posovszky, 2022). Even though considerable efforts must be taken to make obesity precision medicine a common practice, it seems to have a bright future ahead (Hurtado and Acosta, 2021; Hinney, Körner and Fischer-Posovszky, 2022).

1.2.4. Weight loss diets and dietary supplements

The reduction of energy intake is a strategy to decrease body weight. Dietary guidelines for healthy adults recommend a distribution of macronutrients as follows: 45-65% of calories from carbohydrates, 10-30% from protein and 20-35% from fat (Curioni and Lourenço, 2005; Brehm and D'Alessio, 2008). However, to obtain metabolic improvements, weight loss diets must be

personalized to each patient (Martinez *et al.*, 2014) and, ideally, along with regular exercise (Curioni and Lourenço, 2005; Magkos, Hjorth and Astrup, 2020). The effect of macronutrients in the diet in relation to body weight loss has been examined in numerous studies and clinical trials (Due *et al.*, 2008; Larsen *et al.*, 2010; Martinez *et al.*, 2014; Poulsen *et al.*, 2014; Isenmann, Dissemond and Geisler, 2021; Pomares-Millan *et al.*, 2022). Generally, they found that an increase in diet carbohydrates (especially sugars) and fat led to weight gain, while an increase in diet protein led to weigh loss as well as increased thermogenesis and satiety (Martinez *et al.*, 2014). For instance, a Danish study in individuals with increased waist circumference found that consumption of high-quality carbohydrates and less processed food led to a higher weight loss than eating a Western-like diet comprised by food with refined grains, dairy, sugar products and low-fiber vegetables and fruit (Poulsen *et al.*, 2014). Two different studies which provided a low-calorie diet promoting weight loss in obese and overweight individuals, showed that body weight regain was prevented with a diet consisting of high-quality carbohydrates and less processed food (Due *et al.*, 2008) and a diet with higher glycemic load (high glycemic index and low protein) (Larsen *et al.*, 2010). Nevertheless, longer studies are needed to ensure that these and other weight loss diets have benefits in the long-term weight control (Malik and Hu, 2007; Magkos, Hjorth and Astrup, 2020).

Variations in the quality and quantity of protein can be used to modify parameters altered in obesity and T2D such as body composition, insulin resistance and satiety (Simonson, Boirie and Guillet, 2020). Nevertheless, the amino acid composition of dietary proteins should also be considered, since they not only build proteins but also regulate many metabolic pathways (Simonson, Boirie and Guillet, 2020; Xiao and Guo, 2022). While branched-chain amino acids, methionine, tryptophan and glutamate are associated with obesity and T2D risk (Newgard *et al.*, 2009; Simonson, Boirie and Guillet, 2020), other amino acids such as serine are inversely correlated (Okekunle *et al.*, 2019).

Dietary supplements for body weight loss are also approved by the FDA. However, they have very low effectiveness (National Institutes of Health. Office of Dietary Supplements., 2022). Over-the-counter weight loss supplements are very popular as well. Yet, some might have hidden ingredients that can be harmful (U.S.A. Food & Drug Adminsitration, 2022). L-serine is a dietary supplement approved by the FDA. It is considered GRAS (generally recognized as safe), but only a 8.4% of L-form (from total protein weight) is approved as a food additive (U.S. Food and Drug Administration, 2022). No other applications are contemplated. Later in this thesis, I summarize

the many benefits of L-serine supplementation on obesity and T2D, posing L-serine as a potential candidate for their prevention and/or treatment.

1.3. Serine metabolism

Since its discovery in silk protein by the German chemist Emil Cramer in 1865 (De Koning *et al.*, 2003), L-serine has been traditionally known as a mere non-essential amino acid involved in the synthesis of proteins. However, L-serine is crucial for an overall good metabolic function because it participates in many fundamental pathways.

1.3.1. Sources and biosynthesis

L-serine is a glucogenic amino acid containing three carbon atoms and a polar hydroxyl group. It comes from either diet or its biosynthesis from different intermediates (Newsholme *et al.*, 2011; Holm and Buschard, 2019). L-serine is provided by daily-consumed food products such as cereals, roots, legumes, nuts, vegetables, fruits and different types of meat and fish (**Table 1**) as well as by the protein and phospholipid turnover. Most importantly, L-serine can be synthesized from glycine and *de novo* from 3-phosphopglycerate (from glycolysis), being the major source. Serine hydroxymethyltransferase (SHMT) transfers one carbon to glycine leading to serine production, but this process might be reversed from serine to glycine. *De novo* synthesis of serine is induced not only by lack of serine but also by metabolic stress and takes place in three irreversible steps. Firstly, phosphoglycerate dehydrogenase (PHGDH) converts 3-phosphoglycerate into 3-phosphohydroxypyruvate by using NAD^+. Next, phosphoserine aminotransferase (PSAT) transaminases 3-phosphohydroxypyruvate to obtain 3-phosphoserine. Then, the latter is hydroxylated by phosphoserine phosphatase (PSP) to L-serine. This is known as the phosphorylated pathway (Newsholme *et al.*, 2011; Kohlmeier, 2015; El-hattab, 2016; Yang and Vousden, 2016; Murtas *et al.*, 2020; Maugard *et al.*, 2021).

1.3.2. Catabolism

As long as the protein consumption is sufficient for L-serine biosynthesis, only 5% of L-serine contained in body proteins comes directly from the diet (Kohlmeier, 2015). Besides the synthesis of proteins, L-serine is critical to other metabolic processes such as glycolysis, phospholipid and sphingolipid synthesis, glutathione synthesis, folate and methionine cycles and nucleotide production (**Figure 1**) (Parker and Metallo, 2016). L-serine metabolism is linked to glycolysis and gluconeogenesis by their intermediate 3-phosphoglycerate which is derived from glucose or

pyruvate, respectively, according to metabolic needs (Kalhan and Hanson, 2012; Yang and Vousden, 2016).

Cereals and grain products	mg Ser/N g	Fruits	mg Ser/N g	Nuts and seeds	mg Ser/N g
Maize grain or whole meal (*Zea mays*)	311	Apple (*Malus sylvestris*)	270	Hazelnut (*Corylus avellana*)	603
Oats (*Avena sativa*)	294	Banana (*Musa spp.*)	244	Pistachio (*Pistacia spp.*)	346
Quinoa (*Chenopodium quinoa*)	231	Grape (*Vitis spp.*)	300	Sesame (*Sesamum spp.*)	291
Rice brown or husked (*Oryza spp.*)	339	Orange (*Citrus sinensis*)	180	Sunflower seed (*Helianthus spp.*)	270
Starchy, roots and tubers		**Meat and poultry**		**Vegetables**	
Potato (*Solanum tuberosum*)	259	Beef and veal edible flesh (*Bos taurus*)	252	Carrot (*Daucus carota*)	201
Sweet potato (*Ipomoea batatas*)	255	Chicken edible flesh (*Gallus gallus*)	244	Pea seed (*Pisum sativum*)	281
Cassava meal (*Manihot esculenta*)	204	Horse edible flesh (*Equus caballus*)	263	Lettuce leaves (*Lactuca sativa*)	206
Tigernut (*Cyperus esculentus*)	219	Pork edible flesh (Suidae)	275	Eggplant fruit (*Solanum melongena*)	230
Dry legumes and legume products		**Fish and shellfish**		**Eggs**	
Bean (*Phaseolus vulgaris*)	347	Salmon (*Salmonidae*)	243	Hen, whole	478
Chick-pea (*Cicer arietinum*)	318	Cod (*Gadidae*)	312	yolk	564
Lentil (*Lens culinaris*)	329	Tuna (*Scombrinae*)	224	white	456
Soy bean (*Glycine max*)	320				

Table 1. Serine content in food products. Conversion factor (N): Meat, fish: 6.25; nuts: 5.3; soy beans: 5.71, oats: 5.83 and rice: 5.95. Adapted from FAO Food and Nutrition Series (Food Policy and Food Science Service, Nutrition Division, 1981).

Cell membrane basic structure are also associated with L-serine. Phospholipids such as phosphatidylcholine (PC) and phosphatidyletanolamine (PE) constitute together up to 80% of the mammalian membrane bilayer. In the ER, L-serine substitutes choline and ethanolamine groups of these compounds by the action of two different synthases, to produce phosphatidylserine (PS), which represents from the 5 to 10% of phospholipids. Conversely, in the mitochondria, PS can be transported and, further, decarboxylated to PE (Vance, 2015). Sphingolipids are a type of phospholipid, bioactive components involved in many functions such as cell growth, death, proliferation, migration, adhesion, apoptosis, necrosis and cytoskeleton rearrangement (Breslow and Weissman, 2010; Hannun and Obeid, 2018). L-serine, together with palmitate, is the precursor of the *de novo* synthesis of these lipids by condensation of serine palmitoyltransferase

(SPT) (Hannun and Obeid, 2018). Sphingolipids can then be reduced to sphingosines and further N-acetylated to yield ceramides (Breslow and Weissman, 2010).
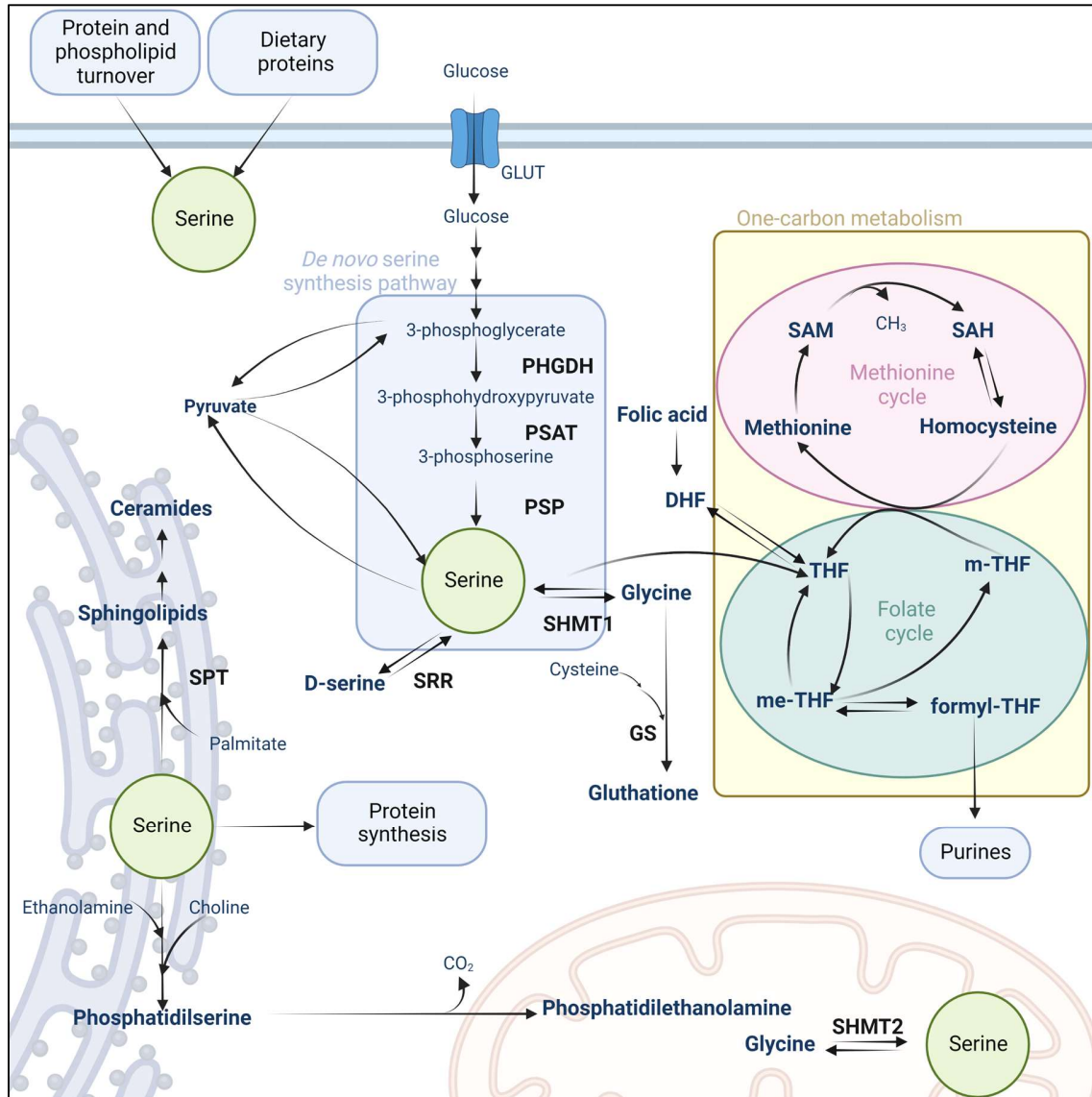
Figure 1. L-serine is essential in cell growth and proliferation. L-serine can be directly obtain from dietary proteins and protein and phospholipid turnover. However, it is mainly synthesized *de novo* in a three step involving PHGDH (phosphoglycerate dehydrogenase), PSAT (phosphoserine aminotransferase) and PSP (phosphoserine phosphatase). It can be converted to D-serine by SRR (serine racemase) action but also to Glycine in the cytosol or mitochondria through SHTM1 (serine hydroxymethyltransferase) and SHTM2, respectively. Glycine derived from serine is then used to synthesize THF (tetrahydrofolate) in the folate cycle, essential substrate also in the methionine cycle, cycles that constitute the one-carbon metabolism. Glycine is also substrate in the synthesis of glutathione. Sphingolipids are produced from serine through SPT (serine palmitoyltransferase), from which ceramides are obtained. Moreover, L-

serine is utilized in phospholipids and protein synthesis. Created with Biorender.com. Based on references in 1.3.1. and 1.3.2.)

Antioxidant defense conferred by glutathione also relies on L-serine catabolism. Serine hydroxymetyltransferase (SHTM1) in the cytosol and serine hydroxymethyltransferase (SHTM2), in the mitochondria, are responsible for the conversion of serine into glycine (Wang *et al.*, 2013; Meiser *et al.*, 2016; Yang and Vousden, 2016). Glutathione is then derived from glycine, cysteine and glutamate (Meiser *et al.*, 2016; Yang and Vousden, 2016). This process consists of a two-step ATP-dependent metabolic reaction, first catalyzed by glutamate cysteine ligase and then, by glutathione synthase (Lu, 2009). Furthermore, glycine yielded by SHTM1 and SHTM2 might be also used as a one-carbon unit in the folate cycle. Tetrahydrofolate (THF) is obtained by the action of dihydrofolate reductase (DHFR) on dihydrofolate (DHF), which is the product from the ingested folate (Newman and Maddocks, 2017). Then, the carbon unit from glycine is added to THF yielding 5,10-methylene-THF. Then, this folate will be further oxidized to 10-formyl-THF, which is a substrate for *de novo* purine synthesis (Yang and Vousden, 2016; Wu and Tam, 2021; Zarou, 2021). However, 5,10-methylene-THF is also involved in the methionine cycle. With an irreversible reaction catalyzed by methylenetetrahydrofolate reductase (MTHFR), 5-10-methylene-THF is converted to 5-methyl-THF. Subsequently, this folate is used to re-methylate homocysteine by methionine synthase yielding methionine (Yang and Vousden, 2016; Wu and Tam, 2021). Methionine is converted to S-adenosyl methionine (SAM), which acts as a methyl donor in different methyl-transferase reactions, by methione adenosyltransferase (MAT). After the donation of a methyl group, SAM turns to S-adenosyl-homocysteine (SAH) that is further hydroxylated to homocysteine. The latter is then methylated to methionine with a group coming from the folate cycle closing the cycle (Yang and Vousden, 2016; Sanderson *et al.*, 2019; Wu and Tam, 2021). Together, folate and methionine cycles mainly comprise the one-carbon metabolism.

Nucleotide production is required for cell proliferation, for DNA and RNA synthesis but also for substrates as ATP and NAD. Both purines and pyrimidines can be synthesized *de novo* or by the savage pathway. While the savage pathway consists of recycling free bases for both types of nucleotides, *de novo* pathways require more energy and different substrates (Moffatt and Ashihara, 2002; David L. Nelson, 2008; Yang and Vousden, 2016; Puigserver, 2018; Yin *et al.*, 2018; Wang *et al.*, 2021). Nevertheless, either savage or *de novo* pathways in both purines or pyrimidines, folate derivatives and phosphoribosyl pyrophosphate (PRPP) substrates are essential (Puigserver, 2018). As mention earlier, purine synthesis relies on serine metabolism.

Purines are the result of a highly-consuming enzymatic process that uses, among other substrates, glutamine and glycine (Yin *et al.*, 2018).

Neurotransmission is also connected to serine metabolism due to the production of the two co-agonists of the N-methyl-D-aspartate receptor (NDMAR): glycine and D-serine. Although L-serine may effectively cross the blood brain barrier, it is also synthesized *in situ,* mainly in astrocytes (Maugard *et al.*, 2021). D-serine is converted from its enantiomer L-serine by serine racemase (SRR) action. By binding to the glycine modulator site (GMS) of NMDARs, D-serine regulates synaptic transmission and plasticity (De Koning *et al.*, 2003; Suwandhi *et al.*, 2018; Wolosker and Balu, 2020; Maugard *et al.*, 2021).

1.4. Role of serine in metabolic and neurological diseases

1.4.1. Genetic diseases altering serine metabolism

1.4.1.1. Serine deficiencies

Serine deficiency disorders are the result of low activity of one of the three enzymes involved in the serine biosynthesis pathway. Most of the cases are due to deficiency in PHGDH; only a limited number of cases showed a deficiency of PSAT or PSP activity. PHGDH deficient patients are mainly children showing neurodevelopmental disorder with microcephaly, several types of seizures and psychomotor retardation. Low serine levels in cerebrospinal fluid (CSF) and plasma are key for the diagnosis (Van Der Crabben *et al.*, 2013). The most severe case of serine deficiency is Neu-Laxova syndrome. This is a rare autosomal-recessive disorder caused by mutations in PHGDH, PSAT1 and PSP. Clinical manifestations are head and limb malformations as well as skin abnormalities leading to a pre- or post-natal death (Aslan *et al.*, 2002; Acuna-hidalgo *et al.*, 2014; Shaheen *et al.*, 2014; Murtas *et al.*, 2020). In children and juvenile patients with serine deficiency disorder, treatment with oral L-Serine supplementation (200-500mg/kg/day) together with glycine (200mg/kg/day) led to improvements in seizures and well-being (De Koning TJ, Duran, M, Dorland L, Gooskens R, Van Schaftingen E, Jaeken J, Blau N, Berger R, 1998; de Koning, 2006; Van Der Crabben *et al.*, 2013).

1.4.1.2. Hereditary sensory autonomic neuropathy 1 (HSAN1)

Genetic alterations in L-serine-dependent lipid synthesis enzymes may also develop in a neurological disease known as hereditary sensory autonomic neuropathy type 1 (HSAN1). HSAN1 is the result of missense mutations in genes SPTLC1 and SPTLC2, which encode for SPT. Alterations in SPT lead to increased affinity to alanine and glycine instead of L-serine, thus

yielding atypical and neurotoxic 1-deoxysphingolipid (1-deoxySL) (Eichler *et al.*, 2009; Zitomer *et al.*, 2009; Penno *et al.*, 2010; Garofalo *et al.*, 2011; Fridman *et al.*, 2019). Levels of 1-deoxySL were reduced in HSAN1 mice (Garofalo *et al.*, 2011) and patients (Garofalo *et al.*, 2011; Fridman *et al.*, 2019) by L-serine administration (10% serine diet and 200-400mg/kg/day, respectively). Both of these studies suggested L-serine as an aid for slowering down the progression of HSAN1 (Garofalo *et al.*, 2011; Fridman *et al.*, 2019).

1.4.1.3. GRIN-encephalopathies

As described previously, L-serine is also the precursor of the NMDAR co-agonists glycine and D-serine. NMDAR is a receptor expressed in the central nervous system (CNS), where it is partly responsible for the excitatory neurotransmission (Mielnik *et al.*, 2021; Tajima *et al.*, 2022). GRIN disorder encompass the set of pathologies resulting from mutations in the GRIN genes, which encode for NMDAR subunits. These GRIN alterations cause several neurological conditions such as encephalopathies, intellectual disability, attention deficit hyperactivity disorder (ADHD), autism spectrum disorder (ASD) and schizophrenia (Xiangwei, Jiang and Yuan, 2018; Mielnik *et al.*, 2021). L-serine supplementation improved motor and cognitive symptoms as well as communication in a pediatric patient with a Rett-like syndrome with severe encephalopathy. The therapeutic strategy of using L-serine supplementation (500mg/kg/day) was to provide a D-serine precursor that would compensate for the neurological symptoms derived from genetic alteration of the NMDAR GRIN12B subunit (Soto *et al.*, 2019). Furthermore, an ongoing clinical trial is studying the tolerability and efficacy of L-serine in pediatric patients with GRIN-related encephalopathy (ClinicalTrials.gov, 2020).

1.4.2. Neurodegenerative diseases and serine.

Neurodegenerative diseases such as Alzheimer's disease (AD), amyotrophic lateral sclerosis (ALS) and Parkinson's disease (PD) have also been linked to L-serine or serine metabolism. The main features of AD are the presence of β-amyloid-containing (Aβ) plaques and tau-containing neurofibrillary tangles in the cortex, leading to synaptic and neuronal loss (Benarroch, 2018; Knopman *et al.*, 2021). Clinical symptoms in AD patients generally manifest when they are older than 65 years and their cognitive impairment may vary from mild to very severe (Knopman *et al.*, 2021). Even though Aβ and tau proteins seem to have normal roles in synapses, when accumulated are toxic and cause neurodegeneration (Spires-Jones and Hyman, 2014; Knopman *et al.*, 2021). Aβ directly binds to NMDARs, impairing synaptic plasticity and triggering synaptic loss. Hence, using NMDAR antagonists, such as memantine, is one of the pharmaceutical

approaches of AD treatment (Spires-Jones and Hyman, 2014; Bach, Halmos and Smith, 2015; Benarroch, 2018; Knopman *et al.*, 2021). Nevertheless, L-serine is currently used in a phase IIa clinical trial as a potential treatment for AD, in 15g twice daily dose (ClinicalTrials.gov, 2017).

ALS, also referred as motor neuron disease (MND), is a rare disease with an unclear gene/environment interaction etiology and low life expectancy after diagnosis (2-5 years) (Hardiman *et al.*, 2017; Levine *et al.*, 2017; Davis *et al.*, 2020). ALS is presented as muscle weakness and paralysis due to the degeneration of the upper and lower motor neurons. As in AD, the damage of these motor neurons is the result of the aggregation and accumulation of protein inclusions (Hardiman *et al.*, 2017; Davis *et al.*, 2020). Moreover, half of the patients show cognitive or behavioral deterioration (Hardiman *et al.*, 2017; Levine *et al.*, 2017). Due to its neuroprotective effect *in vitro* and *in vivo*, L-serine has been proposed as a potential agent to treat ALS, but also to PD (Dunlop, J. Powell, *et al.*, 2018; Dunlop, J. T. Powell, *et al.*, 2018; Davis *et al.*, 2020; Dunlop and Carney, 2021). Furthermore, a phase I clinical trial suggested that oral L-serine administration (up to 15g twice a day) was safe in ALS patients (Levine *et al.*, 2017).

PD is a progressive disease caused by the loss of dopaminergic neurons in the midbrain leading to rest tremor, rigidity, bradykinesia, postural instability and cognitive and behavioral problems (Vanle, 2018; Louise *et al.*, 2019). Glycine levels were found to be elevated in PD patients compared to healthy controls (Iwasaki, Y; Ikeda, K; Shiojima, T; Kinoshita, 1992). However, metabolomics data showed that plasma serine levels were inversely correlated to PD progression. Thus, suggesting plasma serine as a biomarker of disease progression (Lewitt, Lu and Auinger, 2017). The overactivation of the target receptor of D-serine and glycine, NMDAR, is also an important physiological feature of PD. Hence, NMDARs are also a target in the PD therapy (Vanle, 2018). Interestingly, D-serine has been shown to be safe and beneficial as an adjuvant for treating PD, improving behavioral and motor symptoms, in a dose of 2g/day (Gelfin *et al.*, 2012). Furthermore, repeated dosing of D-serine (60mg/kg) was shown to improve auditory plasticity (Kantrowitz *et al.*, 2016) and cognition (120mg/kg) (Garrigue *et al.*, 2020) as well as negative, positive, and depression symptoms in combination with olanzapine and risperidone (30mg/kg/day) (Heresco-levy *et al.*, 2005) in schizophrenic patients. There is also an ongoing clinical trial studying a potential cognitive improvement by increasing D-serine (ClinicalTrials.gov, 2022), but another trial using D-serine as an adjuvant for treating depression (ClinicalTrials.gov, 2021).

1.4.3. Obesity, T2D and L-serine

L-serine and its metabolism have been also linked to obesity and T2D. Studies in animals have shown that L-serine supplementation reduced the body weight of non-obese diabetic (NOD) mice (Holm *et al.*, 2018) and 2% supplementation in female mice led to a decrease in the body weight of their offspring (Nagamachi *et al.*, 2018). A similar effect was observed in mice chronically supplemented with 1% D-serine, whose body weight gain decreased under high-fat diet (HFD) (Suwandhi *et al.*, 2018). Furthermore, L-serine supplementation reduced and prevented severity of pancreatitis (Chen *et al.*, 2020), increased glucose tolerance and insulin sensitivity, protected from hepatic lipid accumulation, reduced oxidative stress in mice (Zhou, He, Zuo, Zhang, Wan, Long, *et al.*, 2018) and ameliorates alcoholic fatty liver in rats (Sim *et al.*, 2015). All these findings show the potential benefits of L-serine supplementation in body weight control, glucose and lipid metabolism. Indeed, there is a clinical trial studying the supplementation of L-serine in obese subjects with fatty liver disease (ClinicalTrials.gov, 2016). Moreover, there is an ongoing phase IIa human study investigating L-serine as co-adjuvant with fenofibrate (drug used to reduce lipids in blood) to reduce serum deoxysphinganine levels in patients with macular telangiectasia (ClinicalTrials.gov, 2019). Interestingly, L-serine has already been patented for using as a supplement in type 1 pre-diabetic subjects, based on a previous study on mice (Holm *et al.*, 2018). Early diagnosis is essential to attenuate symptoms in T2D. In this regard, plasma 1-deoxySLs (Othman, Saely, *et al.*, 2015; Mwinyi *et al.*, 2017) and other sphingolipid species including ceramides (Boslem, Meikle and Biden, 2012; Field, Gordillo and Scherer, 2020; Turpin-Nolan and Brüning, 2020; Yun *et al.*, 2020) have been shown to be a biomarker for the development of T2D. Nevertheless, these novel sphingolipid species are associated to T2D through β-cell dysfunction (Boslem, Meikle and Biden, 2012; Yun *et al.*, 2020), while ceramides have been identified in insulin-resistant muscle in rodents and humans (Summers and Nelson, 2005). Moreover, ceramides are negatively correlated with insulin sensitivity in human (Straczkowski *et al.*, 2004; Summers and Nelson, 2005). A study with streptozotocin (STZ)-induced diabetic mice showed that 1-deoxySLs are toxic for pancreatic acinar cells, by triggering mitochondrial dysfunction and oxidative stress (Chen *et al.*, 2020). These effects were reduced by oral administration of L-serine (10% contained in chow diet food) (Chen *et al.*, 2020). Sphingolipids play also a role in type 1 diabetes (T1D) pathogenesis (Gurgul-Convey, 2020). Moreover, the reduction of these toxic sphingolipids in plasma improves diabetic neuropathy in diabetic rats (Othman, Bianchi, *et al.*, 2015). Formation of these toxic sphingolipid species observed *in vitro* is the result of L-serine deficiency (Esaki *et al.*, 2015). Even though pancreatic sphingolipid levels remained unchanged, L-serine supplementation (28.7g/L in water) in a T1D mice model improved glucose tolerance and

hyperglycemia and reduced insulitis score as well as diabetes incidence (Holm *et al.*, 2018). In addition, L-serine levels in plasma or serum were inversely correlated to diabetes risk in human (Gunther *et al.*, 2020) and mice (Arimura, Emi Ushika Miharu, Horiuchi, 2021) and reduced in children with T1D and adults with T2D (Holm and Buschard, 2019). Therefore, L-serine seems to be a potential candidate as a dietary supplement for prevention and/or treatment of obesity and T2D.

- **Supplementation**:
  - L-serine:
    - prevents LPS-induced intestinal inflammation and oxidative stress.

- **Deficiency**: enzymes involved in serine biosynthesis: PHGDH, PSAT, PSP
- **Biomarker**:
  - serine deficiency disorders: ↓ L-serine in CSF and plasma
  - HSAN1: ↑ 1-deoxySL
- **Supplementation**:
  - *L-serine*: serine deficiency disorders, Alzheimer's disease, ALS, Parkinson's disease, GRIN-related encephalopathies, HSAN1. Also reduces oxidative stress in hypothalamus,
  - *D-serine*: Parkinson's disease, Schizophrenia and Depression.

- **Deficiency**: Homocysteinemia
- **Supplementation**:
  - L-serine: ↓ homocysteine with a methionine load.

- **Supplementation**:
  - L-serine: ↓ body weight under HFD, ↓ body weight regain by increasing BAT thermogenesis after fasting, ↓ body weight in offspring

- **Supplementation**:
  - L-serine:
    - protected from hepatic lipid accumulation, ↓ oxidative stress and alcoholic fatty liver

Serine

- **Supplementation**:
  - L-serine:
    - ↑ sleeping satisfaction and sleeping time and ↓ awake episodes.
    - advance light-induced phase

- **Biomarker**:
  - T2D:
    - ↑ 1-deoxySL: beta cell dysfunction
    - ↑ ceramides: ↑ insulin resistance in muscle, ↑ insulin sensitivity
    - ↓ L-serine levels
  - T1D
    - ↓ L-serine levels
- **Supplementation**:
  - L-serine:
    - T1D: ↓ 1-deoxySL, ↓ neuropathy, ↓ glucose tolerance and hyperglycemia, ↓ insulitis score, ↓ diabetes incidence, ↓ severity of pancreatitis

- **Biomarker**:
  - chronic renal failure: ↓ L-serine in plasma, ↑ D-serine (↓ reabsorption)

Figure 2. Serine roles in metabolism. The scheme shows how L-serine or L-serine metabolites are associated with metabolism in different organs, blood and circadian rhythms at three levels: deficiency, as a biomarker and supplementation. 1-deoxySL: 1-deoxysphingolipid; ALS: Amyotrophic lateral sclerosis; BAT: Brown adipose tissue; HFD: High-fat diet; HSAN1: Hereditary sensory autonomic neuropathy type 1; LPS: Lipopolysaccharide; PHGDH: phosphoglycerate dehydrogenase; T1D: type 1 diabetes; T2D: Type 2 diabetes. Created with Biorender.com. Based on references in 1.4.

1.4.4. Other diseases and L-serine

Besides the effects on neurological disorders and metabolic diseases described in this thesis, L-serine supplementation has shown to have other beneficial metabolic effects in several diseases

and disorders, such as chronic renal failure, homocysteinemia, sleeping disorders, circadian rhythms disturbances as well as oxidative stress. Homocysteinemia is described as elevated homocysteine levels in blood (> 15 µmol/L) leading to elevated blood pressure, cardiovascular problems, neurocognitive diseases (Xu *et al.*, 2020; Cheng *et al.*, 2022) and osteoporotic fractures (Xu *et al.*, 2020). Human studies have shown that serine lowered 30-32% total homocysteine in plasma after methionine load (Verhoef *et al.*, 2004; Olthof *et al.*, 2006). These results suggested that high serine concentrations in diet protein might be beneficial to lower homocysteine levels, and so, the risk of cardiovascular events. Moreover, D-serine, the L-serine enantiomer, is considered a biomarker for the diagnosis and progression of chronic kidney disease due to a lower D-serine reabsorption capacity in the kidney proximal tubules and glomerulus (Hesaka *et al.*, 2019, 2021; Kimura, Hesaka and Isaka, 2020). Moreover, due to its accumulation, D-serine is toxic in tubular cells through activation of the general control nonderepressible 2 (GCN2) enzyme, which is also activated by L-amino acid deficiency, causing apoptosis (Okada *et al.*, 2017). Interestingly, in that *in vitro* study, D-serine toxicity was counteracted by L-serine-containing compared to L-serine-free media; moreover, D-serine levels, in turn, activated L-serine synthesis pathway (Okada *et al.*, 2017).

Sleep deprivation can be defined as abnormal sleep measured as sleep quantity, structure or quality (Krause *et al.*, 2017). Lack of sleep affects humans at multiple levels, such as in attention, learning, memory, emotional processing and mood (Krause *et al.*, 2017; Umemura *et al.*, 2021). Moreover, there is also evidence that sleeping deprivation is positively correlated with BMI, and so, with the risk of developing obesity (Gangwisch *et al.*, 2005). A human study showed that L-serine intake (3g) for four days 30 min before going to sleep improved sleeping satisfaction, the sleeping time and decreased the frequency as well as the times of the awake episodes (Ito *et al.*, 2014).

Circadian rhythms define sleep-awake cycles in mammals (Zisapel, 2018). Set by genetic and environmental factors and controlled by the suprachiasmatic nucleus (SCN) of the hypothalamus, circadian rhythms are 24 h oscillations controlling many physiological processes in the body. They also vary during several stages of life (Logan and McClung, 2019). Besides sleeping and wakefulness, circadian rhythms regulate behavior, body temperature, food intake and neuroendocrine and autonomic effects according to light-dark cycles (Zisapel, 2018; Logan and McClung, 2019). Alterations of these internal rhythms might lead to sleep disturbances, but also represent a risk factor for the development of obesity, T2D and, then, their co-morbidities (Gimble *et al.*, 2011; Stenvers *et al.*, 2019) as well as brain disorders (Logan and McClung, 2019).

Additionally, circadian rhythms and nutrition are related reciprocally. Processes such as gastric emptying, gastrointestinal motility, microbiota functions, insulin sensitivity, concentrations in blood of glucose, lipids and other nutrients as well as diet-induced thermogenesis follow a daily rhythm. In turn, food intake timing, patterns and composition modify circadian rhythms at the molecular and behavioral levels (Potter *et al.*, 2016). Composition of the diet alters the synchronicity with environmental cues (e.g. caffeine and cinammic acid), amplitude (e.g.: L-theanine and harmine) and phase (e.g: resveratrol and DHA/EPA) of circadian rhythms (H. Cheng *et al.*, 2021). Experiments in mice showed that L-serine administration (≥5 mmol/kg) induced light-induced phase delay after light pulse exposure, regulated clock-gene expression in the SCN and affected the light-induced phase advance. In humans, administration of L-serine also leads to an advance in the light-induced phase. These results suggested that L-serine might be used as a method to reset the circadian rhythm during the light cycle (Yasuo *et al.*, 2017).

Imbalance between the production of oxidative species and antioxidant defenses (superoxide dismutase (SOD) and glutathione system (GSH)) leads to oxidative stress. This process is part of aging, but also of the pathologies such as AD, T2D, atherosclerosis, hypertension, and chronic obstructive pulmonary disease (COPD) (Forman, 2021). Therefore, reduction of oxidative stress may represent an improvement in these diseases. In this regard, chronic L-serine supplementation (0.1, 0.2 and 0.5% in drinking water) in aged mice not only reduced food intake and body weight, but also improved oxidative stress and modulated Sirt1/NFkB (oxidative stress regulators) signaling in the hypothalamus (Zhou, Zhang, *et al.*, 2018). Moreover, L-serine administration (0.1, 0.5 and 1% in drinking water) in mice reduced oxidative stress in mice by promoting GSH synthesis and methionine cycle (Zhou, He, *et al.*, 2017). Furthermore, L-serine supplementation (1% in drinking water) prevented HFD-induced oxidative stress (Zhou, He, Zuo, Zhang, Wan and Long, 2018) and lipopolysaccharide (LPS)-induced intestinal inflammation involving GSH synthesis and AMP-activated protein kinase (AMPK) activation (Zhou, Zhang, *et al.*, 2017). *In vitro*, L-serine also conferred protection to oxidative stress in mouse hippocampal cells (HT22 cells) by upregulating GSH synthesis (Kim *et al.*, 2019).

1.5. Maintaining energy homeostasis

Physiological conditions are in dynamic equilibrium tending towards a steady state, known as homeostasis. Energy homeostasis is the balance between energy intake and energy expenditure. Imbalance in this equilibrium, leads to obesity and T2D (Tran *et al.*, 2022). Previously in this thesis, we focused on L-serine and the regulation of energy intake. In this part, we will tackle the

components affecting both energy intake and energy expenditure as well as the potential role of NMDAR in energy balance regulation and insulin secretion.

1.5.1. White adipose and brown adipose tissues

Resting metabolic rate (RMR) is an important component of energy expenditure. RMR is defined as the minimal energy needed in order to maintain physiological function in the organism. The composition of the organism (lean and fat mass) determines the RMR (Tran *et al.*, 2022). Here, we focus on investigating the contribution of fat mass. Fat mass or adipose tissue comprises three types of cells: white, beige and brown adipocytes (**Figure 3**). White adipocytes contain one big lipid droplet and their functions include storing energy as triglycerides, insulating from ambient temperatures and secreting endocrines, which regulate several biological processes. These cells constitute fat depots, white adipose tissue (WAT), such as perigonadal fat (PGF) or subcutaneous fat (SCF) (Schoettl, Fischer and Ussar, 2018; Suchacki and Stimson, 2021). Conversely, brown adipocytes contain many small lipid droplets and their main function is to dissipate energy as heat in a process known as thermogenesis. These fat cells compose the brown adipose tissue (BAT). While WAT contains few mitochondria, BAT contains a high number of mitochondria expressing uncoupled protein 1 (UCP1). However, there are some adipocytes in WAT with the capability to function as brown adipocytes when stimulated by cold in a process known as beiging. These cells are known as beige adipocytes, expressing UCP1 and containing a high number of mitochondria and lipid droplets (Schoettl, Fischer and Ussar, 2018; Suchacki and Stimson, 2021). Both types of cells also have some endocrine functions (Whitehead *et al.*, 2021). Beige adipocytes are present in fat depots such as SCF. Activating WAT browning and BAT activity are strategies to increase energy expenditure in order to recover energy balance in obesity and T2D (L. Cheng *et al.*, 2021; McNeill, Suchacki and Stimson, 2021).
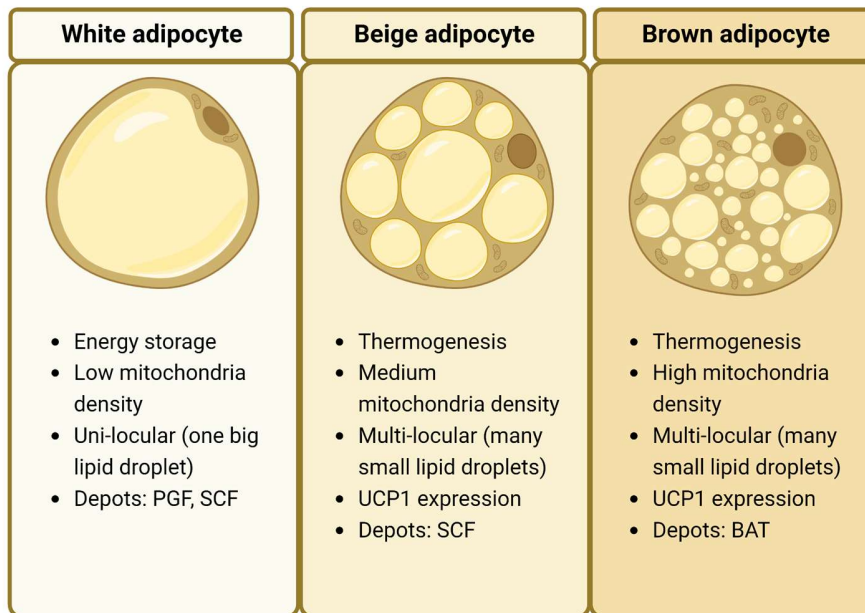
Figure 3. Characteristics of white, beige and brown adipocytes. Adapted from Suchacki and Stimson, 2021. Created with Biorender.com.

1.5.2. BAT thermogenesis

The major function of non-shivering thermogenesis is to maintain body temperature under cold exposure. Sympathetic nerves innervating BAT are stimulated by cold temperature, thus, triggering noradrenaline release, which will activate β₃-adrenergic receptors. Then, signaling cascades from the activation of these receptors will trigger hydrolysis of triglycerides and subsequent release of long-chain fatty acids (McNeill, Suchacki and Stimson, 2021; Suchacki and Stimson, 2021; Cavalieri *et al.*, 2022). Thermogenesis takes place in the inner membrane of mitochondria of brown and beige adipocytes when UCP1 protein activated by the long-chain fatty acids released, uncouples the respiratory chain from the proton gradient generating heat instead of ATP (McNeill, Suchacki and Stimson, 2021; Cavalieri *et al.*, 2022). As mentioned, this process can be triggered by cold exposure, but also by food intake (**Figure 4**). Regarding diet-induced thermogenesis, there are two components: an obligatory and a facultative component. The obligatory thermogenesis is necessary for all processes related to ingestion of food such as digestion, absorption and storage of nutrients. The facultative thermogenesis is regulated by the hypothalamus and represents an increase in energy expenditure in relation to food composition and volume (Brychta and Chen, 2017; Suchacki and Stimson, 2021). Activating BAT thermogenesis with cold, diet or drugs in humans as an approach to treat and/or prevent obesity

and T2D is controversial because of the different contribution of BAT in rodents and human as well as due to the complexity of studies in human. Nevertheless, there is the unanimous view that more research in BAT human is necessary to consider BAT activation a therapeutic strategy for these diseases (Whittle, Relat-Pardo and Vidal-Puig, 2013; Brychta and Chen, 2017; McNeill, Suchacki and Stimson, 2021; Suchacki and Stimson, 2021).
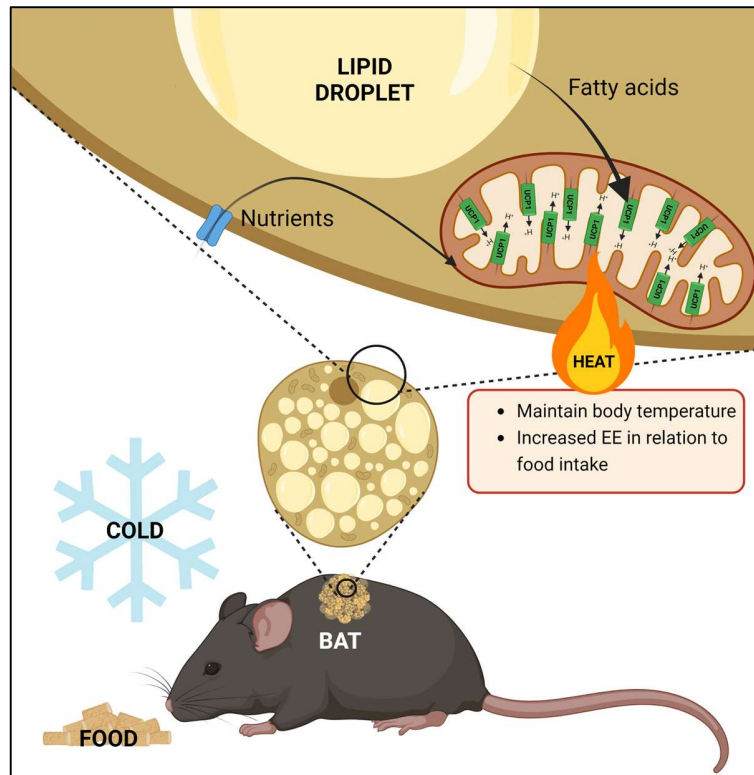
Figure 4. Cold and food-induced thermogenesis in mice. Adapted from McNeill, Suchacki and Stimson, 2021; Suchacki and Stimson, 2021. Created with Biorender.com.

1.5.3. Central control of energy homeostasis

Persistent crosstalk between the CNS and the peripheral tissues ensures energy supply for the organism cellular functions (Dietrich and Horvath, 2013). Energy homeostasis is controlled by several neuronal populations in an area of the ventral diencephalon in the brain known as the hypothalamus (Schneeberger, Gomis and Claret, 2014; Labbé *et al.*, 2015; Tran *et al.*, 2022). Factors such as RMR, physical activity, height, age, thyroid hormone levels, thermogenesis and body composition also affect the hypothalamic control of energy homeostasis (Tran *et al.*, 2022). The hypothalamus is comprised by distinct nuclei: arcuate nucleus (ARC), paraventricular nucleus (PVN), ventromedial nucleus (VMN), dorsomedial nucleus (DMN), pre-optic area (POA) and

lateral hypothalamus (LH) (Schneeberger, Gomis and Claret, 2014; Labbé *et al.*, 2015; Tran *et al.*, 2022) (**Figure 5**). ARC is a key nucleus in the regulation of energy homeostasis involving the melanocortin system. Its location in the brain and its semi-permeable blood-brain barrier poses it in a strategic position for sensing hormones and nutrient changes (Schneeberger, Gomis and Claret, 2014). The melanocortin system consists of two neuronal populations: anorexigenic pro-opiomelanocortin (POMC) neurons and orexigenic neuropeptide Y (NPY)/AgRP-producing neurons (Dietrich and Horvath, 2013). POMC neurons suppress food intake by releasing α-melanocyte stimulating hormone (α-MSH), which activates melanocortin 4 receptors (MC4Rs). Conversely, AgRP/NPY neurons release NPY and AgRP peptides, promoting food intake. These neurons project to the PVN, but also to the VMN and LH (Dietrich and Horvath, 2013; Schneeberger, Gomis and Claret, 2014). In addition, VMN, DMN and POA are also involved in energy homeostasis by their contribution in thermogenesis. Moreover, POA receives thermal inputs from the skin through the thermoreceptors (Labbé *et al.*, 2015). LH regulates orexigenic responses and these orexigenic neurons involved project to ARC and PVN (Schneeberger, Gomis and Claret, 2014). All these nuclei together integrate signals to regulate coordinately energy balance.
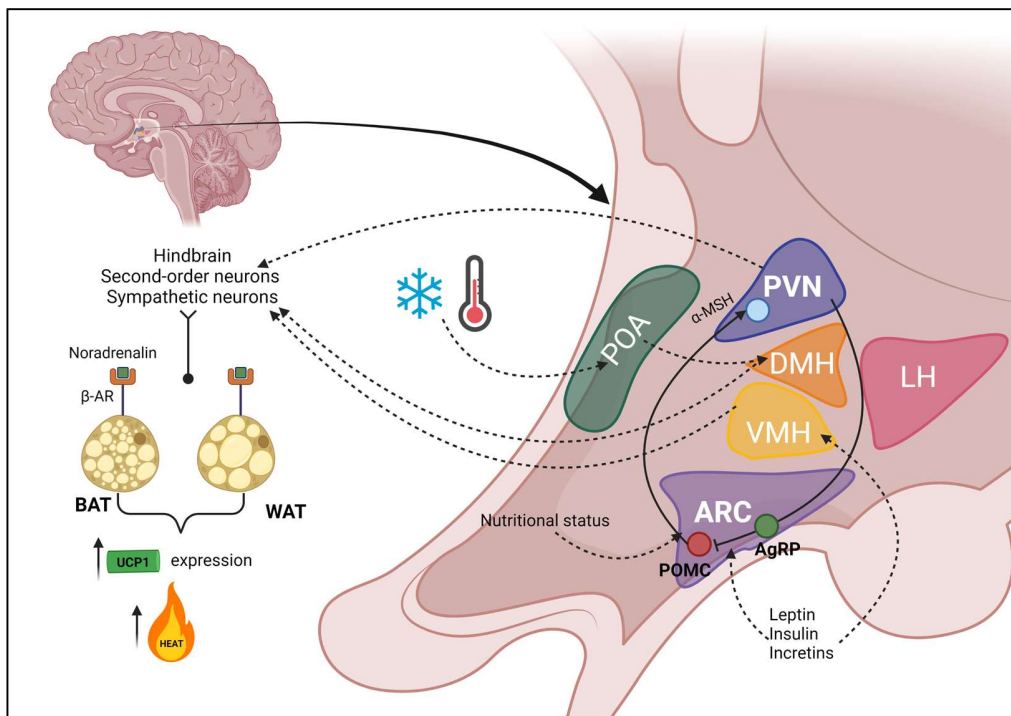
Figure 5. Hypothalamic nuclei involved in thermogenesis. Adapted from Tran *et al*. 2022. Created with Biorender.com.

1.5.3.1. Paraventricular nucleus (PVN) of the hypothalamus

The PVN serves as a hub in the regulation of energy balance responses. Located in the anterior hypothalamus, just above the third ventricle, the PVN receives input signals from the ARC, LH, POA, DMN among other centers in the hypothalamus and hindbrain (Jennifer W. Hill, 2012; Schneeberger, Gomis and Claret, 2014; Labbé *et al.*, 2015; Qin, Li and Tang, 2018; Tran *et al.*, 2022). As discussed later in this thesis, the PVN contribution to energy homeostasis regulation, specifically to BAT thermogenesis, is controversial. However, all evidence indicate some sort of PVN contribution in BAT thermogenesis. Several types of PVN neurons have been identified in the PVN. For instance, parvocellular and magnocellular neurons; but also, gamma-aminobutyric acid (GABA) and glutamatergic neurons (Hill, 2012; Labbé *et al.*, 2015). Parvocellular neurons project to the nucleus tractus solitarius (NTS) linking the PVN to peripheral tissues such as WAT, BAT, liver and pancreas (Hill, 2012). NTS has been proposed as a center for hunger modulation and is highly connected to PVN. Because of the few GABAergic neurons in the PVN, transmission from PVN to NTS might be excitatory and so, mediated by glutamatergic neurons (Nakamura and Nakamura, 2018). Additionally, there are some neuronal populations in the PVN that control energy homeostasis by altering neuroendocrine outflow and, subsequently activation of brainstem and sympathetic and parasympathetic neurons. These are the corticotrophin-releasing hormone (PVN^{CRH}), thyrotropin-releasing hormone (PVN^{TRH}) and oxytocin neurons (PVN^{OXT}). PVN^{CRH} and PVN^{TRH} neurons functions are triggered by hormone secretion to hypothalamic-pituitary-adrenal (HPA) axis and hypothalamic-pituitary-thyroid (HPT) axis, respectively (Hill, 2012; Qin, Li and Tang, 2018). PVN^{CRH} neurons respond to stress, but also, when activated, decrease food intake as well as body weight gain and induce locomotor activity, BAT thermogenesis and lipolysis. PVN^{TRH} neurons induce the release of thyroid hormone, which is crucial for cold-induced thermogenesis (Hill, 2012). In the case of PVN^{OXT} neurons, they release oxytocin and vasopressin in the systemic circulation regulating reproduction processes. Moreover, these neurons sense leptin and modulate food intake and energy expenditure (Hill, 2012; Qin, Li and Tang, 2018).

Further research should focus on unrevealing the specific conditions in which PVN neurons contribute to energy homeostasis and the connections to other hypothalamic neurons regulating peripheral tissues.

1.5.4. Peripheral and central regulation of insulin secretion

Insulin secretion takes places in the β-cells of pancreatic islets and its regulation contributes to glucose homeostasis. During fasting, insulin is secreted in low concentrations to limit catabolism;

whereas post-pandrially, insulin secretion increases. Thus, ensuring energy storage, inhibiting hepatic glucose production and promoting signaling cascades in order to increase glucose transporter in cell membranes (Mathieu, 2021). In β-cells, glucose is taken up and ATP and glutamate are produced. High levels of ATP trigger the closing of ATP-sensitive potassium channels (K_{ATP}) in the membrane and thereby causing depolarization of the cell. Then, the Ca^{2+} influx will trigger insulin exocytosis and release. There are other receptors involved in the regulation of insulin secretion such as GLP1R and NMDAR. During the depolarization of the cell, glutamate and glycine/D-serine NMDAR activation promote concomitant Ca^{2+} and Na^+ influx and K^+ efflux (**Figure 6**) (Marquard *et al.*, 2015; Wollheim and Maechler, 2015). A study by Marquard *et al.* showed that NMDARs limited glucose-stimulated insulin secretion (GSIS) in β-cells and that drugs based on NMDAR antagonism might have beneficial effects on glucose-lowering effects of some drugs as well as on insulin content, islet mass and viability in the long-term (Marquard *et al.*, 2015).

Insulin also exerts its effects on the brain by modulating hepatic glucose production. In addition, hypothalamic insulin controls glucose homeostasis in peripheral organs. Hypothalamic overexpression of insulin signaling molecules (insulin receptor substrate-2 (IRS2) and Akt) enhances insulin action in diabetic rats (Obici, Feng, *et al.*, 2002; Obici, Zhang, *et al.*, 2002). Moreover, alteration of hypothalamic K_{ATP} channels modified glucose production and central insulin action (Pocal *et al.*, 2005). Although insulin secretion is regulated by mechanisms in the pancreatic islet, the CNS also plays a role in its regulation. The pancreas is innervated by both parasympathetic and sympathetic neurons, controlling insulin and glucagon secretion. Parasympathetic neurons activation promotes insulin secretion while sympathetic neurons activation inhibits it (Thorens, 2010; Roh, Song and Kim, 2016). Nevertheless, the interplay between hypothalamic nuclei and specific neurons involved in insulin secretion are yet to be elucidated.
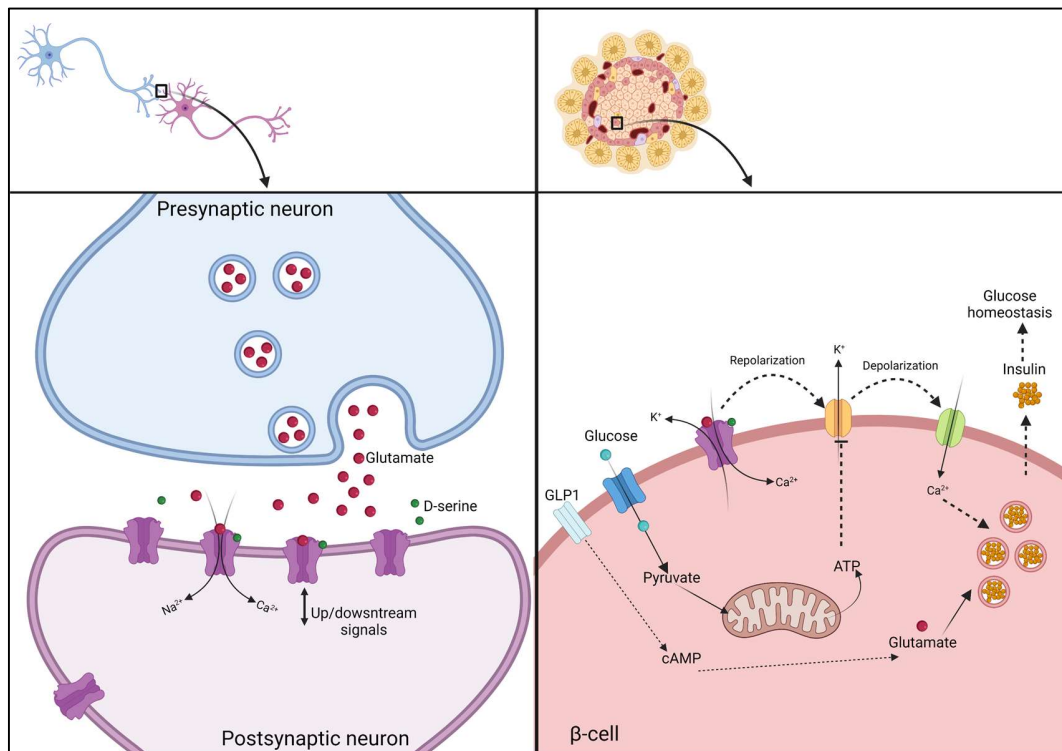
Figure 6. NMDARs in neurons and β-cells. Adapted from Lau & Zukin, 2007 and Wollheim & Maechler, 2015. Created with Biorender.com.

1.5.4.1. D-serine and NMDAR

D-serine is the enantiomer of L-serine and co-agonist of the NMDAR. As described before in this thesis, D-serine can be converted from L-serine through SRR action, which is present in the pancreas and brain. NMDARs are an ionotropic glutamate receptors found in the CNS and β-cells of pancreatic islets (**Figure 6**). They are heterotetrameric cation channels consisting of a combination of GluN1, GluN2 and GluN3 subunits. Furthermore, two of their subunits are GluN1, which are encoded by the Grin1 gene, and constitute the co-agonist binding site or GMS (Hansen *et al.*, 2017; Zhang *et al.*, 2022). NMDARs are clustered in post-synaptic densities, in postsynaptic neurons, and they are crucial for synapse enlargement and stabilization (structural plasticity) as well as long-term potentiation (LTP) and long–term depression (LTD) (functional plasticity, involved in learning and memory) (Lau and Zukin, 2007; Pérez-Otaño, Larsen and Wesseling, 2016; Kono *et al.*, 2019).

Because NMDAR-dependent neurotransmission has fundamental functions in the brain, alterations in these receptors can lead to the development of neurological diseases such as

epilepsy, intellectual disability, ASD, schizophrenia, AD (Lau and Zukin, 2007; Zhang *et al.*, 2022), anxiety disorders and post-traumatic stress disorder (Wolosker and Balu, 2020). Interestingly, a group of patients in a study showing eating disorders, epilepsy, schizophrenia, depression and AD (Thakur, Tyagi and Shekhar, 2019; Wimberley *et al.*, 2022) were also diabetic. Moreover, another study with diabetic patients showed that they were prone to develop depression and AD (Nouwen *et al.*, 2010; Athanasaki *et al.*, 2022). These findings suggest that there are strong associations between these neurological diseases and diabetes. Nevertheless, further research is necessary to discern which are the common mechanisms and how they are involved.

Several factors may determine the link between T2D and neurological diseases. Pancreatic β-cells and neurons possess common features such as glutamate signaling. Glutamate signaling is essential for both neurotransmission as well as vesicular glutamate transporters, amino acid transports and NMDAR function in β-cells (Scholz, Welters and Lammert, 2017). The brain requires high levels of glucose to meet its physiological functions. Therefore, pancreas impairments leading to alterations in glucose homeostasis (hypoglycemia and hyperglycemia) will alter brain functions and so, can evolve into neurological disorders. Indeed, alterations in hypothalamic circuits to sense glucose and insulin levels are involved in the development of T2D and obesity (Scholz, Welters and Lammert, 2017; Thakur, Tyagi and Shekhar, 2019). Another similarity is the presence of NMDARs in both pancreatic β-cells and neurons. Then, studying NMDAR might elucidate the crosstalk between T2D and neurological diseases and a potential target for diabetes treatment.

Indeed, pharmacological treatments based on the inhibition of NMDARs have been long used in depression, AD-related dementia, schizophrenia (Olivares *et al.*, 2012; Adell, 2020), and cerebrovascular diseases (Takahashi *et al.*, 2015). Currently, some NMDAR inhibitors, such as dextromethorphan, have been proposed as an alternative in T2D treatment (Welters *et al.*, 2017; Šterk *et al.*, 2021). In mice, glutamate activation of NMDARs resulted in reduced insulin sensitivity and lipid accumulation upon chow diet (CD); whereas NMDAR blockade with memantine (used as symptomatic therapy in AD) prevented HFD-induced obesity, insulin resistance and hepatic steatosis and promotes glucose tolerance on HFD. Thus, suggesting the NMDAR as a potential target in metabolic syndrome, obesity and T2D treatment (Huang *et al.*, 2021). Furthermore, a study by Suwandhi *et al.* found that chronic NMDARs activation by D-serine supplementation in mice led to hyperglycemia due to insulin secretion impairment; whereas insulin secretion was not affected by direct D-serine supplementation in pancreatic islets. However, increased insulin secretion and improved glucose levels were observed by treating the D-serine-supplemented

mice with an α-adrenergic receptor inhibitor (BRL 44408). Moreover, D-serine was found in the brain 3 h after of oral gavage and neuronal activity within the different hypothalamic nuclei was decreased. These results suggest that D-serine activation of hypothalamic NMDARs regulates insulin secretion in the pancreas via the sympathetic nervous system (Suwandhi *et al.*, 2018).

Taken together, studying NMDAR role in the brain could shed a light on the mechanisms involved in insulin secretion regulation and glucose homeostasis.

2. Aim of the work

Considering the exponential increase in obesity and T2D prevalence worldwide, especially in young adults and children, finding new strategies to tackle obesity and its co-morbidities is of utmost importance. In this regard, dietary supplements such as amino acids might help to intervene metabolically the pathophysiological pathways underlying these diseases. Besides being fundamental in some metabolic reactions involving from cell growth and proliferation to the synthesis of proteins, serine supplementation has shown beneficial effects on food intake as well as on insulin secretion and pancreatic beta cell function in animal models (Zhou, He, Zuo, Zhang, Wan, Long, *et al.*, 2018). Moreover, in humans, serine has been associated with improved insulin secretion and sensitivity, better glucose tolerance (Vangipurapu *et al.*, 2019) and inversely correlated to obesity risk (Okekunle *et al.*, 2019) and T2D (Gunther *et al.*, 2020). Therefore, **the first aim of this work was to elucidate the whole-body metabolic effects of L-serine supplementation in wild-type mice**. D-serine is the enantiomer of L-serine, converted by SRR action and characterized by its completely different role: NMDAR co-agonist. Moreover, chronic D-serine supplementation altered glycemia in mice potentially as result of insulin secretion modulation through the sympathetic stimulation of the hypothalamus (Suwandhi *et al.*, 2018). Based on these findings, **the second aim of this work was to study the potential role of NMDARs in the regulation of insulin secretion as well as whole-body metabolism by specific knockout in the PVN of the hypothalamus of GRIN1$^{flox/flox}$ mice**.

3. Materials and methods

3.1. *In vivo* experiments

3.1.1. Animals and housing conditions

C57BL/6N-Rj male mice aged seven weeks old were purchased from Janvier for the L-serine supplementation study and GRIN1$^{flox/flox}$ mice were obtained from The Jackson Laboratory for the study of PVN-NMDAR role in the insulin secretion. All mice were kept under a cycle of 12 h light and 12 h dark at a temperature of 22°C and fed with either a regular CD (Altromin 1314) or a HFD (Research Diets D12331). For L-serine supplementation study, C57BL/6N-Rj male mice were provided with sterile water or sterile water supplemented with L-serine (Sigma-Aldrich) *ad libitum* for eight or 16 weeks. For the study of PVN-NMDAR role in the insulin secretion, GRIN1$^{flox/flox}$ mice were mated in order to obtain as many male mice as needed to perform the experiments. Animal experiments were performed according to the German animal welfare law, guidelines and regulations of the district of Upper Bavaria (Munich, Germany), protocol number ROB-55.2-2532.Vet_02-16-52 and ROB-55.2-2532.Vet_02-18-63.

3.1.2. Genotyping Grin1$^{flox/flox}$ mice

Ear tags were obtained from GRIN1$^{flox/flox}$ mice at the moment of weaning at three-four weeks of age. To obtain the DNA samples ear tags were boiled with 100µl 50 mM NaOH at 95°C with shaking (1000 rpm) (Thermomixer, Eppendorf) for 30 min. Then, 10 µl 1M Tris pH=8 was added to the mixture to stop the reaction. Samples were cooled down or stored at 4°C before proceeding. For the PCR reaction (**Table 4**), 0.5 µl of DNA samples were used together with a 9.5 µl master mix of platinum green master mix and Grin1 master primer premix.

Grin1 primer premix was obtained by diluting 1:45 the following primers in RNAse-free water:
Grin1 fwd: GTGCTGGGATCCACATTCAT
Grin1 rev: AAACAGGGCTCAGTGGGTAA

PCR samples were loaded in a 2% Agarose (Sigma-Aldrich) gel in TAE (2 M Tris, 1 M glacial acetic acid, 0.5 M EDTA) buffer with PeqGREEN DNA dye (7.5µl / TAE ml). Flox bands were expected at 350 bp.

3.1.3. Stereotaxic injections with AAV vectors in Grin1[flox/flox] mice (Collaboration)

All the adenoviral injections were performed by Tim Gruber, Elena García-Clavé and Cristina García-Cáceres (Institute for Diabetes and Obesity, Helmholtz Zentrum München German Research Center for Environmental Health (GmbH), 85764 Neuherberg, Germany).

In order to ablate the NMDARs in the PVN of Grin1[flox/flox] mice, and adeno-associated virus (AAV) carrying the Cre recombinase (AAV2/1-EF1a-EGFP-T2A-iCre, Vector Biolabs, Cat. No VB2069) or GFP as control (AAV2/1-EF1a-EGFP) were bilaterally injected (0.5 µl/hemisphere; 1x10^13 viral genomes/nl) using a motorized stereotaxic system (Neurostar, Tubingen, Germany) combined with a binocular 3.5x-90x stereomicroscope (AMScope, USA) and a glass micropipette (Drummond) at a flow rate of 250nl/min. To target the PVN, we used the following stereotaxic coordinates: posterior -0,7mm and +/- 0,25mm to bregma, and -4,7mm ventral from the dura. Surgeries were performed using a mixture of ketamine and xylazine (100 and 7 mg/kg, respectively) as anesthetic agents and metamizol (200 mg/kg, subcutaneous), followed by meloxicam (1 mg/kg, on three consecutive days, subcutaneous) for postoperative analgesia.

3.1.4. Metabolic phenotyping

Body weight and blood glucose (FreeStyle Freedom lite, Abbott) were measured weekly in C57BL/6N-Rj and GRIN1[flox/flox] mice.

3.1.5. Body composition

Body composition of mice was measured at the beginning, middle and end of the experiments by non-invasive nuclear magnetic resonance (EchoMRI).

3.1.6. Glucose tolerance test (GTT), Glucose-stimulated insulin tolerance test (GSIS) and Pyruvate tolerance test (PTT)

Glucose tolerance tests (GTT) was carried out after 4 h fasting. Fasting glucose levels (0 min) were measured in all experiments prior to injection with a glucometer (FreeStyle Freedom lite, Abbott). Mice were intraperitoneally (i.p.) injected with a 2g/kg glucose solution (Braun). Then, glucose levels were measured from the blood collected from the tail tip of the mice at 0, 15, 30, 60, 90 and 120 min after the injection. GSIS was performed after 4 h fasting. Then, glucose levels were measured from the tail tip (0, 2, 5, 10 and 15) and blood samples collected (0, 2, 5, 10 and 15). After collection, blood samples were centrifuged (10 min, 10000 xg at 4°C) and serum insulin concentration was determined with an insulin ELISA kit (CrystalChem). Pyruvate tolerance test

(PTT) was conducted after overnight fasting (16 h). Mice were i.p. injected with 2g/kg sodium pyruvate solution and glucose concentrations were measured at 0, 15, 30, 60, 90 and 120 min.

3.1.6.1.1. GSIS after two weeks 0.1% D-serine challenge

GSIS (as described in 3.1.6) was carried out after two weeks of supplementing with 0.1% D-serine (Sigma-Aldrich) in the drinking water of AAV-injected mice. This experiment was performed in a cross over design, so each mouse was its own control.

3.1.7. Indirect calorimetry measurement

Mice were singled-housed in metabolic cages assigned randomly in the different cabinets of the indirect calorimetry system (TSE Phenomaster). After one day of acclimatization, energy expenditure (EE), respiratory exchange ratio (RER), locomotor activity and food and water intake were measured. The health status of the mice was monitored daily.

3.1.7.1. Overnight fasting

While mice were in the system, food hopers were removed from each cage and added again after 16 h overnight fasting.

3.1.7.2. Cold exposure and thermoneutrality

While the mice were in the system, the temperature of the cabinets was decreased to 4°C for 4 h or increased to 30°C for 24 h.

3.1.8. Food preference test

Grin1$^{flox/flox}$ mice were single-housed and starved for 16 h. Afterwards, mice were exposed to known amounts of CD and HFD for 3 h. Then, mice were transferred to their original cages and leftover food was weighed to calculate the amount of each diet consumed per mouse.

3.1.9. Sacrifice and organ withdrawal

For the L-serine supplementation study, at the end of the experiment, mice were euthanized with an anesthesia overdose of ketamine/xylazine (400 µl ketamine, 150 µl xylazine in 2 ml of 0.9% NaCl). Subsequently, blood samples were collected and processed to obtain blood serum (4000 rpm, 15 min); tissues were either frozen on dry ice and stored at -80°C or processed for histology (see chapter 3.5). For the study of PVN-NMDAR role in the insulin secretion, blood was previously collected from the tip tail of GRIN1$^{flox/flox}$ mice. Then, they were either sacrificed with CO_2 or

anesthesia overdose and perfused transcardially with a peristaltic pump, first with cooled PBS (1.37 M NaCl, 27 mM KCl, 100 mM NaHPO$_4$, 18 mM KH$_2$PO$_4$, pH=7.4) and then, with 4% PFA/PBS. Serum was obtained from the blood collected after 10 min centrifugation at 10000 xg for 10 min. In some experiments, after perfusion with PBS, organs were withdrawn and treated as described above. After perfusion, brains were carefully kept in 4%PFA overnight and, then, transferred to a 30% sucrose/TBS (1.21g Tris, 8.5g NaCl in 1 l deionized water) solution.

3.2. *Ex vivo* experiments

3.2.1. Lipolysis assay

Perigonadal fat pads from wild-type mice were obtained after sacrifice by cervical dislocation. Tissues were cut into small pieces (3-5 mg) and pre-equilibrated with pre-warmed Dulbecco's Modified Eagle Medium (DMEM) (Life Technologies, Thermo Fisher Scientific) at 37°C, 5% CO$_2$ for 30 min in a 96-well plate. Subsequently, tissues were incubated with either 200 μM L-serine, 400 μM L-serine with or without 1 μM isoproterenol (Sigma-Aldrich) or with 1 μM isoproterenol alone in DMEM at 37°C, 5% CO$_2$ for 3 h. After the incubation, the media was used for glycerol quantification with glycerol colorimetric assay kit (Biovision) and the tissues were delipidated with a 2:1 chloroform/methanol solution at 37°C. Delipidated tissues were transferred to a 0.3 N NaOH/0.1%SDS solution and kept at 40°C overnight with shaking at 600 rpm. The solutions obtained were used to determinate the protein concentration with a BCA protein kit assay (Thermo Fisher Scientific). Lipolysis was calculated based on the glycerol content in the assay media normalized by the protein content of the tissues.

3.2.2. Brain slices preparation and electrophysiological recordings (Collaboration)

All the electrophysiology experiments were performed by Cahuê Murat and Cristina García-Cáceres (Institute for Diabetes and Obesity, Helmholtz Zentrum München German Research Center for Environmental Health (GmbH), 85764 Neuherberg, Germany).

Two weeks after adenoviral injection, GRIN1[flox/flox] mice were sacrificed by cervical dislocation. Brain was quickly ablated and placed in ice-cold artificial cerebrospinal fluid (aCSF) modified for slicing, containing (in mM): 87 NaCl, 2.69 KCl, 1.25 NaH$_2$PO$_4$, 26 NaHCO$_3$, 7 MgCl$_2$, 0.2 CaCl$_2$, 25 D-glucose, and 75 sucrose (330 mOsm/Kg H2O, pH 7.4 bubbled with a carbogen mixture of 95% O2 and 5% CO2). The specimen was glued to a sectioning stage and submerged in ice-cold slicing aCSF in a vibratome chamber (7000 smz-2; Campden Instruments). Coronal brain slices (250 μm) containing the paraventricular nucleus of the hypothalamus were sectioned and

incubated at 32-33º for 30 min in aCSF, containing (in mM): 124 NaCl, 2.69 KCl, 1.25 NaH_2PO_4, 26 $NaHCO_3$, 1.2 $MgCl_2$, 2 $CaCl_2$, 2.5 D-glucose, and 7.5 sucrose (298 mOsm/Kg $H2O$, pH 7.35 constantly bubbled with carbogen mixture). After this step, the slices were kept under the same conditions but at room temperature for at least 40 min until electrophysiological recordings.

Single brain slices were transferred to a chamber mounted on a stage of an upright microscope (SliceScope; Scientifica) coupled with a video camera (optiMOS sCMOS; QImaging) and continuously perfused with Mg_2+-free aCSF in order to optimize NMDAR activation, containing (in mM): 124 NaCl, 2.69 KCl, 1.25 NaH2PO4, 26 $NaHCO_3$, 4 $CaCl_2$, 2.5 D-glucose, 7.5 sucrose, and 10 µM glycine (298 mOsm/Kg $H2O$, pH 7.35 constantly bubbled with a carbogen mixture of 95% O2 and 5% CO2) in the presence of 6-Cyano-7-nitroquinoxaline-2,3-dione (CNQX; 20 µM) and picrotoxin (100 µM), at a rate of ~2 mL/min by a gravity-driven perfusion system. Neurons were visualized under infrared differential interference contrast (IR-DIC) optics with a 40x immersion objective using the µManager 1.4 software (Edelstein *et al.*, 2010). Accordingly, GFP+ neurons were identified by blue (λ = 488 nm) light illumination. Patching pipettes were made with thick-walled borosilicate glass (GC150TF-10; Harvard Apparatus) pulled using a horizontal puller (P-1000; Sutter Instruments) and filled with an internal solution, containing (in mM): 128 K-gluconate, 8 KCl, 10 HEPES, 0.5 EGTA, 4 Mg-ATP, 0.3 Na-GTP, and 10 Na-phosphocreatine (295 mOsm/Kg H_2O, pH 7.3), resulting in a pipette tip resistance between 4 and 7 MΩ. Whole-cell recordings were performed with an EPC 10 USB Double patch-clamp amplifier (HEKA Elektronik) in voltage-clamp mode. Signals were acquired at 20 kHz and low-pass filtered at 5 kHz (Bessel) using the PatchMaster 2x90.2 software (HEKA Elektronik). To check NMDAR activation, neurons were held at -70 mV and the holding current was monitored in response to bath-applied NMDA (25 µM). Data were visualized and analyzed using custom-written codes in MATLAB (MathWorks).

3.3. *In vitro* experiments

3.3.1. Primary brown adipocyte culture

3.3.1.1. Isolation and maintenance of primary brown adipocytes

Brown preadipocytes were obtained from the stromal vascular fraction (SVF) of five-six week-old wild-type mice BAT. Tissues were minced with scissors and introduced in 15 ml tubes (2 mice per tube) containing 10ml of digestion media (DMEM, 1% BSA, 1mg/ml collagenase IV) and digested at 37°C with shaking (1000 rpm) for 45 min. Cell suspension was filter through 100 µM strainer in order to remove undigested tissue. Cells were centrifuged at room temperature at 500 xg for 5

min. Then, cells were re-suspended with pre-warmed growth media (37°C; DMEM, 10% fetal bovine serum (FBS), 1% penicillin/streptomycin and 100 µg/ml normocin). After a second centrifugation, cells were again re-suspended in 5 ml growth media. Preadipocytes were grown in 6-well plates and re-plate either in 6-well plate or 24-well regular/Seahorse plates (Agilent technologies). Cell culture medium was changed every other day.

3.3.1.2. Differentiation of primary brown adipocytes

At confluence, differentiation was induced in preadipocytes for two days with induction media (DMEM, 10% FBS, 0.5 mM 3-Isobutyl-1-methylxanthine (IBMX), 5 µM dexamethasone, 125 µM indomethacin, 100 nM human insulin and 1 nM 3,3',5'-Triiodo-L-thyronine (T3)). Then, cells were maintained with differentiation media (growth media with 100 nM human insulin and 1nM T3) until the day of the experiment.

3.3.2. L-serine stimulation in primary brown adipocytes

Preadipocytes were differentiated in 6-well plates. At differentiation day eight, brown adipocytes were stimulated with 400 µM L-serine for 0, 10, 60 and 120 min using differentiation media. Next, protein was isolated from the 6-well plate by adding RIPA buffer (50 mM Tris pH 7.4, 150mM NaCl, 1mM EDTA, 1% Triton-X) with 1% protease inhibitor, 1% phosphatase inhibitor cocktail II, 1% phosphatase cocktail III and 0.1% SDS; scraping the cells from the wells and collecting all the volume in tubes. Then, cells were lysed using a syringe and let stand on wet ice for 10 min. Tubes were centrifuged for 10 min at 14000 rpm at 4°C. Supernatant was collected in new tubes and protein concentration was measured with BCA protein assay kit (Thermo Fisher Scientific).

3.3.3. Cellular respiration experiments (Seahorse)

Primary brown preadipocytes were seeded and differentiated in the 24-well Seahorse plate for seven days. On day seven, brown adipocytes were pre-incubated with or without 200 or 400 µM L-serine in DMEM with 0.2% BSA fatty acid-free (Sigma Aldrich), 2.8 mM glucose and 0.8 mM sodium pyruvate for 3 h. Prior to measurement, brown adipocytes were treated with or without 200 or 400 µM L-serine in XF Assay Medium-Modified DMEM 0.2% BSA fatty acid-free, 2.8 mM glucose and 0.8 mM sodium pyruvate. Assay ports were loaded with: (A) assay media, 2 or 4 mM L-serine, 10 µM isoproterenol or 4 mM L-serine and 10µM isoproterenol, (B) 20 µg/mL oligomycin (Merck), (C) 20 µM carbonyl cyanide-p-trifluoromethoxyphenylhydrazone (FCCP) (R&D systems) (D) 25 µM rotenone; 25 µM antimycin A (Sigma Aldrich) and 1 M 2-deoxy-D-glucose (Alfa Aesar). Compounds for the injections were prepared either in Krebs buffer or assay media. Oxygen

consumption rates (OCR) were measured with the Seahorse XF24 Analyser (Seahorse Bioscience-Agilent). Each cycle consisted of 2 min mixing, 2 min waiting and 2 min measuring.

3.4. Metabolic parameters measurement

3.4.1. Liver glycogen and triglycerides measurement

Glycogen and triglyceride (TG) levels in liver were measured with Glycogen colorimetric/fluorimetric assay kit (Biovision) and Triglyceride Quantification colorimetric/fluorimetric kit (Biovision), respectively.

3.4.2. Liver metabolomics (Collaboration)

All liver metabolites experiments were conducted by Silke Heinzmann (Research Unit Analytical BioGeoChemistry, Department of Environmental Sciences, Helmholtz Center Munich 85764 Neuherberg, Germany). Liver samples were obtained with a two-phase extraction procedure including water and chloroform. 50 mg liver powder were added to 600 µl of a methanol/water mix (1:1) and homogenized in Precellys 3 x 20 sec at 5800 rpm at -10 °C. Afterwards, 300 µl methyl tert-butyl ether (MTBE) were added and thoroughly vortexed for 2 min to wash out lipids from the homogenate. After centrifugation at 13000 rpm for 10 min, the upper organic phase was transferred to a tube and the procedure repeated (300 µl methanol, 300 µl H_2O and 300 µl MTBE). The upper phase was merged to the previous supernatant and the lower aqueous phase was transferred into a separate tube. The aqueous phase extract was added to the SpeedVac for solvent evaporation, reconstituted in D_2O buffer (PO_4-buffered pH=7.4, TSP (0.1 % trimethylsilyl-tetradeuteropropionic acid) as internal standard for chemical shift correction) and submitted to nuclear magnetic resonance (NMR) spectroscopy analysis for an overview of hydrophilic metabolites. All aqueous extract (AE) samples were manually phased, baseline-corrected and calibrated to internal standard TSP. Then imported to MATLAB (MathWorks), where the water residual peak was cut out and all peaks aligned (RSPA algorithm) and spectra normalized using probabilistic quotient normalization to account for minor variation in liver net weight and extraction efficiency.

3.5. Histology

Tissues were fixed in 4% PFA/PBS overnight. Then, they were transferred into 70% ethanol (Merck Millipore) and stored at 4°C.

3.5.1. Paraffin embedding and tissue sectioning

Tissues stored with 70% ethanol were dehydrated consecutively with 80%, 90% and twice 100% ethanol for 1 h at room temperature. Afterwards, tissues were cleared with xylol for 10 min at room temperature for three times. Subsequently, they were transferred to pre-warmed paraffin for 1 h at 65 °C twice. Then, in the third paraffin step, tissues were incubated overnight. Tissues were embedded with paraffin and, later, sectioned with a microtome (HM390E, Thermo Fisher Scientific). Sections were 2µM thick and mounted on microscope slides.

3.5.1.1. Haematoxylin and Eosin (H&E) staining

Tissue sections were deparaffinised by submerging them in xylol for 5 min two times. Then, they were rehydrated in consecutive ethanol solutions: 100% (twice), 90% and 70% ethanol for 5 min; and submerged in deionized water for 2 min. Afterwards, tissue sections were stained with haematoxylin (Mayer's solution) for 1 min, then submerged for 10 s in deionized water and kept in running tap water for 2 min. Subsequently, tissue sections were incubated in 96% ethanol for 2 min, in 100% ethanol for 2 min and, after, in eosin (chromotrope II R: 100 mg chromotrope II R, 100 ml 100 % ethanol, 100 µl acetic acid and filtered) for 3 min. Steps in 96% ethanol and 100% ethanol were repeated. Finally, tissue sections were submerged in xylol for 2 min twice and, immediately after, mounted with Rotti-Histokitt™ (Carl Roth) and the cover glass. Then, dried at room temperature. Images were taken with a Zeiss Scope A1 (Carl Zeiss).

3.5.1.2. Adipocyte size measurements (Collaboration)

All the adipocyte size measurements were performed by Andreas Israel and Siegfried Ussar (Institute for Diabetes and Obesity, Helmholtz Zentrum München German Research Center for Environmental Health (GmbH), 85764 Neuherberg, Germany). Adipocyte size was measured using three pictures taken per adipose tissue from each mouse, using Adiposoft plugin for ImageJ version 1.52v. Outliers were removed using ROUT (Q = 1%) in GraphPad Prism 8 version 8.4.3 (GraphPad software).

3.5.2. Brain sectioning

Brains soaked in 30% sucrose/TBS were frozen at -20 °C in the cryostat (CM3050S, Leica). Brains were sectioned in coronal slices of 30-40 µM. Brain sections containing the PVN were preserved in TBS and the remaining brain slices were kept in cryoprotectant (300g sucrose, 300ml glycerol, 300 ml ethylene glycol, 0.5 g sodium azide in 1l deionized water) at -20 °C.

3.5.2.1. Brain immunostaining

Brain slices were washed with TBS three times for 5 min. Then, they were blocked with SUMI (0.25% gelatin and 0.5% Triton-X in TBS) for 1 h. Next, brain slices were incubated overnight with the primary antibody, shaking, at 4°C. After primary antibody (**Table 7**) incubation, brain slices were washed with TBS three times with TBS for 10 min. Then, they were incubated with the secondary antibody (**Table 7**) diluted in SUMI (1:1000) for 2 h. Brain slices were incubated with DAPI in TBS (1:5000) for 10 min and washed with TBS three times for 10 min. Sections were mounted on microscope slides, dried in the dark and, then, covered with a coverglass with 100 - 150 µl of mowiol-based mounting solution containing the anti-fading agent DABCO (elvanol). Images were acquired using a confocal microscope (Leica TCS SP8, Germany) and LAS X software (version 3.5.7.23225).

3.5.2.2. *In situ* hybridization

Brains were obtained from mice transcardially perfused with PBS (Gibco) and 4% PFA prepared in PBS (Gibco). After overnight incubation with 4%PFA/PBS, brains were subsequently immersed overnight in 10, 20 and 30% sucrose prepared in PBS (Gibco). Next, they were frozen and sectioned as in 3.5.2. *In situ* hybridization was performed with RNAscope® Target Retrieval kit (ACD). Brain sections were washed with PBS (Gibco) in the Tissue-Tek® slide rack for 5 min. Then, brain sections were baked in the HybEZ™ II (ACD) oven for 30 min at 60 °C and fixed with pre-chilled 4%PFA in PBS (Gibco) for 15 min. Brain sections were dehydrated with consecutive ethanol solutions in sterile deionized water (with 10% reagent retriever (ACD)) 50, 70 and 100%(twice) for 5 min at room temperature and air-dried for 5 min. Brain sections in the slide rack were submerged into 1x boiling Target Retrieval solution (ACD) for 5 min. Immediately after, they were transferred to sterile distilled water for 10s, rinsed with 100% ethanol and air dried. Create a barrier around the brain sections with ImmEdge™ hydrophobic barrier pen and let it dry overnight at room temperature. Next day, few drops of Protease II (ACD) were added onto each section. Then, brain sections were incubated for 30 min at 40 °C and subsequently washed with sterile distilled water, shaking, for 2 min. After removing excess liquid, few drops of Grin1 probe (1:50) (ACD), positive and negative controls were added onto the brain sections. Brain sections were incubated for 2 h at 4°C and then washed for 2 min. Incubation and washing steps were repeated for hybridization probes Amp1-Fl, Amp2-Fl, Amp 4-Fl. To continue immunostaining for GFP, sections were blocked with 10% goat serum in TBS-T for 1 h and then incubated with primary antibody (**Table 7**) overnight at 4°C, keeping them in a humid chamber. Next, remove primary and incubate with secondary antibody (**Table 7**) for 1 h at room temperature. Add few

drops of DAPI (from the kit) for 30 seconds and then mount the slides with cover slides with DAKO. Finally, slides were air dried overnight and stored at 4°C.

3.6. Gene and protein analysis

3.6.1. RNA isolation

Total RNA was isolated from tissues using RNAeasy Kit (Qiagen). Tissues were lysed with 1ml Qiazol lysis reagent (Qiagen) and magnetic beads in the Tissue Lyser II (Qiagen) for 2 min at 30 Hz twice and, then, centrifuged for 5 min at 10000 xg at 4°C. After 5 min incubation at room temperature, 200 ml chloroform were added to each tube, shaken for 15 s and incubated at room temperature. Next, tubes were centrifuged for 15 min at 12000 xg at 4°C and upper phase was transfer to a new tube. Then, the same volume of 70% ethanol was added to the tube and mixed thoroughly with the phase extracted in the previous step. The mixture was transferred to the RNeasy column. Next steps were performed according to the manufacturer's instructions. Total RNA concentration of each sample was measured with NanoDrop 2000 (Thermo Scientific).

3.6.2. cDNA synthesis

0.5 µg total RNA was used to transcribe to cDNA using the High-Capacity cDNA Reverse Transcription Kit (Applied Biosystems).

3.6.3. Real-time qPCR

Real time quantitative PCR was performed using 300 nM forward and reverse gene-specific primers (**Table 5**) and iTAq Universal SYBR Green Supermix (BioRad) in a CFX384 Touch (BioRad) thermocyler.

3.6.4. Tissue protein isolation

Tissues were lysed with 250 µl of lysis buffer (RIPA buffer +1% protease inhibitor, 1% phosphatase inhibitor cocktail II, 1% and phosphatase inhibitor cocktail III) and magnetic beads in the Tissue Lyser II (Qiagen) for 3 min 25 Hz. 0.1% SDS was added to the tubes, gently inverted to mix and incubated for 10 min on wet ice. Next, samples were centrifuged for 30 min at 15000 xg and 4°C. Supernatant was collected and protein concentration was measured with BCA protein assay kit (Thermo Fisher Scientific).

3.6.5. Western blot

Protein samples from tissues or cells were prepared with a volume containing 15-30 µg protein, 4x sample buffer and 2.5% β-mercaptoethanol or 5% DTT and, then, boiled for 5 min at 95 °C. After cool down, protein samples were loaded in a SDS gel and electrophoresis was performed in Mini PROTEAN® Tetra Cell (Bio-Rad) or Criterion™ Cell (Bio-Rad) with running buffer (3 g Tris, 14.4 g glycine in 1 l deionized water) with 0.1% SDS at constant 80-100V for 10 min and at constant 100-120V (PowerPac basic, Bio-Rad) until the end of the run.

SDS gel (**Table 6**) was blotted to a 0.45 µm polyvinylidene difluoride (PVFD) membrane in transfer buffer (running buffer with 20% methanol) in Mini Trans-Blott Cell (Bio-Rad) or Criterion™ Blotter (Bio-Rad) for 1.5 h at constant 0.35 A. Blotted membranes were rinsed with TBS-T (1 l TBS and 1 ml Tween 20) and blocked with 5% skim milk/TBS-T and shaking. Blocked membranes were incubated overnight with a primary antibody (**Table 7**) diluted in 5% BSA/TBS-T at 4 °C and shaking. After washing three times with TBS-T at room temperature, membranes were incubated for 2 h with the secondary antibody (**Table 7**) diluted in 5% milk/TBS-T at room temperature with shaking. Next, membranes were washed three times with TBS-T at room temperature, the membranes were incubated in 2 ml ECL solution for 1 min and target proteins were visualized and imaged in ChemiDoc MP (BioRad). Quantification of the protein bands was performed using ImageJ software (version 1.52v).

3.7. Statistics

All statistics were calculated using Graph Pad Prism 8 version 8.4.3 unless stated differently in the figure legend. Data are represented as a mean ± standard error of the mean (SEM). Statistical significance was determined by unpaired Student's t-test between two groups or, for multiple comparisons, using one or two-way ANOVA, followed by Tukey's or as stated in the figure legend. Differences reached statistical significance with $p < 0.05$. For liver metabolomics, data were analysed by unsupervised multivariate analysis (PCA) and supervised orthogonal partial least-squares discriminant analysis (OPLS-DA) analysis. Seahorse Data were obtained with Wave software version 2.6.1.53 (Agilent technologies) before Graph Pad analysis. A univariate general linear model was performed to study the effect of the diet and L-serine treatment on EE, adjusting for body weight in SPSS version 24 (SPPS). The mean difference was calculated for each paired comparison. ANCOVA was calculated using RStudio 2022.07.1+554 to study the effect of PVN-NMDAR knockout in EE at room temperature and during cold exposure.

4. Results

4.1. L-serine supplementation blunts body weight regain after overnight fasting in mice

4.1.1. L-serine supplementation alters liver metabolism and decreases body weight regain after consecutive overnight fasting

L-serine supplementation had no major effects on metabolism of random fed mice. Neither body weight, body composition, blood glucose levels, insulin levels nor glucose tolerance were affected after eight weeks of supplementation with L-serine. However, it seemed to alter metabolism of liver. Liver weight tended to decrease under HFD as well as glycogen levels in both CD and HFD. Moreover, expression of a key enzyme in gluconeogenesis, phosphoenolpyruvate carboxykinase (*Pepck*), was upregulated in CD-fed mice (López-Gonzales *et al.*, 2022). Based on these findings, we investigated whether L-serine supplementation could promote liver gluconeogenesis in mice. To do so, we performed a PTT at week one and at week six of the eight-week experiment. However, there was no increased glucose production in L-serine supplemented mice under CD or HFD (**Figure 7A**). Blood glucose levels after overnight fasting at week eight did not change between groups (**Figure 7B**). Insulin levels after overnight fasting at week eight did not change with L-serine supplementation, but increased in serum of HFD-fed mice (**Figure 7C**). Kidney, a major player in gluconeogenesis, did not show differences in tissue weight between groups (**Figure 7D**). To determine any important effects of L-serine in the liver, we analysed liver weight, histology and measured metabolic parameters as well as the expression of glucose metabolism-related genes. Liver weight did not change between diets, with or without L-serine supplementation (**Figure 7E**). Liver H&E staining showed fewer lipid droplets in CD-fed L-serine supplemented mice. However, in HFD, L-serine supplementation seemed to decrease the size but not the number of lipid droplets (**Figure 7F**). In line with these findings, we observed that L-serine supplementation significantly decreased TG levels and tended to increase glycogen content in CD-fed mice with no effects on HFD feeding (**Figure 7G and H)**. Regarding the expression of glucose metabolism-related genes in the liver, there were no differences between diets and L-serine supplemented groups in expression glucose-6-Phosphatase (*G6Pase*) and forkhead box protein 1 (*Foxo1*). Liver *Pepck* expression did not change with L-serine supplementation, but it was significantly downregulated in HFD-fed compared to CD-fed control mice. For the expression of glycogen metabolism-related genes in the liver, glycogen synthase-2 (*Gys-2*) and glycogen phosphorylase (*Pgyl*) did not show any differences between diets or L-serine supplemented groups (**Figure 7I**).
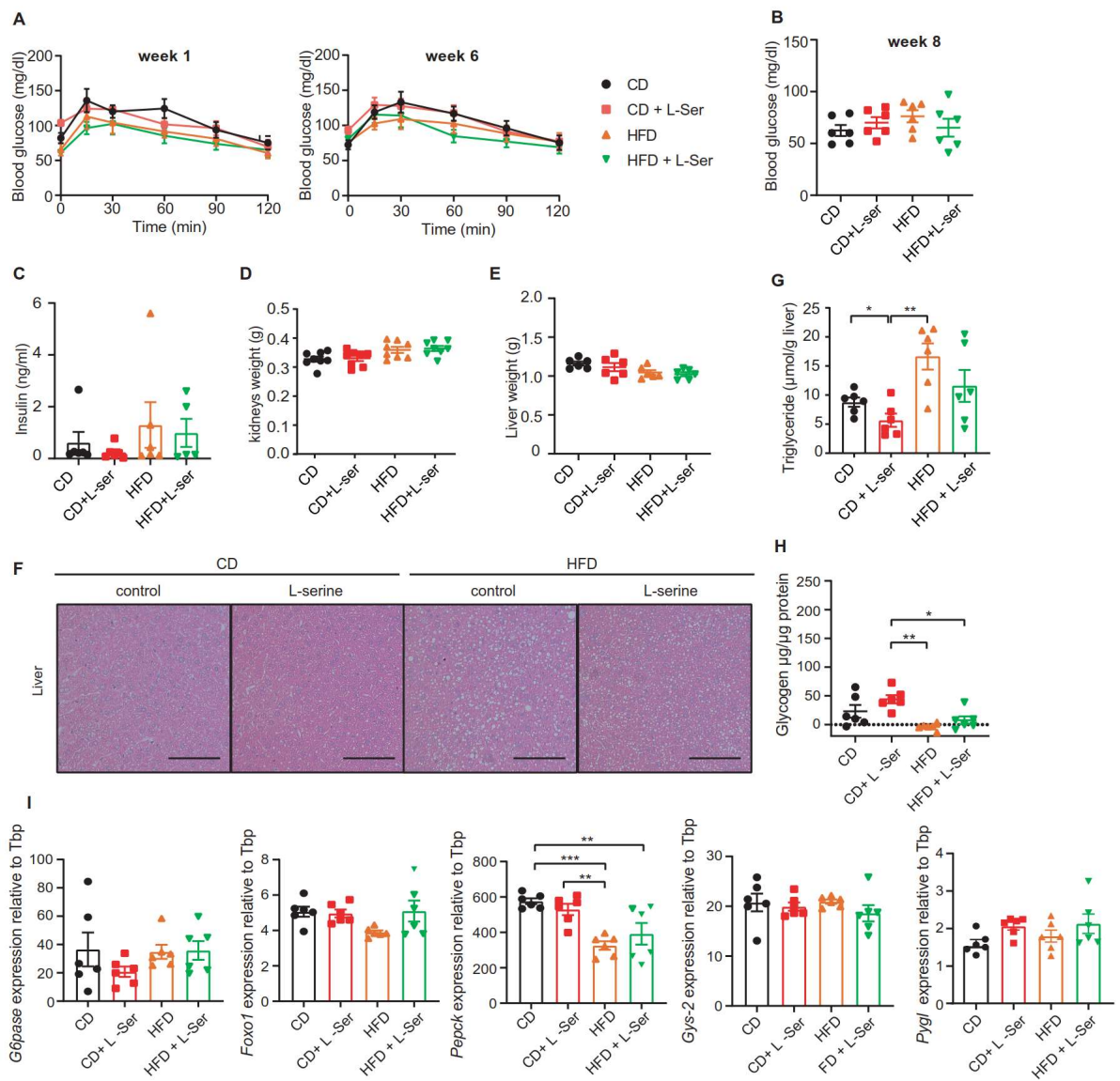
Figure 7. L-serine supplementation does not promote liver gluconeogenesis but alters liver metabolism after subsequent overnight fasting. (A) Pyruvate Tolerance test (PTT) after one and six weeks L-serine supplementation (n=6). **(B)** Blood glucose levels after L-serine supplementation and repeated overnight fasting at week eight (n=6). **(C)** Plasma insulin levels after L-serine supplementation and repeated overnight fasting at week eight (n=6). **(D)** Kidneys weight after L-serine supplementation and repeated overnight fasting at week eight (n=6). **(E)** Liver weight after L-serine supplementation and repeated overnight fasting at week eight (n=6). **(F)** Representative H&E stainings of liver after eight weeks of L-serine supplementation. Size bar represents 100 µM. **(G)** TG levels in liver after L-serine supplementation and repeated overnight fasting at week eight (n=6). **(H)** Glycogen levels in liver after L-serine supplementation and repeated overnight fasting at week eight (n=6). **(I)** Liver gene expression after L-serine supplementation and repeated overnight fasting at week eight (n=6). Data are shown as mean ± SEM, one or two-way ANOVA with Tukey's post-hoc test. * $p < 0.05$, ** $p < 0.01$, *** $p < 0.001$.

Interestingly, body weight and body composition were altered in these mice after being subjected to overnight fasting. We observed how body weight regain tended to decrease in CD and decreased in HFD-fed mice supplemented with L-serine (**Figure 8A**) due to a reduction in fat mass (**Figure 8B**). In line with these results, WAT weights in HFD-fed mice also decreased (**Figure 8C**). The histology of these tissues revealed no changes in CD with or without L-serine supplementation (**Figure 8D**). Under HFD, PGF displayed smaller adipocyte size with L-serine supplementation. However, SCF with L-serine supplementation did not show differences in adipocyte size compared to control (**Figure 8D**). We confirmed that the size of perigonadal adipocytes with L-serine supplementation decreased under HFD, but also decreased in subcutaneous adipocytes under CD and HFD (**Figure 8E**). In order to investigate whether L-serine supplementation triggered inflammation, we measured the gene expression of some inflammatory markers. In PGF, there were no changes in gene expression between groups for *IL-6*. However, *TNFα* and *CD68* were upregulated in HFD compared to CD. Moreover, L-serine supplementation downregulated *TNFα* expression under HFD feeding. No changes in gene expression of tumor necrosis factor *α* (*TNFα),* interleukin 6 (*IL-6)* or cluster of differentiation 68 (*CD68)* were observed in SCF (**Figure 8F**).
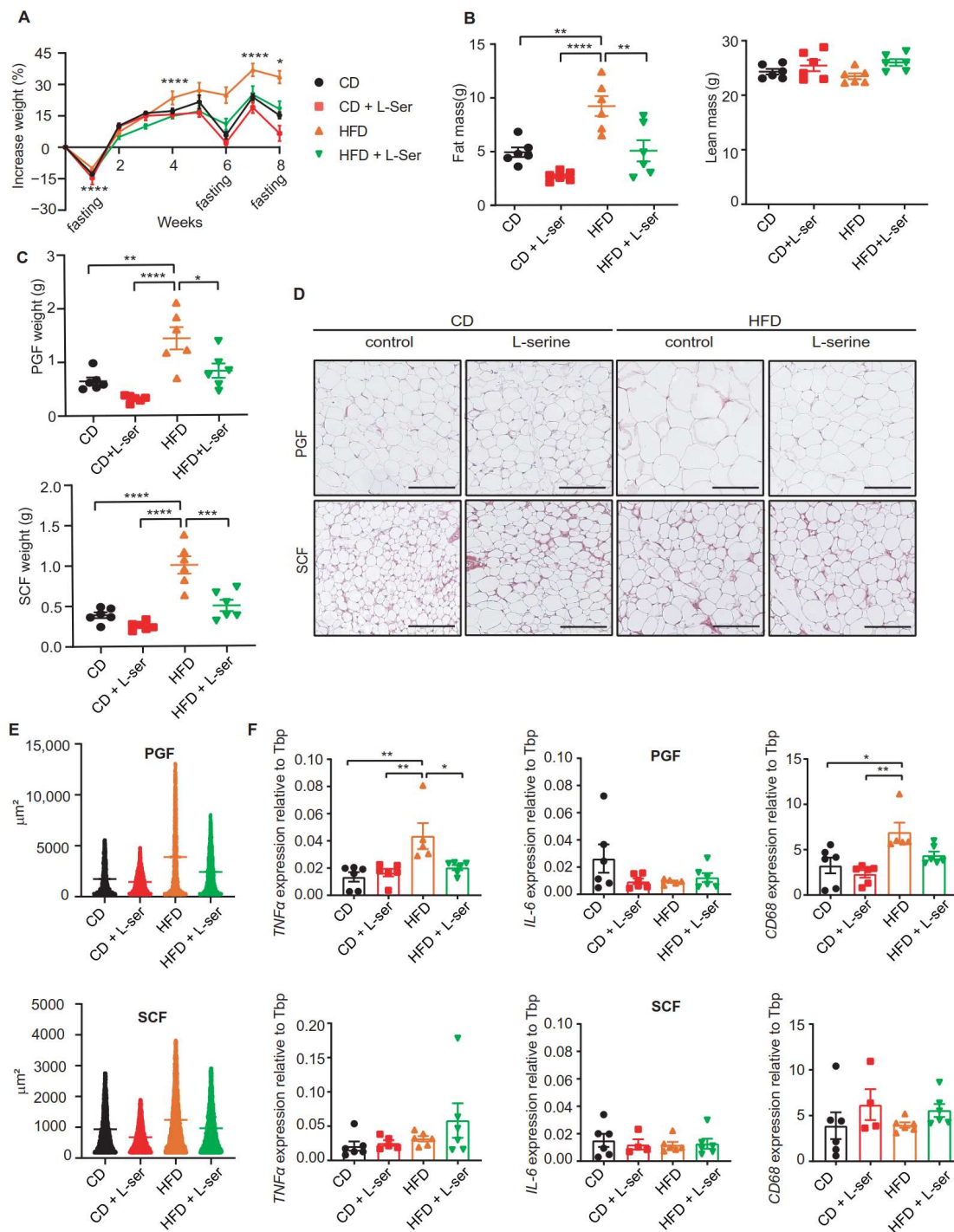
Figure 8. L-serine supplementation decrease body weight in HFD-fed mice due to a decrease in fat mass after subsequent overnight fasting. (A) Body weight increase (%) of mice with or without L-serine supplementation and repeated overnight fasting (n=6). **(B)** Body composition (fat and lean mass) of mice with or without L-serine supplementation and repeated overnight fasting at week eight (n=6). **(C)** Weights of perigonadal fat (PGF) and subcutaneous fat (SCF) after eight weeks L-serine supplementation and repeated overnight fasting (n=6). **(D)**

Representative H&E stainings of PGF and SCF after eight weeks of L-serine supplementation and repeated overnight fasting. Size bar represents 100 µM. **(E)** Adipocyte sizes of SCF and PGF after eight weeks L-serine supplementation and repeated overnight fasting (n=4 mice; >7000 adipocytes per group for PGF and >10000 adipocytes per group for SCF). **(F)** Gene expression of inflammatory markers in PGF and SCF after eight weeks of L-serine supplementation (CD, HFD, HFD+L-ser: n=6; CD+L-ser: n=4-5). Data are shown as mean ± SEM, one or two-way ANOVA with Tukey's post-hoc test. * $p < 0.05$, ** $p < 0.01$, *** $p < 0.001$, **** $p < 0.0001$.

4.1.2. Decrease in body weight regain is not the result of a decrease in lipogenesis or increase in lipolysis in WAT

The decrease in body weight regain was due to a reduction in fat mass (**Figure 8A and B**). Hence, we intended to discern the cause of the decrease in fat mass. With this aim, we measured the expression of genes involved in lipogenesis and the expression of lipolysis proteins in WAT. L-serine supplementation did not alter the expression of genes related to *de novo* lipogenesis (DNL) acetyl-CoA carboxylase (*Acaca*) and fatty acid synthase (*Fasn*) in PGF. Interestingly, the transcription factor sterol regulatory element-binding protein 1 (*Srebp1*) was downregulated in PGF of HFD-fed mice compared to CD-fed. However, its expression was upregulated L-serine-supplemented HFD-fed mice compared to their HFD control. For SCF, expression of *Acaca*, *Fasn* and *Srebp1* did not change between diets and with or without L-serine supplementation (**Figure 9A**). To assess lipolysis, we quantified hormone-sensitive lipase (HSL) phosphorylation at the activating sites Ser563 and Ser660, as well as the inhibitory Ser565 site in SCF and PGF following an overnight fasting. We observed increased Ser660 and lower Ser565 phosphorylation in HSL in the HFD compared to the CD-fed mice in PGF. However, we did not observe any differences between the L-serine-supplemented and control mice irrespective of the diet. In addition, L-serine supplementation led to a reduction in phosphorylation of Ser565 in the CD compared to the HFD in SCF (**Figure 9B**). Thus, these data did not suggest an increased lipolysis in WAT due to the interaction of fasting and L-serine supplementation. Because of the increasing lipolysis trend in PGF of HFD-fed mice supplemented with L-serine, we focused on PGF to study lipolysis *ex vivo*. We quantified free glycerol released in culture medium as a measure of lipolysis under 200 µM and 400 µM L-serine, 1 µM isoproterenol as positive control and 1 µM isoproterenol together with 400 µM L-serine. Any L-serine concentration in the media promoted lipolysis in PGF fat pads. Moreover, 400 µM L-serine did not potentiate isoproterenol-induced lipolytic effect (**Figure 9C**).
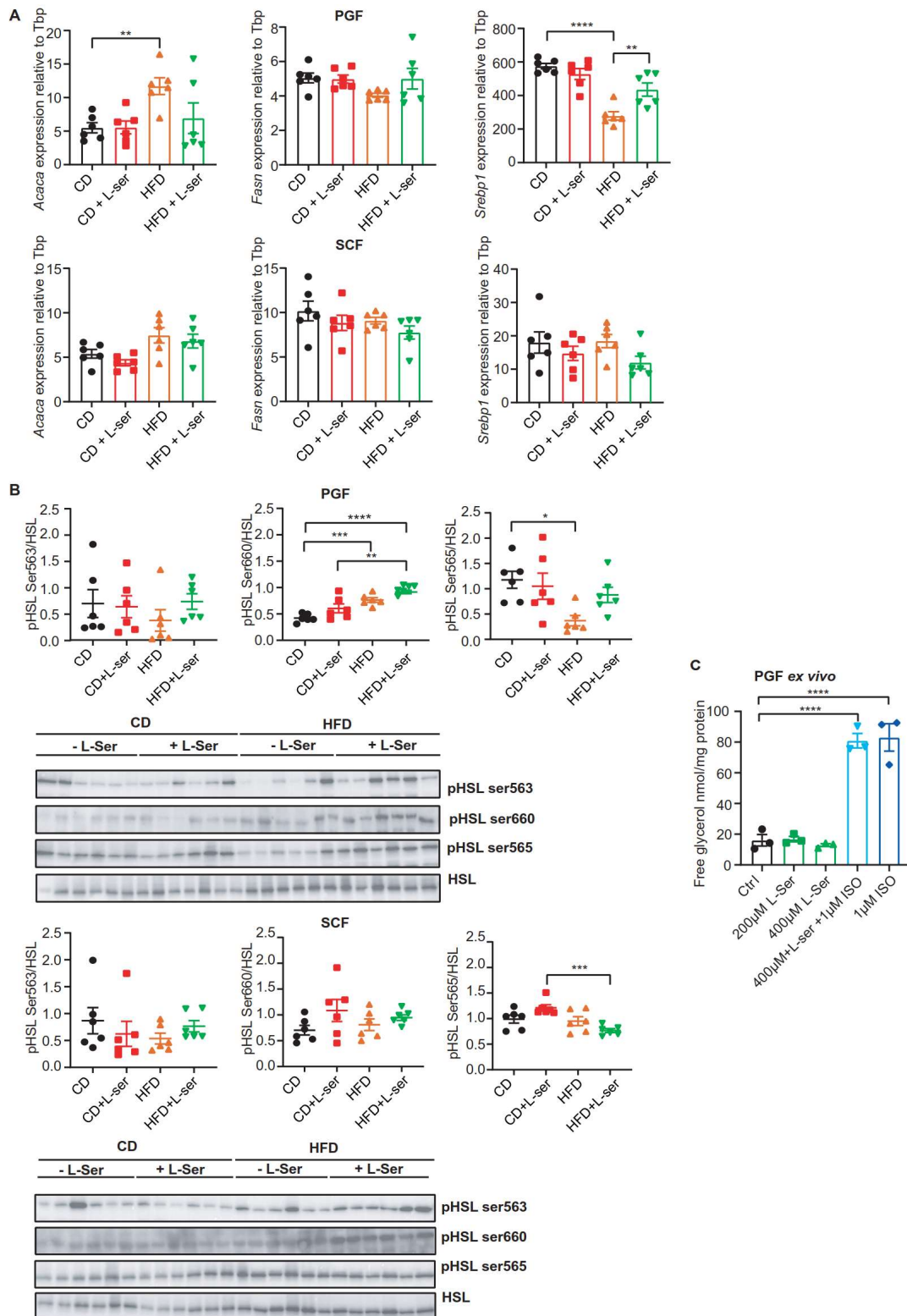
Figure 9. L-serine supplementation did not decrease fat mass as a result of a decreased lipogenesis or increased lipolysis in WAT. (A) Expression of lipogenesis-related genes in PGF and SCF of mice with or without L-

serine supplementation and repeated overnight fasting (n=6). **(B)** Western blots and quantifications for phosphorylated HSL (Ser563,Ser660, Ser565) and total HSL of PGF and SCF of mice with or without L-serine supplementation and repeated overnight fasting (n=6). **(C***)* Ex vivo* lipolysis assay of PGF with L-serine supplementation (n = 3). Data are shown as mean ± SEM, one-way ANOVA with Tukey's post-hoc test. * $p < 0.05$, ** $p < 0.01$, *** $p < 0.001$, **** $p < 0.0001$.

Regarding BAT, there was a significant decrease in weight in CD after L-serine supplementation, but there were no changes in HFD (**Figure 10A**). In line with the weight, BAT histology in CD displayed decreased lipid droplet size after L-serine supplementation. In HFD, BAT weight tended to decrease in BAT of some mice, but it was not significant (**Figure 10B**).
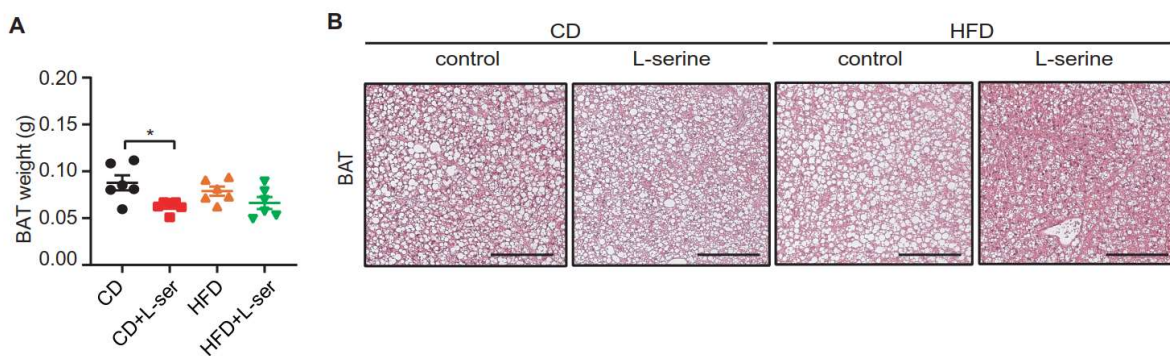
Figure 10. L-serine supplementation decreased BAT weight and lipid droplet size after repeated overnight fasting. (A) BAT weight after eight weeks L-serine supplementation and repeated overnight fasting (n=6) **(B)** Representative H&E stainings of BAT after eight weeks of L-serine supplementation and repeated overnight fasting. Size bar represents 100 µM. Data are shown as mean ± SEM, one-way ANOVA with Tukey's post-hoc test. * $p < 0.05$.

4.1.3. L-serine supplementation does not affect glucose tolerance, but alters liver metabolism in random fed and fasted mice

Those findings could still not elucidate the reduction in fat mass leading to a decrease in body weight regain after subsequent overnight fasting in L-serine-supplemented mice. Neither did they help us comprehend the alterations in liver metabolism under these conditions. In order to better understand these events, we reproduced our experiment in parallel with mice treated in the same conditions but *ad libitum*, with no overnight fasting. We intended to reproduce the decrease in body weight regain in fasted HFD-fed mice supplemented with L-serine, but also to investigate alterations in glucose tolerance, liver metabolism, metabolic parameters by indirect calorimetry and changes in BAT.

As we previously showed (López-Gonzales *et al.*, 2022), random fed mice under a CD and a HFD did not show any differences in body weight regain with L-serine supplementation. There were only differences between CD and HFD control mice. In overnight fasted mice, we also detected differences between CD and HFD control mice. Although body weight regain decreased in fasted HFD-fed mice supplemented with L-serine, as shown in figure 8A, differences did not reach statistical significance. In line with figure 8A, CD-fed mice supplemented with L-serine body weight regain was similar (**Figure 11A**). L-serine supplementation did not affect glucose tolerance in random fed nor overnight fasted mice (**Figure 11B**). Regarding the liver, weight decreased with L-serine supplementation only under CD. Interestingly, liver weight of random fed CD control mice was significantly higher than that of HFD control mice. In contrast to random fed, fasted mice did not show any differences in liver weight between the groups (**Figure 11C**). Concerning expression of gluconeogenesis-related genes, L-serine supplementation upregulated expression of the transcription factor *Foxo1*, but downregulated *G6Pase* in random fed CD mice. Moreover, *Pepck* and pyruvate carboxylase (*PC)* tended to be upregulated in these L-serine-supplemented mice. There were no changes gene in expression in HFD-fed mice. In fasted mice, L-serine supplementation tended to increase expression of *Foxo1*, downregulated *G6Pase* and tended to decrease *Pepck* expression in CD-fed mice. No changes were observed in *PC* expression. While there were no changes in most genes in HFD, there was a trend towards *Pepck* downregulation in L-serine supplemented mice (**Figure 11D**).
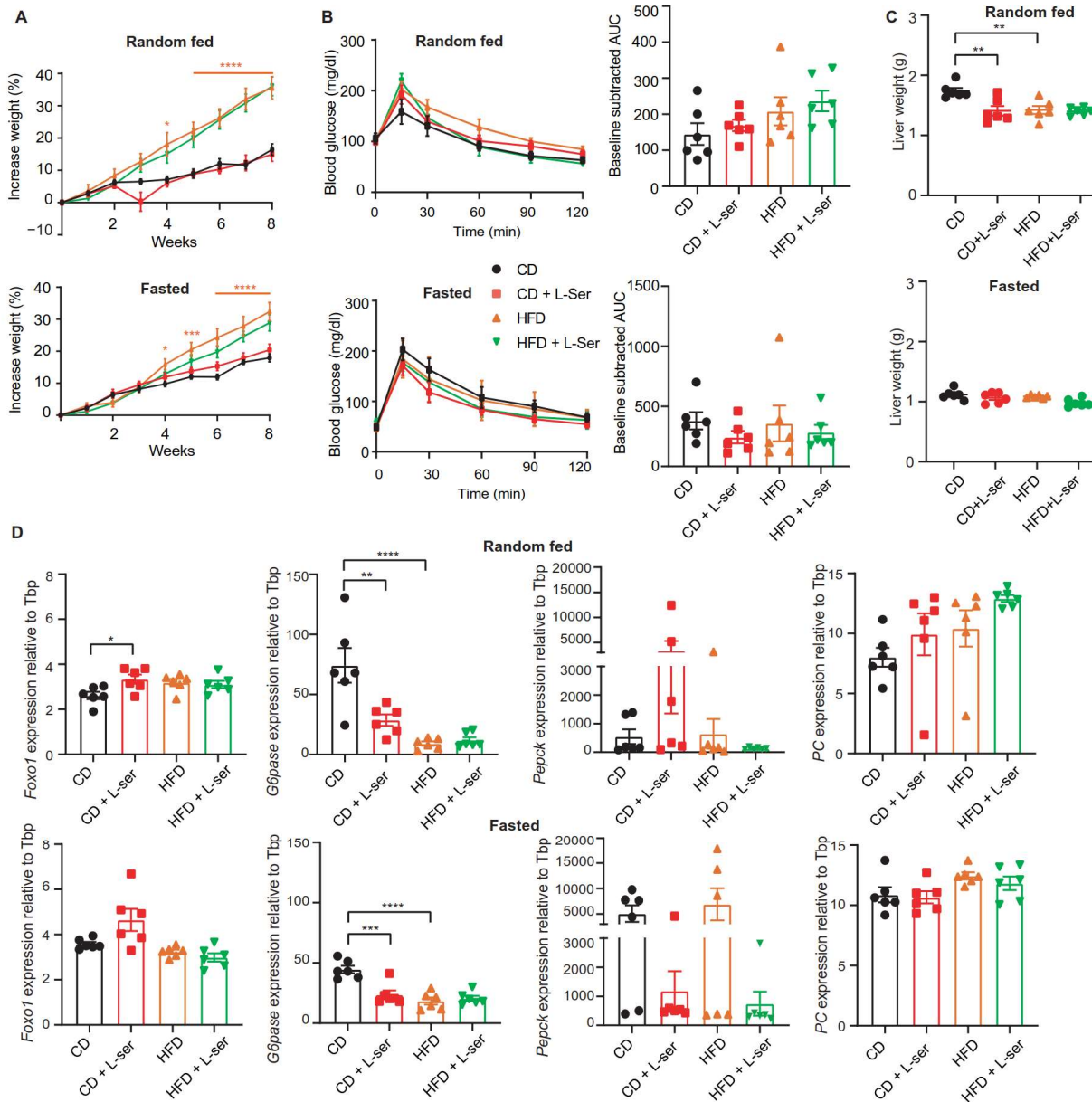
Figure 11. L-serine supplementation had no impact on glucose tolerance, but altered liver metabolism after repeated overnight fasting. (A) Body weight increase (%) of mice with or without L-serine supplementation *ad libitum* and overnight fasted (n=6). **(B)** GTT of mice with or without L-serine supplementation *ad libitum* and overnight fasted. **(C)** Liver weights of mice with or without L-serine supplementation *ad libitum* and overnight fasted (n=6). **(D)** Expression of glucose metabolism-related genes in liver of mice with or without L-serine supplementation *ad libitum* and overnight fasted. Data are shown as mean ± SEM, one or two-way ANOVA with Tukey's post-hoc test. * $p < 0.05$, ** $p < 0.01$, *** $p < 0.001$, **** $p < 0.0001$. Statiscal significance in panel A is compared to CD control.

Aiming to discern overnight fasting and L-serine supplementation effects on liver metabolism, we supplemented with L-serine another cohort of mice under CD and HFD, for one week and sacrificed them right after fasting. One-week L-serine supplementation and overnight fasting did not change body weight in CD or HFD-fed mice, but CD-fed mice tended to have a higher body weight. After overnight fasting, all mice had similar weight with no changes between diets or L-serine supplementation (**Figure 12A**). Interestingly, blood glucose levels after fasting were higher in CD than in HFD-fed mice and tended to be higher in L-serine-supplemented mice compared to their HFD-fed control (**Figure 12B**). NMR-based metabolomics was performed to identify altered metabolites in the liver. PCA analysis revealed that HFD (red) had an impact on liver metabolism (left), but L-serine supplementation (magenta) did not (right) (**Figure 12C**). Three main comparisons were carried out using OPLS-DA analysis: the impact of HFD, CD and HFD combined and CD- and HFD-specific impact of L-serine supplementation on the liver AE samples. The HFD feeding made a significant impact on the metabolite profiles of AE samples (R^2X=38.8%, R^2Y=83.8%, Q^2Y=74.6%). Affected metabolites were glycogen, glutathione, glucose, lactate and taurine (**Figure 12D**).
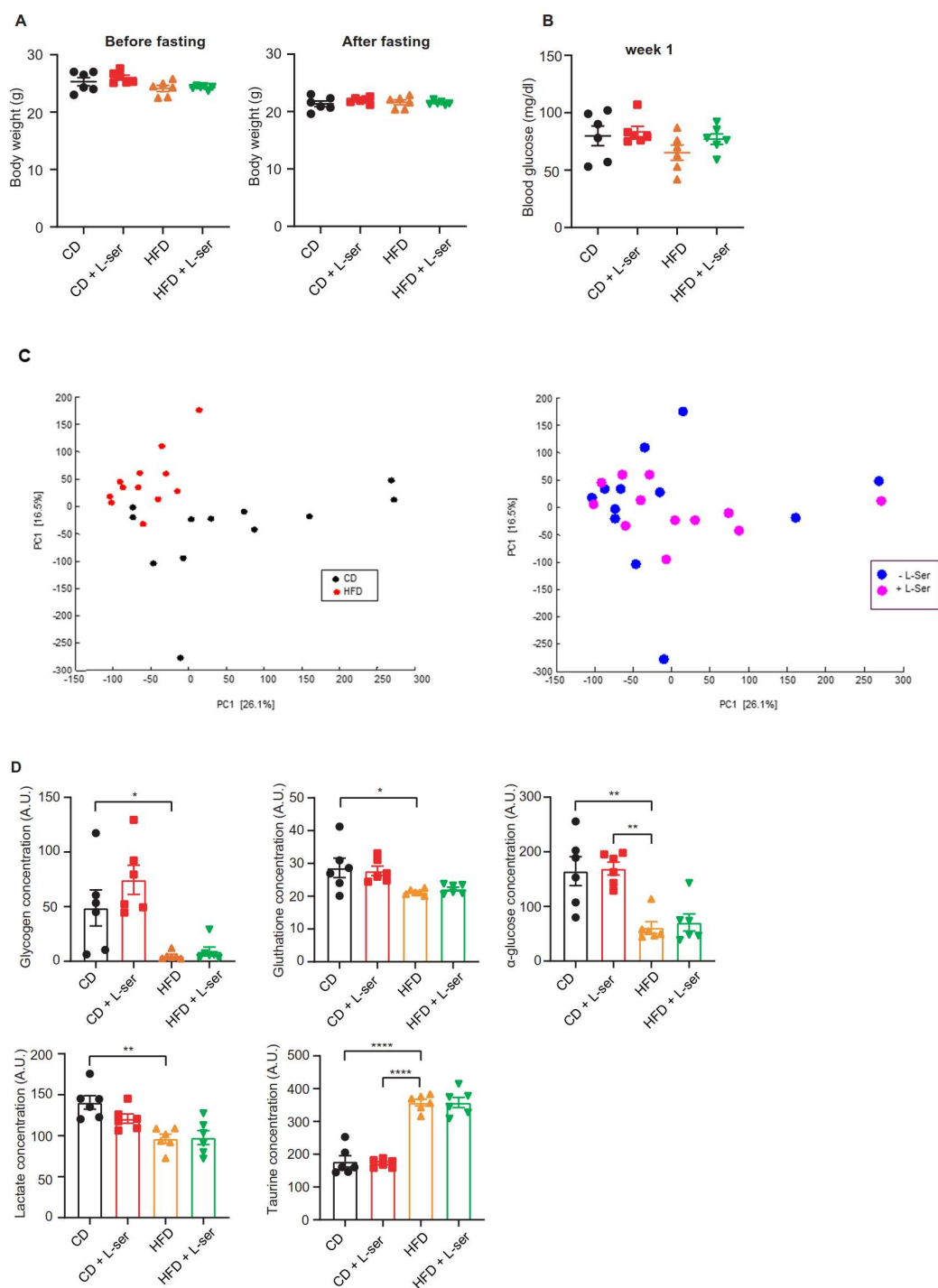
Figure 12. Overnight fasting and one-week L-serine supplementation did not alter body weight, blood glucose or liver metabolomics in mice. (A) Body weight of L-serine supplemented mice for one week under CD and HFD before and after overnight fasting (n=6). **(B)** Blood glucose levels without or with one-week L-serine supplementation and overnight fasting in mice under CD and HFD (n=6). **(C)** PCA analysis of the impact of HFD(red) compared to CD (black) and impact of L-serine supplementation (magenta) compared to no L-serine supplementation (blue) (n=12). **(D)**

Altered metabolites in liver AE of CD and HFD-fed mice with or without L-serine supplementation and subjected to overnight fasting (n=6). Data are shown as mean ± SEM, one-way ANOVA with Tukey's post-hoc test. * $p < 0.05$, ** $p < 0.01$, **** $p < 0.0001$. In panel **(C)**, data were analyzed by unsupervised multivariate analysis (PCA) and supervised OPLS-DA analysis.

4.1.4. L-serine supplementation activates BAT thermogenesis after overnight fasting

To further investigate the body weight regain decrease after repeated fasting in L-serine-supplemented mice, we introduced them in metabolic cages. Using indirect calorimetry, we obtained data on their EE, locomotor activity, RER, food and water intake. Interestingly, we observed several changes in CD-fed mice. L-serine supplementation decreased EE in CD random fed mice (p= 0.002); however, after overnight fasting, it significantly increased EE compared to respective CD control (p=0.013). We also observed that overnight fasting increased EE in L-serine-supplemented CD-fed mice compared with their random fed control (p=0.0003). Regarding HFD-fed mice, we observed a trend to reduce EE with L-serine supplementation in random fed mice, but to increase EE after overnight fasting (**Figure 13A**). Locomotor activity of mice under CD and HFD with or without L-serine supplementation did not change neither in random fed nor in fasted mice (**Figure 13B**). L-serine supplementation did not alter total RER, RER during light or RER during dark phase in CD random fed mice. However, total RER and RER during light and RER during dark phase in CD-fed mice supplemented with L-serine increased after overnight fasting compared to random fed. Overnight fasting also increased RER (total, light and dark phase) in CD-fed control mice. Moreover, we observed increased total RER and RER during the light phase in L-serine-supplemented CD-fed mice compared to their fasted CD-fed controls. There were no differences between groups in HFD neither in total RER nor in light or dark phase RER (**Figure 13C**). Total food intake decreased with L-serine supplementation in random fed mice under CD. However, overnight fasting increased total food intake resulting from the increasing intake in the light phase for both L-serine-supplemented CD-fed and control mice compared to random fed. Moreover, L-serine supplementation increased the overnight fasting effects on total food intake. With respect to HFD, food intake changes were observed only during the light phase in fasted control compared to random fed mice (**Figure 13D**). In line with food intake, changes in water intake were observed only in CD-fed mice. Overnight fasting increased water intake in CD-fed mice supplemented with L-serine. Furthermore, water intake increased in fasted L-serine-supplemented mice compared to control (**Figure 13E**). These findings could not elucidate the root cause of the decrease in body weight regain. However, the unexpected changes in CD were compelling.
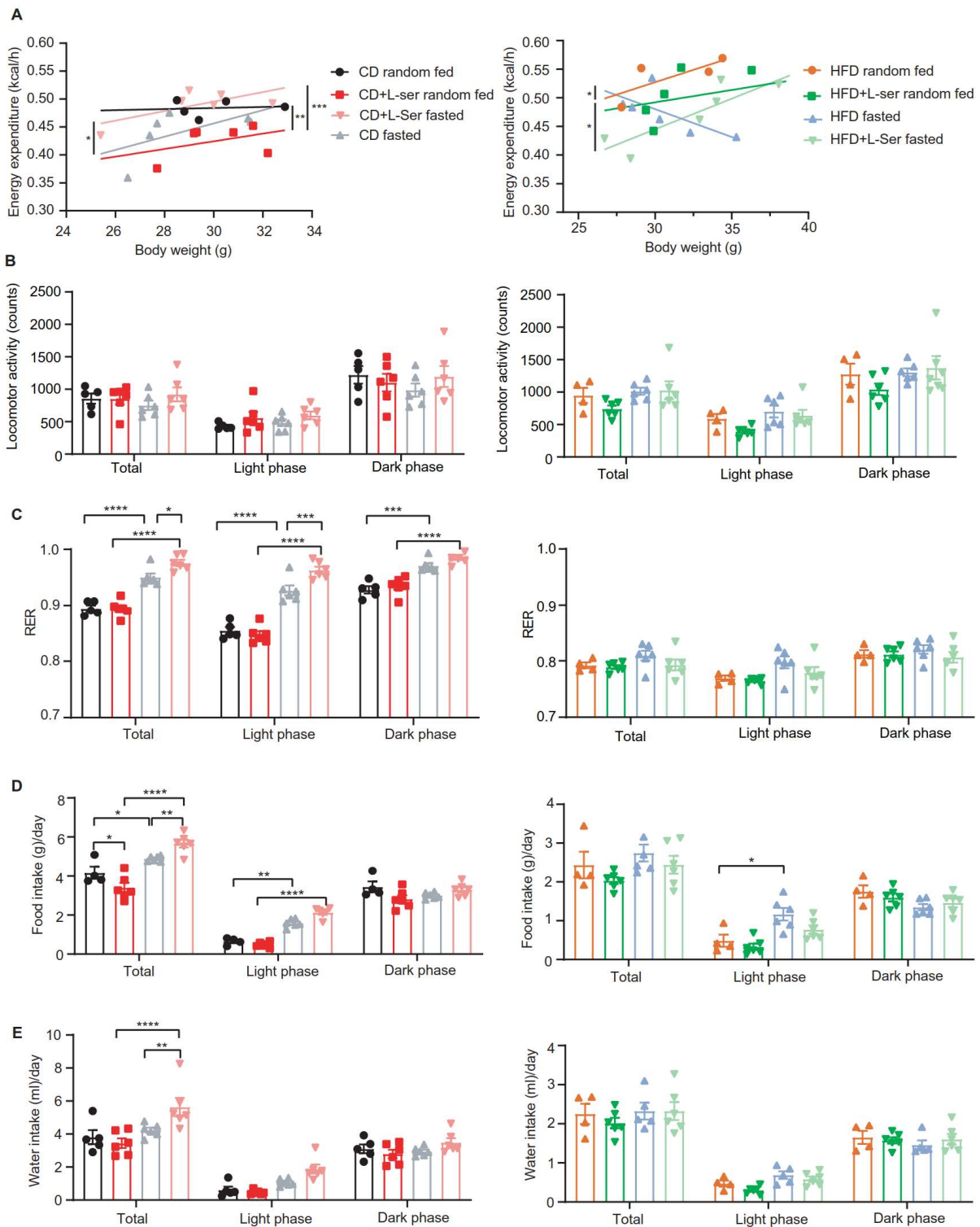
Figure 13. Overnight fasting after L-serine supplementation leads to changes in EE, RER, food and water intake in CD-fed mice, but not in HFD-fed mice. (A) EE in relation to body weight of random fed and overnight fasted mice under CD and HFD and with and without L-serine supplementation (CD random fed: n = 5; CD fasted, CD+L-ser random

fed, CD+L-ser fasted: n = 6; HFD random fed: n = 4; HFD fasted, HFD+L-ser random fed, HFD+L-ser fasted: n = 6). **(B)** Locomotor activity of random fed and overnight fasted mice under CD and HFD and with and without L-serine supplementation (CD random fed: n = 5; CD fasted, CD+L-ser random fed, CD+L-ser fasted: n = 6; HFD random fed: n = 4; HFD fasted, HFD+L-ser random fed, HFD+L-ser fasted: n = 6). **(C)** RER of random fed and overnight fasted mice under CD and HFD and with and without L-serine supplementation (CD random fed: n = 5; CD fasted, CD+L-ser random fed, CD+L-ser fasted: n = 6; HFD random fed: n = 4; HFD fasted, HFD+L-ser random fed, HFD+L-ser fasted: n = 6). **(D)** Food intake of random fed and overnight fasted mice under CD and HFD and with and without L-serine supplementation (CD random fed: n = 5; CD fasted, CD+L-ser random fed, CD+L-ser fasted: n = 6; HFD random fed: n = 4; HFD fasted, HFD+L-ser random fed, HFD+L-ser fasted: n = 6). **(E)** Water intake of random fed and overnight fasted mice under CD and HFD and with and without L-serine supplementation (CD random fed: n = 5; CD fasted, CD+L-ser random fed, CD+L-ser fasted: n = 6; HFD random fed: n = 4; HFD fasted, HFD+L-ser random fed, HFD+L-ser fasted: n = 6). Statistical analysis in panel **(A)** is described in Section 3.7.Data are shown as mean ± SEM, two-way ANOVA with Tukey's post-hoc test. * $p < 0.05$, ** $p < 0.01$, *** $p < 0.001$,**** $p < 0.001$.

To better understand the changes in CD-fed mice described in figure 13, we challenged these mice with cold exposure and housing at thermoneutrality. After overnight fasting, mice were exposed to cold (4°C) for 4 h and subsequently for 24 h to thermoneutrality (30°C). After cold exposure, EE increased in all groups and no differences were observed. Conversely, EE decreased after thermoneutrality, displaying no differences between the groups (**Figure 14A**). In random fed mice, RER followed the diurnal rhythm of increasing during the dark phase, indicating that mice are active and eat; and decreasing during the light phase, when mice rest or sleep. During the dark phase, mice are fueling their metabolism with carbohydrates provided with the food, indicated by a RER of 0.85-0.95. During the light phase, mice usually eat less and maintain their basal metabolism partly with their fat storages, by lipid oxidation, indicated by a lower RER, 0.80-0.90. In fasted mice, we observed a decreased RER (0.75-0.80) during overnight fasting, indicating that they were mobilizing the fat storage and using more fat as a substrate to maintain their metabolism. When the fasted mice had access to food again, RER increased to almost 1.0 and was maintained for almost 24 h. During cold exposure, RER tended to be higher in fasted mice as well as during thermoneutrality and for the next 36 h. Subsequently, fasted mice followed the same RER cycles as random fed mice. We did not observe differences in RER with L-serine supplementation (**Figure 14B**). Regarding cumulative food intake, we observed an increase in fasted L-serine supplemented mice compared to their random fed control at the end of the experiment. In thermoneutrality, there were no differences with L-serine supplementation, but fasted mice ate more than random fed mice (**Figure 14C**).
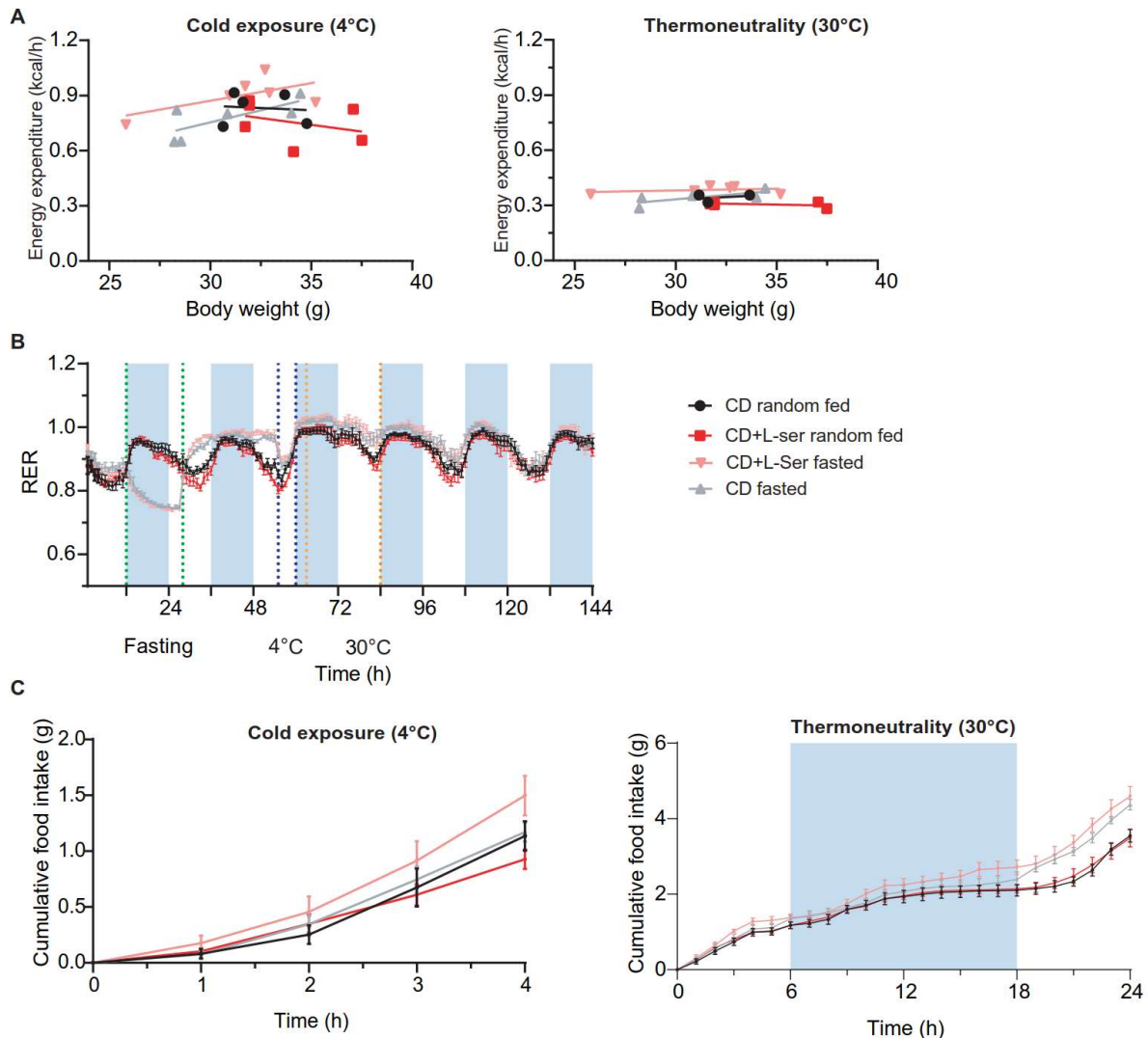
Figure 14. L-serine supplementation had no impact on EE, RER and cumulative food intake under cold or thermoneutrality exposure. (A) EE in relation to body weight of random fed and overnight fasted mice under CD with and without L-serine supplementation under cold and thermoneutrality exposure (CD random fed: n = 5; CD fasted, CD+L-ser random fed, CD+L-ser fasted: n = 6). **(B)** RER values of random fed and overnight fasted mice under CD with and without L-serine supplementation under cold and thermoneutrality exposure (CD random fed: n = 5; CD fasted, CD+L-ser random fed, CD+L-ser fasted: n = 6). **(C)** Cumulative food intake of random fed and overnight fasted mice under CD with and without L-serine supplementation under cold and thermoneutrality exposure (CD random fed: n = 5; CD fasted, CD+L-ser random fed, CD+L-ser fasted: n = 6). Statistical analysis in panel **(A)** is described in Section 3.7 .Data are shown as mean ± SEM, two-way ANOVA with Tukey's post-hoc test. * $p < 0.05$, ** $p < 0.01$, *** $p < 0.001$,**** $p < 0.001$.

Because of the changes in food intake in CD-fed mice after L-serine supplementation, we intended to investigate whether these changes were due to a L-serine effect in the hypothalamus,

a brain region responsible for regulating food intake. We measured hypothalamic *Npy* and *Pomc* genes, which promote hunger or satiety by increasing or decreasing food intake, respectively. While the expression of these genes did not change in HFD-fed mice, there were some changes in CD-fed mice. However, differences in expression were between random fed and fasted mice and not due to L-serine treatment. *Npy* expression was upregulated in fasted CD-fed mice, suggesting that hunger and food intake were promoted in fasted mice. Conversely, *Pomc* expression was downregulated in fasted mice with L-serine supplementation, suggesting that satiety was reduced and so, food intake was promoted. The same trend was observed in CD-fed control mice, but it was not statistically significant (**Figure 15A**).
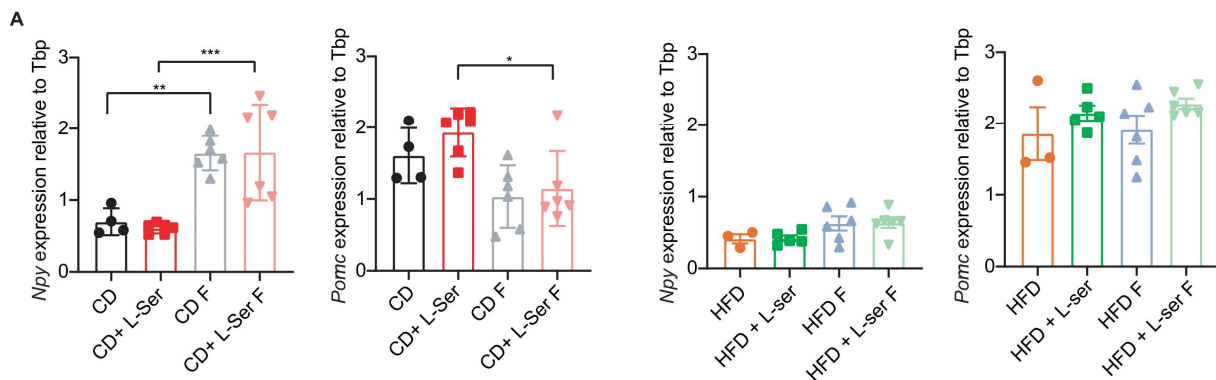
Figure 15. L-serine did not impact on expression of genes related to food intake in the hypothalamus. (A) Expression of *Npy* and *Pomc* genes in the hypothalamus of random fed and fasted mice supplemented with L-serine for 16 weeks (CD random fed: n=4; CD fasted, CD+L-ser random fed, CD+L-ser fasted: n=6; HFD random fed: n=4; HFD fasted, HFD+L-ser random fed, HFD+L-ser fasted: n=6). Data are shown as mean ± SEM, one-way ANOVA with Tukey's post-hoc test. * $p < 0.05$, ** $p < 0.01$, *** $p < 0.001$.

To investigate whether changes in EE and food intake in CD-fed mice were due to L-serine and/or overnight fasting effects on BAT, we analysed weight, gene and protein expression of this tissue. Moreover, we aimed to discern any changes in BAT, which could lead to a decrease in body weight regain in HFD-fed mice. BAT weight of random fed mice did not change with L-serine supplementation neither in CD nor in HFD-fed mice. There were only differences between the CD and HFD control mice. Similarly, BAT of fasted mice did not show differences upon L-serine supplementation; however, there was a trend to decrease in both CD and HFD-fed mice. Nevertheless, we observed that the overall BAT weight decreased in fasted compared to random fed mice and a significant increase in HFD compared to CD control in both random fed and fasted mice (**Figure 16A**). The higher EE might be associated with an increase in BAT thermogenesis. Therefore, we measured the expression of thermogenesis-related genes. In random fed mice, we

did not detect any changes in expression of peroxisome-proliferator activated receptor gamma co-activator 1α (*Pgc1α*), PR domain containing 16 (*Prdm16*) or *Ucp1* genes. Nonetheless, we revealed a trend to up-regulated *Pgc1α* in fasted CD-fed mice supplemented with L-serine as well as in HFD-fed mice. *Prmd16* and *Ucp1* gene expression in fasted mice did not change between groups (**Figure 16B**). Although we did not observe any significant changes in the expression of *Ucp1*, we measured the UCP1 protein expression in BAT of these mice. There were no differences in UCP1 levels with L-serine supplementation neither in CD nor in HFD in random fed mice. However, in fasted mice, while no changes were detected in HFD, L-serine-supplemented mice showed a higher UCP1 expression than their CD control (**Figure 16C**). Then, we measured phosphorylated AMPKα (Thr172), which is a protein activated by changes in energy homeostasis. In random fed mice, L-serine supplementation increased phosphorylated AMPKα levels in CD-fed mice, whereas it decreased the levels in HFD-fed mice. In fasted mice, in line with UCP1, phosphorylated AMPKα was upregulated in CD-fed mice with L-serine supplementation (**Figure 16D**). In summary, L-serine supplementation did not significally change weight or expression of thermogenesis-related genes in BAT. However, it increased UCP1 expression and phosphorylation levels of AMPKα after repeated overnight fasting.

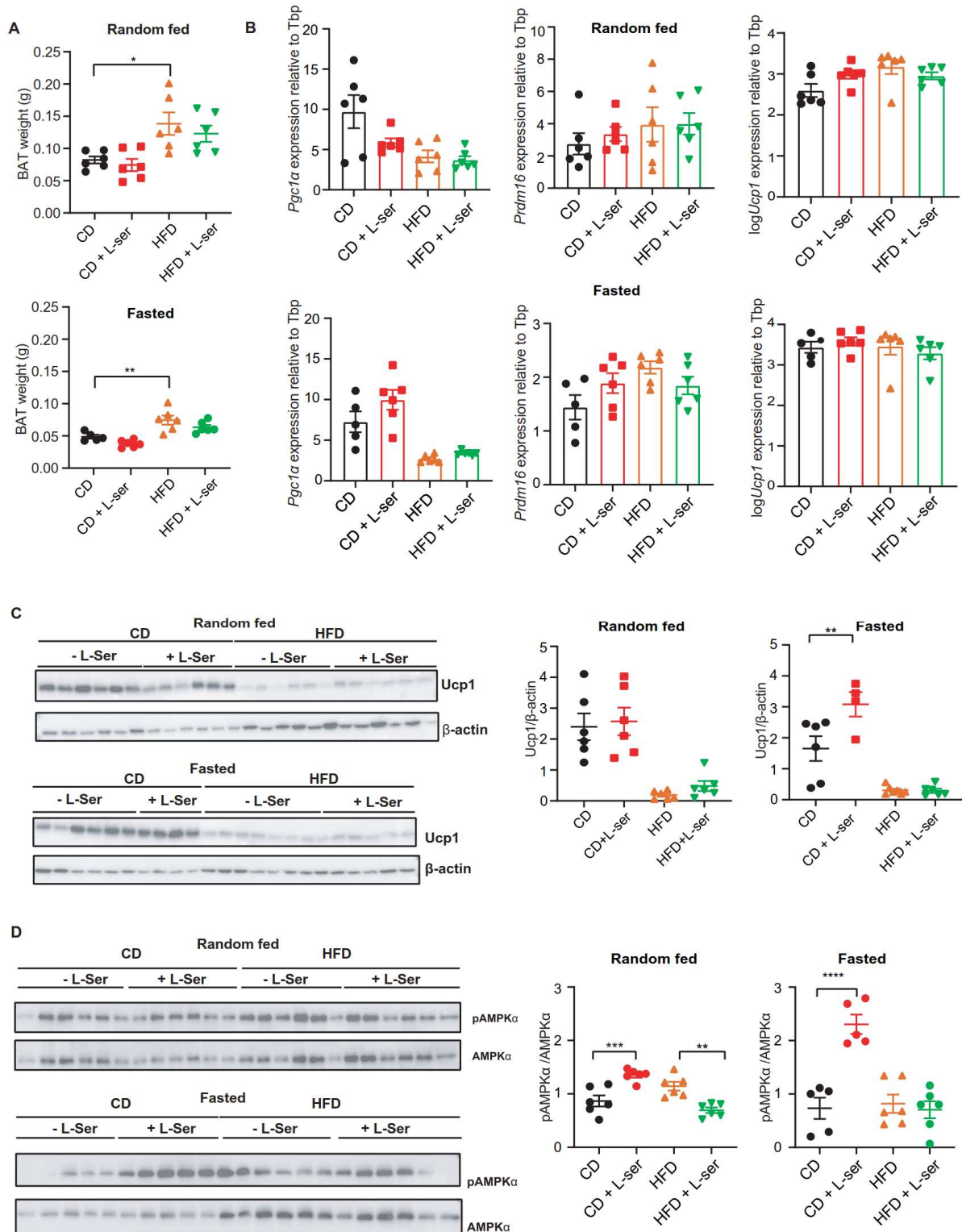**Figure 16. L-serine supplementation activates UCP1 and AMPKα in BAT in CD-fed mice. (A)** BAT weight of random fed and fasted mice with or without L-serine supplementation (n=6). **(B)** Expression of thermogenesis-related

genes in BAT of random fed and fasted mice with or without L-serine supplementation. **(C)** Western blot and quantifications of UCP1 in random fed and fasted mice with and without L-serine supplementation (n=6). (**D**) Western blot and quantifications of phosphorylated AMPKα in random fed and fasted mice with and without L-serine supplementation (n=6) Data are shown as mean ± SEM, one-way ANOVA with Tukey's post-hoc test. * $p < 0.05$, ** $p < 0.01$, *** $p < 0.001$, **** $p < 0.0001$.

4.1.5. L-serine supplementation activates primary brown adipocytes

To explore the effects of L-serine on brown adipocytes, preadipocytes from wild-type mice were isolated, differentiated to adipocytes and then, stimulated them with 400 µM L-serine. We observed trend to increase the phosphorylation of AMPKα after 10 min. Nevertheless, phosphorylation of AMPKα was similar to the control after 60 min (**Figure 17A**). To investigate whether L-serine supplementation promoted brown adipocytes mitochondrial respiration, we performed a 3 h pre-incubation with 400 µM L-serine supplementation and measured oxygen consumption rate (OCR). Basal mitochondrial respiration increased significantly in adipocytes injected with L-serine in combination with isoproterenol compared to control. However, when preadipocytes were previously exposed to L-serine, mitochondrial respiration slightly increased but not significantly. We observed the same trend in all groups after oligomycin injection, an inhibitor of the ATP synthase. After injection with FCCP, which is an uncoupler of mitochondrial oxidative phosphorylation, mitochondrial respiration tended to increase in adipocytes pre-incubated with L-serine compared to control, but did not reach statistical significance. However, adipocytes injected with L-serine increased the maximal mitochondrial respiration compared to control (**Figure 17B**). Taken together, these findings indicate that L-serine supplementation increases phosphorylation levels of AMPKα as well as mitochondrial respiration in brown adipocytes.
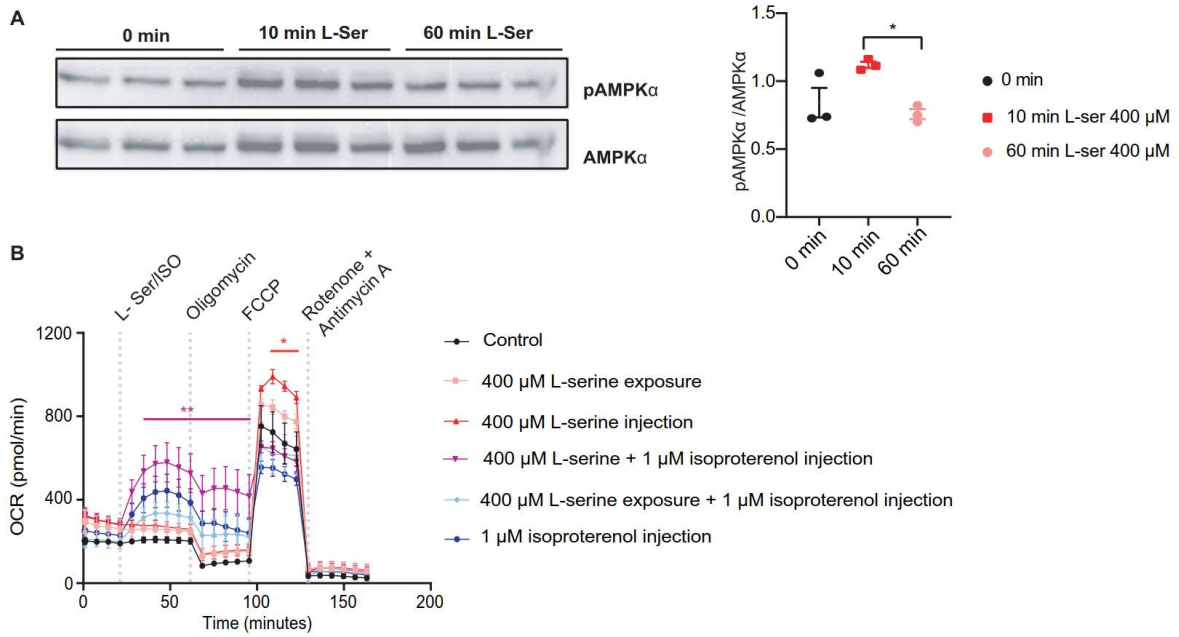
Figure 17. L-serine promotes maximal mitochondrial respiration in primary brown adipocytes. (A) Western blot and quantifications of phosphorylated AMPKα in differentiated primary brown adipocytes after L-serine stimulation (n=3). **(B)** Oxygen consumption rate (OCR) of differentiated primary brown adipocytes pre-treated or not with 400 µM L-serine and injected with 400 µM L-serine, 400 µM L-serine in combination with 1 µM isoproterenol or 1 µM isoproterenol (n=3 replicates from 2 mice). Data are shown as mean ± SEM, one or two-way ANOVA with Tukey's post-hoc test. * $p < 0.05$, ** $p < 0.01$, *** $p < 0.001$.

4.2. Metabolic effects of NMDAR knockout in PVN neurons of Grin1$^{flox/flox}$ mice

In order to study the PVN-NMDAR role in insulin secretion and whole-body metabolism, we specifically knockout the NMDA receptors by using AAV stereotaxic injections in Grin1$^{flox/flox}$ mice. Grin1$^{flox/flox}$ mice have a loxP sites flanking the sequence of the *Grin1* gene, which encodes for the essential subunit of the NMDAR (The Jackson Laboratory, 2022). Two weeks after the injections, we performed the validation of the PVN-specific knockout of Grin1 as well as the metabolic phenotyping of the mice.

4.2.1. PVN-NMDAR knockout validation of AAV-injected Grin1$^{flox/flox}$ mice
4.2.1.1. NMDAR currents recordings on PVN-GFP-expressing neurons of GFP (control) and Cre mice

NMDAR currents of GFP-expressing neurons on brain slices containing the PVN were measured in GFP (control) and Cre mice after stimulation with 25 µM NMDA. Whole-cell currents in GFP-expressing neurons in the PVN of GFP (control) mice responded to NMDA stimulation. However, GFP-expressing neurons of Cre mice did not respond to NMDA (**Figure 18A and B**). We also observed a decrease in the peak current amplitude in GFP-expressing neurons of Cre mice (**Figure 18C**). These results suggest that in the GFP-expressing neurons of mice injected with the Cre virus there were no NMDA currents as a result of NMDARs knockout.
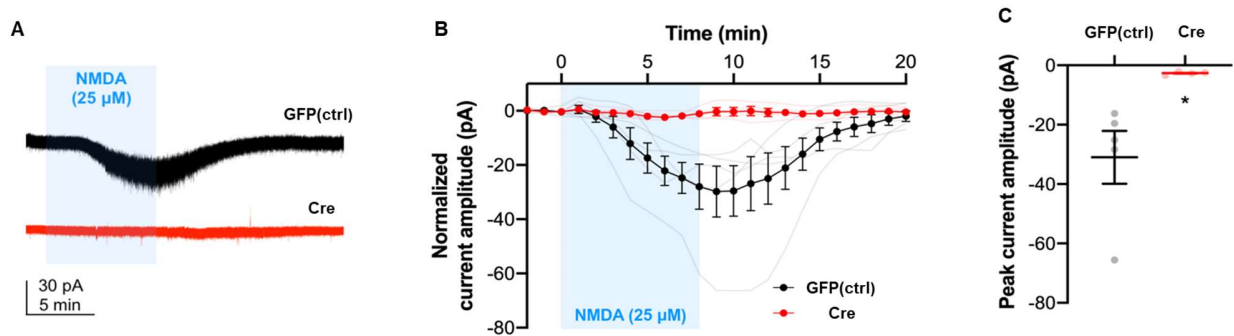
Figure 18. NMDAR currents are lost in GFP-expressing neurons in mice injected with a GFP-Cre-recombinase expressing virus. (A) Representative whole-cell currents in Cre and GFP (control) neurons of the PVN within brain slices of a Grin1$^{flox/flox}$ mouse after two weeks after injection, showing the response to 25µM NMDA stimulation (n=3). **(B)** Time course of average NMDA-induced (25µM) responses for 20 min in Cre and GFP (control) neurons of the PVN within brain slices of a Grin1$^{flox/flox}$ mouse after two weeks after injection (light lines are the individual recordings; strong lines are the average values) (Neurons: GFP (control), n=5; Cre, n=4). **(C)** Maximal amplitude response from in GFP+ and control neurons of the PVN within brain slices of a Grin1$^{flox/flox}$ mouse (Neurons: GFP (control), n=5; Cre, n=4). Data are shown as mean ± SEM, *p< 0.05.

4.2.1.2. GFP and GRIN1 expression in PVN neurons of AAV-injected Grin1^{flox/flox} mice

The efficiency of the virus targeting neurons in the PVN was validated by immunostaining for GFP in the PVN-containing slices. As observed in figure 19A, both GFP (ctrl) and Cre mice showed GFP-expressing neurons in the PVN. However, there were differences in the number of cells targeted as well as the areas reached by the virus. Moreover, in some mice, regardless of the Cre or control virus injection, one hemisphere of the brain showed more GFP-positive cells or GFP expression in the PVN was unilateral instead of bilateral. Nevertheless, we confirmed that the AAV vector infected and recombined with the DNA of the neurons by expressing GPF protein in their cytosol. In order to investigate whether there was a NMDAR deletion in PVN-GFP-expressing neurons in mice injected with AAV vectors expressing Cre recombinase, we combined GFP immunostaining with GRIN1 *in situ* hybridization. Although, GRIN1 signal remained in GFP-expressing neurons from the Cre mice, it decreased compared to GFP (ctrl) mice (**Figure 19B).**
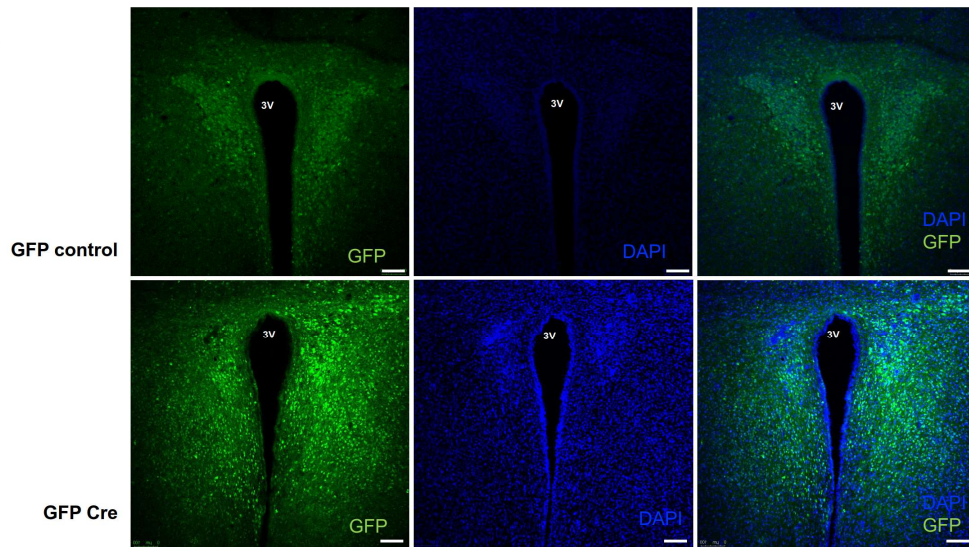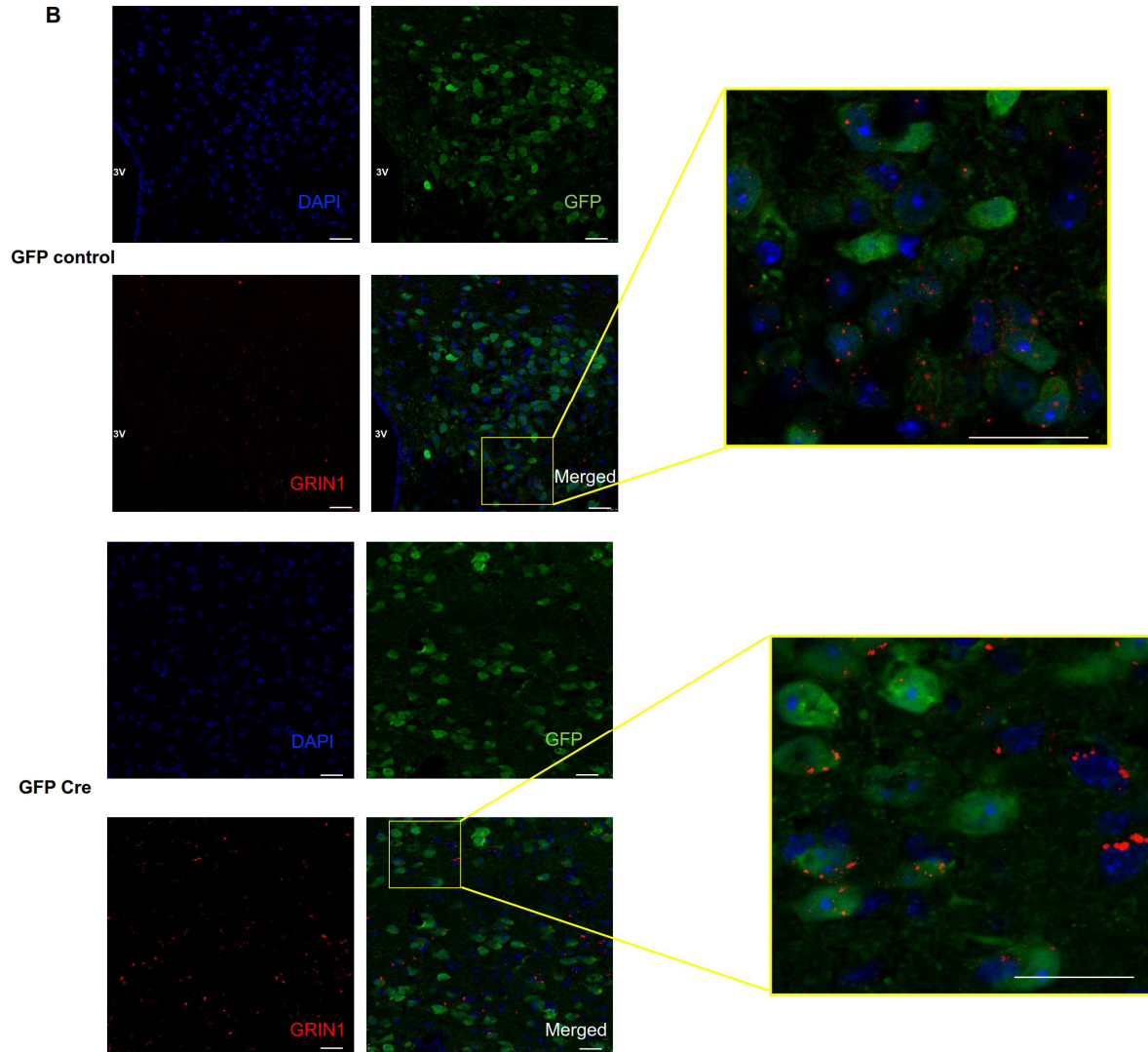
Figure 19. GRIN1 expression decreases in GFP-expressing neurons in GFP-Cre-AAV-injected Grin1$^{flox/flox}$ mice. **(A)** Confocal images of GFP-expressing neurons (green) in slices containing the PVN of control (GFP control) and Grin1^{PVN-KO} mice (Cre) 14 weeks post-injection (nuclei in blue). **(B)** Confocal images of GFP (green) and GRIN1 (red)-expressing neurons on brain slices containing PVN of control (GFP control) and Grin1^{PVN-KO} mice (Cre) (nuclei in blue) 14 weeks post-injection. Size bar represents 100 μM.

4.2.2. Grin1^{PVN-KO} mice did not show any differences on body weight, body composition or glucose levels in blood compared to control mice

Grin1^{PVN-KO} mice (Cre) did not exhibit differences in body weight or blood glucose levels after 12 weeks compared to control (GPF(ctrl)) (**Figure 20A and B**). While there were no differences in lean mass, there was a trend to decrease the fat mass of Grin1^{PVN-KO} (**Figure 20C**). There were no changes in WAT weight (PGF and SCF) and liver weight of Grin1^{PVN-KO} mice compared to control after 15 weeks (**Figure 20D**).
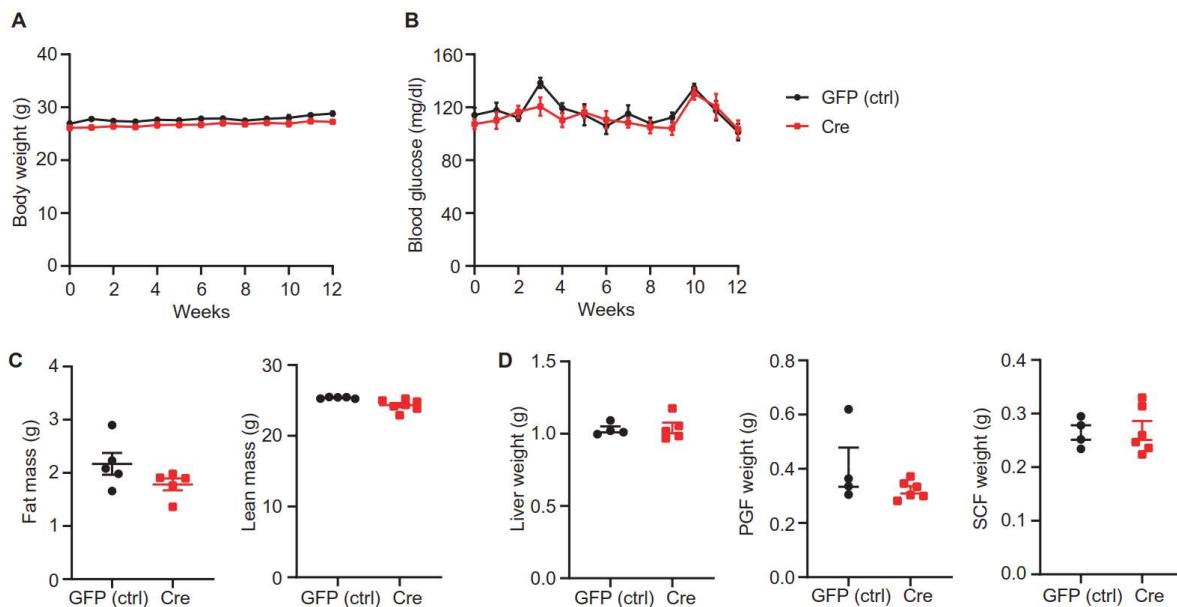
Figure 20. Grin1^{PVN-KO} mice did not show phenotypical differences compared to control mice. (A) Body weight of Grin1^{PVN-KO} (Cre) and control (GFP (ctrl)) mice at week 12 (GFP (ctrl): n=6; Cre: n=7). **(B)** Blood glucose levels of Grin1^{PVN-KO} (Cre) and control (GFP (ctrl)) mice at week 12 (GFP (ctrl): n=6; Cre: n=7). **(C)** Body composition (fat and lean mass) of Grin1^{PVN-KO} (Cre) and control (GFP (ctrl)) mice at week 12 (GFP (ctrl): n=6; Cre: n=7). **(D)** Tissue weight of Grin1^{PVN-KO} (Cre) and control (GFP (ctrl)) mice at week 15 (GFP (ctrl): n=4; Cre: n=6). Data are shown as mean ± SEM, unpaired t-test or two-way ANOVA with Sidak's post-hoc test.

4.2.3. Grin1^{PVN-KO} mice do not show differences in glucose tolerance or insulin secretion compared to control mice

To assess glucose tolerance and insulin secretion, GTT and oral GSIS (oGSIS) were performed on weeks seven and 11, respectively. Glucose tolerance did not change in Grin1^{PVN-KO} mice compared to control (**Figure 21A**). Insulin secretion in Grin1^{PVN-KO} mice after an oral glucose bolus did not change compared in Grin1^{PVN-KO} mice compared to control (**Figure 21B**). In a previous study, wild-type mice treated for two weeks with a low concentration of D-serine (0.1% D-serine) showed a slight increase in glucose tolerance due to improved insulin secretion (Suwandhi *et al.*, 2018). Therefore, we carried out this experiment with our mice to investigate whether there were changes in insulin secretion in Grin1^{PVN-KO} mice, whose NMDAR in the PVN are knocked out. Nevertheless, insulin levels after two weeks of 0.1% D-serine treatment did not change in Grin1^{PVN-KO} compared to control mice (**Figure 21C**).
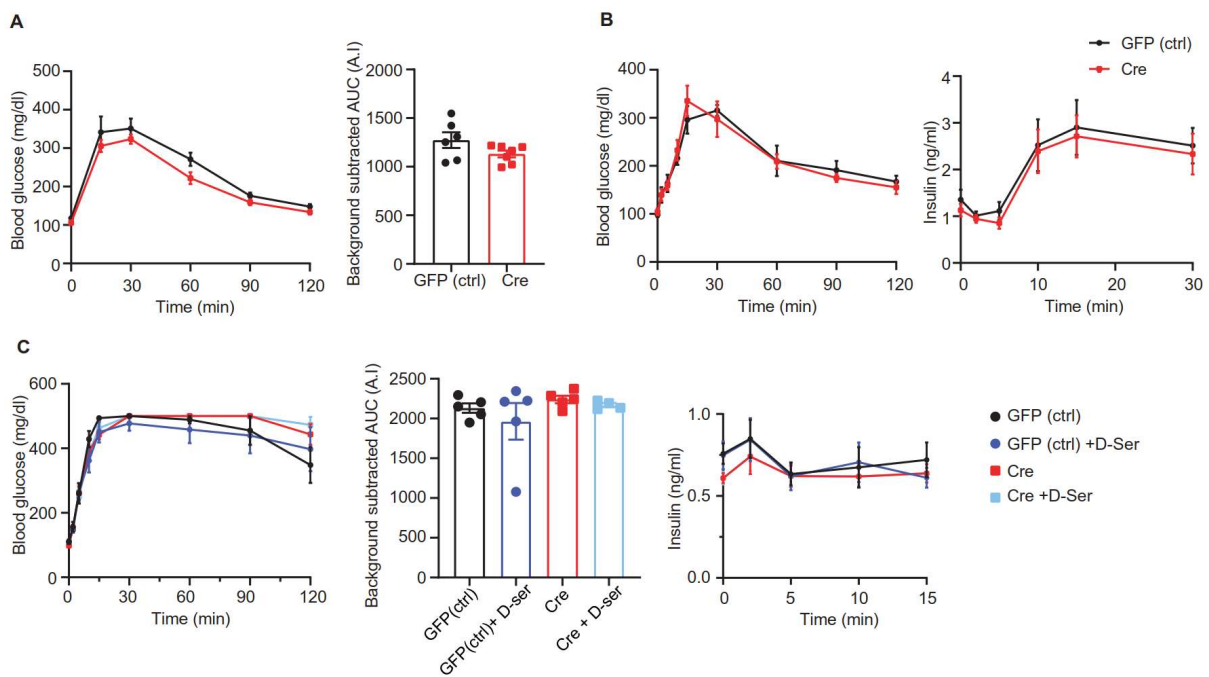
Figure 21. Grin1^{PVN-KO} does not display changes in glucose tolerance or insulin secretion. (A) GTT Grin1^{PVN-KO} (Cre) and control (GFP (ctrl)) mice at week seven (GF (ctrl): n=6; Cre: n=7). **(B)** Oral GSIS (oGSIS) Grin1^{PVN-KO} (Cre) and control (GFP (ctrl)) mice at week 11 (GFP (ctrl): n=6; Cre: n=7). **(C)** ipGSIS after two weeks 0.1% D-serine treatment in of Grin1^{PVN-KO} (Cre) and control (GFP (ctrl)) mice at weeks ten and 12 (GFP (ctrl): n=5; Cre: n=4). Data are shown as mean ± SEM, one or two-way ANOVA with Sidak's post-hoc test.

4.2.4. Grin1^{PVN-KO} mice showed reduced EE at room temperature and decreased food intake during cold exposure

4.2.4.1. Grin1^{PVN-KO} mice showed a lower EE at room temperature compared to control mice

The metabolic phenotypes of Grin1^{PVN-KO} and control mice were analysed by indirect calorimetry. We observed that Grin1^{PVN-KO} mice showed a lower EE compared to control mice (p=0.032) (**Figure 22A**). There were no changes in RER or locomotor activity neither in total nor during light or dark phase between the two groups (**Figure 22B and C**). Moreover, food intake was similar between Grin1^{PVN-KO} mice and control mice (**Figure 22D**). Similarly, water intake was not different between groups (**Figure 22E**). To investigate whether Grin1^{PVN-KO} mice had any diet preference, we fasted the mice overnight and re-fed them for 3 h. During refeeding, mice were fed with a CD and a HFD *ad libitum*. Grin1^{PVN-KO} mice did not eat differently than control mice. It seemed that some Grin1^{PVN-KO} mice tended to eat more CD and some control mice preferred HFD over CD. Nevertheless, there were no differences between groups and, overall, both groups ate more HFD than CD (**Figure 22F**).
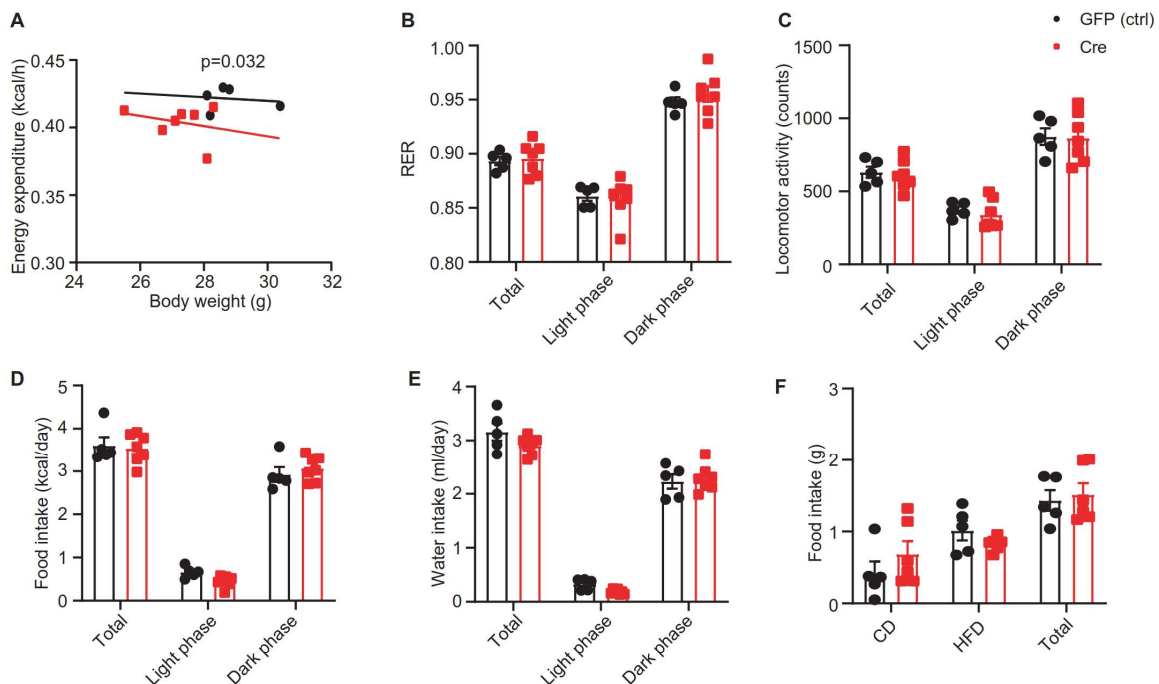
Figure 22. Grin1^{PVN-KO} had a lower EE at room temperature. (A) EE in relation to body weight of Grin1^{PVN-KO} (Cre) and control (GFP (ctrl)) mice (GFP (ctrl): n=5; Cre: n=7). **(B)** Average RER values of Grin1^{PVN-KO} (Cre) and control (GFP (ctrl)) mice (GFP (ctrl): n=5; Cre: n=7). **(C)** Average locomotor activity values of Grin1^{PVN-KO} (Cre) and control (GFP (ctrl)) mice (GFP (ctrl): n=5; Cre: n=7). **(D)** Average food intake of Grin1^{PVN-KO} (Cre) and control (GFP (ctrl)) mice (GFP

(ctrl): n=5; Cre: n=7). **(E)** Average water intake of Grin1^{PVN-KO} (Cre) and control (GFP (ctrl)) mice (GFP (ctrl): n=5; Cre: n=7). **(F)** Food preference test during 3 h re-feeding Grin1^{PVN-KO} (Cre) and control (GFP (ctrl)) mice (GFP (ctrl): n=5; Cre: n=6). Data are shown as mean ± SEM, two-way ANOVA with Sidak's post-hoc test. In panel **(A)**, ANCOVA was calculated with R.

Because of the changes in EE, we analysed BAT in detail. We observed that BAT weight of Grin1^{PVN-KO} mice was lower than that of the control (**Figure 23A**). In line with these results, BAT histological analysis showed a smaller size of lipid droplets (**Figure 23B**). There were no significant changes in expression of *Pgc1α*, *Prdm16* and *Ucp1* of Grin1^{PVN-KO} compared to control mice (**Figure 23C**). Similarly, when we measured the protein levels of UCP1, there was only a trend towards increase in Grin1^{PVN-KO} mice (**Figure 23D**).
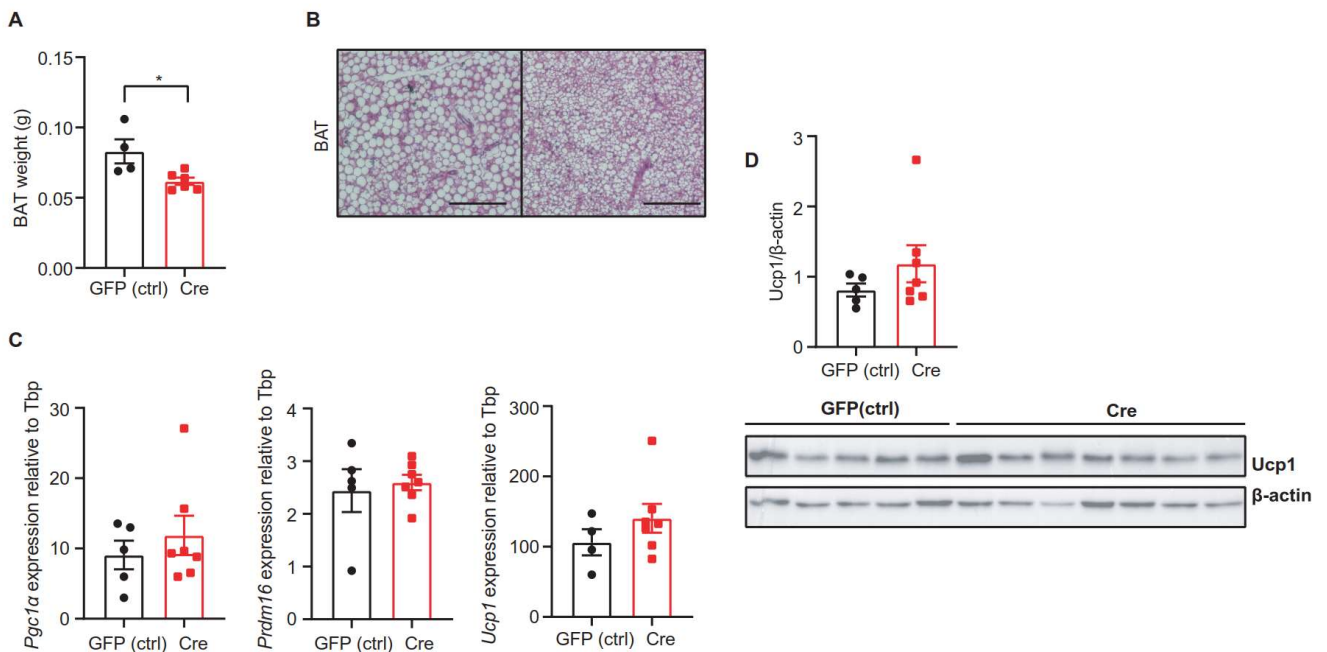
Figure 23. BAT of Grin1^{PVN-KO} mice shows weight and smaller lipid droplet size. (A) BAT weight of Grin1^{PVN-KO} (Cre) and control mice (GFP (ctrl)) (GFP (ctrl): n=4; Cre: n=6). **(B)** Representative H&E stainings of BAT of Grin1^{PVN-KO} (Cre) and control mice (GFP (ctrl)) (GFP (ctrl): n=4; Cre: n=6). Size bar represents 100 µM. **(C)** Expression of thermogenesis-related genes in BAT of Grin1^{PVN-KO} (Cre) and control mice (GFP (ctrl)) (GFP (ctrl): n=4; Cre: n=6). **(D)** Western blot and quantifications of UCP1 in BAT of Grin1^{PVN-KO} (Cre) and control mice (GFP (ctrl)) (GFP (ctrl): n=4; Cre: n=6). Data are shown as mean ± SEM, unpaired t-test, *p< 0.05.

4.2.4.2. Grin1^{PVN-KO} mice decreased their food intake and increased BAT thermogenesis under cold exposure

Aiming to investigate whether there were changes in BAT thermogenesis, we challenged the mice at cold temperature (4 °C) for 4 h inside metabolic cages, measuring the same parameters as in our previous experiment (**Figure 22**). When the mice were exposed to the cold, both Grin1^{PVN-KO} and control mice increased their EE. Although, some Grin1^{PVN-KO} mice showed lower EE, overall EE between groups were not statistically different (p=0.071) (**Figure 24A**). RER tended to be lower in Grin1^{PVN-KO} mice than in control (**Figure 24B**), but the locomotor activity was similar between the groups (**Figure 24C**). Surprisingly, Grin1^{PVN-KO} mice ate very little or did not eat at all. Although there were some control mice also eating little, overall there was a significant decrease in food intake of Grin1^{PVN-KO} mice relative to control (**Figure 24D**). This might also explain the trend to decrease in RER, since Grin1^{PVN-KO} mice might have used some of their lipid storage together with their glycogen reservoir when they did not eat. Interestingly, both groups drank very little or did not drink at all (**Figure 24E**).
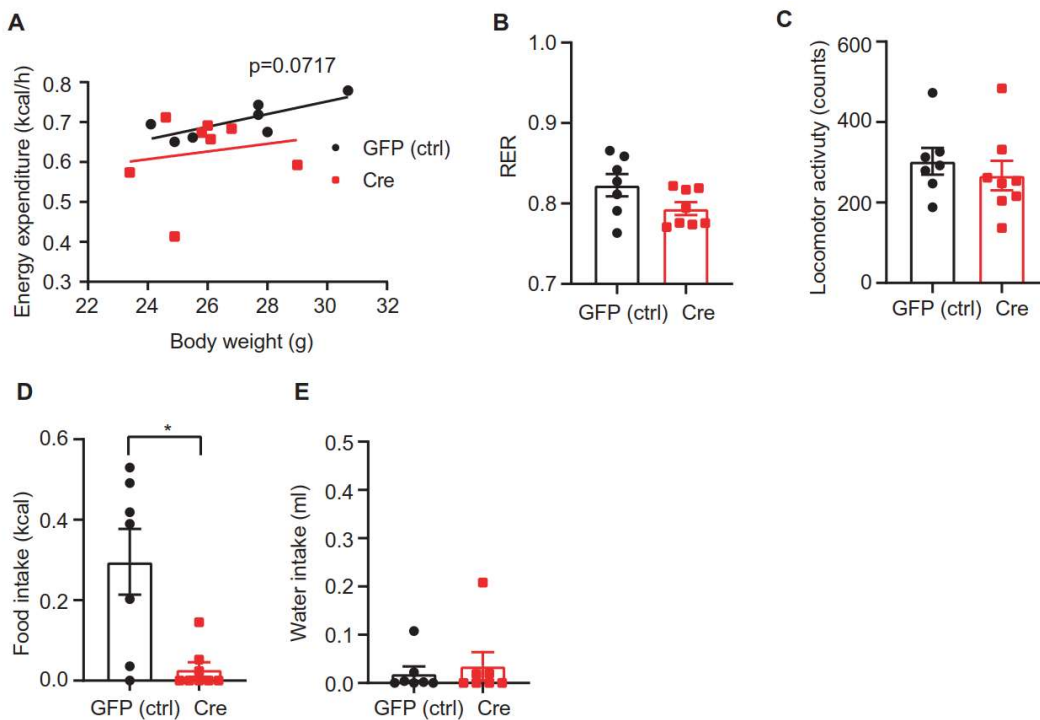
Figure 24. Grin1^{PVN-KO} mice decrease their food intake during cold exposure. (A) EE in relation to body weight during cold exposure of Grin1^{PVN-KO} (Cre) and control (GFP (ctrl)) mice (GFP (ctrl): n=7; Cre: n=8). **(B)** Average RER values during cold exposure of Grin1^{PVN-KO} (Cre) and control (GFP (ctrl)) mice (GFP (ctrl): n=7; Cre: n=8). **(C)** Average

locomotor activity during cold exposure values of Grin1^{PVN-KO} (Cre) and control (GFP (ctrl)) mice (GFP (ctrl): n=7; Cre: n=8). **(D)** Average food intake during cold exposure of Grin1^{PVN-KO} (Cre) and control (GFP (ctrl)) mice (GFP (ctrl): n=7; Cre: n=8). **(E)** Average water intake during cold exposure of Grin1^{PVN-KO} (Cre) and control (GFP (ctrl)) mice (GFP (ctrl): n=7; Cre: n=8). Data are shown as mean ± SEM, unpaired t-test, *p< 0.05. In panel **(A)**, ANCOVA was calculated with R.

To investigate how Grin1^{PVN-KO} mice adapted to the cold, we analysed BAT. After cold exposure, BAT weight of Grin1^{PVN-KO} mice was not different from BAT weight of control mice **(Figure 25A)**. Moreover, there were no differences in the expression of thermogenesis-related genes (*Pgc1α*, *Prdm16* and *Ucp1*) between Grin1^{PVN-KO} and control mice **(Figure 25B)**. However, we observed an increase of BAT UCP1 protein in Grin1^{PVN-KO} mice compared to control **(Figure 25C)**. This result suggests that BAT thermogenesis of Grin1^{PVN-KO} increased under cold exposure compared to control.
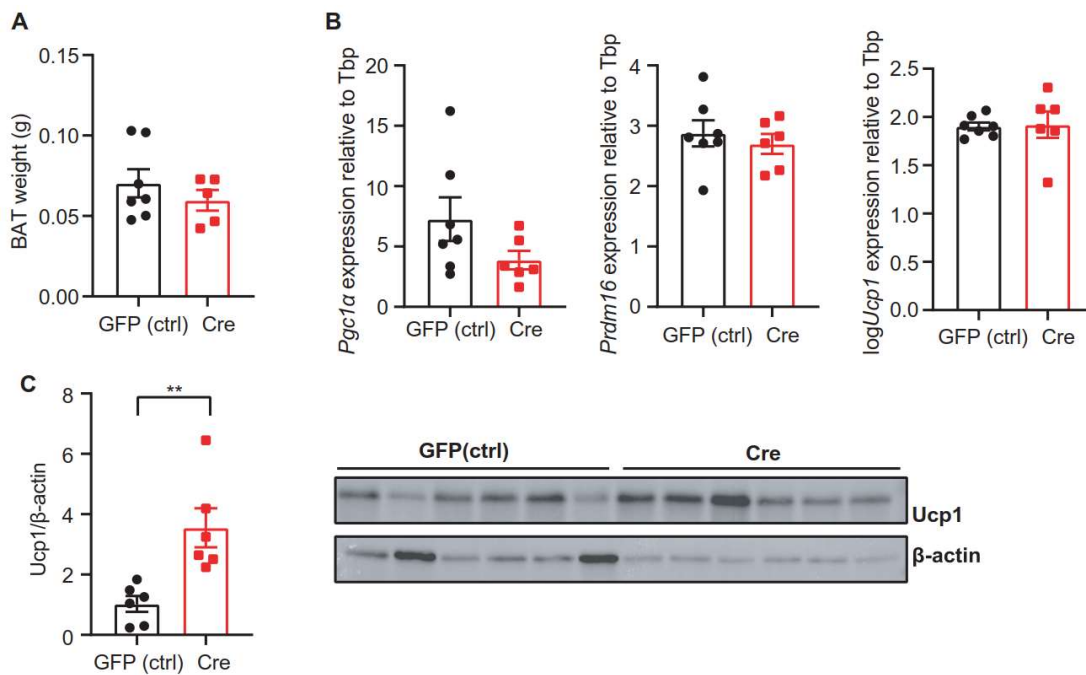
Figure 25. BAT thermogenesis increases in Grin1^{PVN-KO} mice upon cold exposure. (A) BAT weight of Grin1^{PVN-KO} (Cre) and control mice. **(B)** Expression of thermogenesis-related genes in BAT of Grin1^{PVN-KO} (Cre) and control mice (GFP (ctrl)) after cold exposure (GFP (ctrl): n=7; Cre: n=8). **(C)** Western blot and quantifications of UCP1 in BAT cold of Grin1^{PVN-KO} (Cre) and control mice (GFP (ctrl)) after cold exposure (GFP (ctrl): n=7; Cre: n=8). Data are shown as mean ± SEM, unpaired t-test, ** p < 0.01.

5. Discussion

5.1. L-serine supplementation blunts body weight regain after overnight fasting in mice

5.1.1. L-serine supplementation alters liver metabolism and decreases body weight regain after consecutive overnight fasting

In our previous study, L-serine supplementation did not have major effects on metabolism of mice, but altered liver metabolism. Moreover, there was an upregulation of *Pepck* expression in liver, suggesting a potential increase in gluconeogenesis (López-Gonzales *et al.*, 2022). Aiming to further investigate this effect, we reproduced this experiment and conducted PTTs. If L-serine was a substrate or promoted glucose production, we would observe an increase in glucose levels. Even though we did not see differences in glucose levels, we cannot rule out the L-serine impact on gluconeogenesis. Indeed, previous studies show that L-serine is a substrate in gluconeogenesis. L-serine is converted to pyruvate by the action of serine dehydratase (SDH) or to hydroxypyruvate by SPT (Xue *et al.*, 1999; Hagopian, Ramsey and Weindruch, 2005; Milan Holecek, 2022). Both substrates are used in liver for gluconeogenesis. However, SDH pathway plays a major role, especially after caloric restriction (Hagopian, Ramsey and Weindruch, 2005). Furthermore, PTT requires a prior overnight fasting, which has enormous effects on murine metabolism. Sixteen hours of fasting altered water intake, hormone levels such as corticosterone, leptin, neuropeptide Y as well as significantly decreased body weight and tissues mass (Heijboer *et al.*, 2005; Jensen *et al.*, 2013). Moreover, after 16 h fasting gluconeogenic genes such as *Pepck* were upregulated in liver (Heijboer *et al.*, 2005). In addition, an *in vitro* study showed that the presence of fasting hormones (glucagon and corticosterone) induced synergically amino acid-catabolism genes to promote gluconeogenesis in hepatocytes. Furthermore, those hepatocytes produced glucose using L-serine as substrate (Korenfeld *et al.*, 2021). Therefore, one could think that the contribution of L-serine supplementation on gluconeogenesis was blunted by the effect of fasting on metabolism. Insulin and blood glucose levels were not affected in neither *ad libitum* nor overnight fasted mice upon CD or HFD with L-serine supplementation. Nevertheless, the liver was altered with L-serine supplementation in both *ad libitum* and fasted mice. There were changes in glycogen and TG levels. Changes were also clearly displayed on the H&E stainings of this tissue (López-Gonzales *et al.*, 2022). Therefore, we showed that L-serine has an impact on liver, but changes in gluconeogenesis are yet to be elucidated.

Fasting significantly decreases the body weight of mice (Heijboer *et al.*, 2005; Jensen *et al.*, 2013; Tang *et al.*, 2017). In our study, L-serine supplementation significantly decreased the body weight regain after repeated overnight fasting in HFD-fed mice and showed the same trend in CD-fed mice. Moreover, total fat mass and WAT weight decreased in HFD-fed mice. Perigonadal adipocytes were smaller in those mice and *TNFα* inflammatory marker was downregulated. In this context, it is well-known that chronic low-grade adipose tissue inflammation is associated with the development of obesity and metabolic syndrome (Hotamisligil, 2006; Ouchi *et al.*, 2011; Furman *et al.*, 2019). Also, substantial decrease in fat mass in human reduced low-grade inflammation and improved cardiometabolic factors (Sarin *et al.*, 2019). On the other hand, adipose tissue inflammation has also been shown to be necessary for a healthy expansion and remodelling (Wernstedt Asterholm *et al.*, 2014). Thus, impaired adipose tissue inflammation in obese mice after fasting led to lower intensity of adipose tissue loss, thereby to a metabolic inflexibility (Lacerda *et al.*, 2019). However, our findings show that decrease in fat mass in HFD-fed mice after L-serine supplementation and repeated fasting was independent of inflammation. Moreover, these mice showed normal fasting glucose and insulin levels as well as improved TG levels in the liver compared to CD control. Therefore, L-serine supplementation decreased fat mas in fasted mice with no changes in inflammation.

5.1.2. Decrease in body weight regain is not the result of decreased lipogenesis or increased lipolysis in WAT

Overnight fasting affects metabolism of mice, especially decreasing of body weight. Fat accumulation results from an imbalance between lipogenesis and lipolysis/fatty acid oxidation (Kersten, 2001). However, other factors such as food intake, EE and BAT thermogenesis are involved in body weight regulation. Here, possible explanations of the decrease in fat mass from HFD-fed mice supplemented with L-serine might result from the contribution of several events: (1) a decrease in DNL in WAT, (2) an increase in lipolysis in WAT (3) an increase in EE, (4) a decrease in food intake or (5) an increase in BAT thermogenesis. DNL is promoted with substrate availability leading to the activation of several enzymes to convert and store carbohydrates and other substrates as lipids in adipocytes. Even though DNL is essential for metabolic homeostasis, chronic elevation is associated with the development of obesity, T2D, non-alcoholic fatty acid liver disease (NAFLD) and cardiovascular diseases (Kersten, 2001; Solinas, Borén and Dulloo, 2015; Batchuluun, Pinkosky and Steinberg, 2022). Thus, lipogenesis inhibitors are considered potential therapeutic strategies for treating those diseases (Batchuluun, Pinkosky and Steinberg, 2022). DNL takes place in the liver and adipose tissue. However, in our study neither TGs levels nor

histology showed a potential increased DNL in liver. Hence, we analysed the gene expression of key enzyme involved in DNL (*Acaca* and *Fasn*) as well as the transcription factor *Srebp1* in WAT. Nevertheless, no changes were observed in the expression of these genes in PGF or in SCF that could explain the fat mass reduction in fasted mice under HFD supplemented with L-serine. One must bear in mind that DNL is inhibited by fasting (Kersten, 2001), which makes more complex the interpretation of these results.

As well as in DNL, dysfunction of enzymes involved in lipolysis are associated directly with dyslipidaemia and indirectly with pathogenesis of metabolic syndrome, obesity, T2D, NAFLD, cancer and other diseases (Grabner *et al.*, 2021; Wen *et al.*, 2022). Therefore, modulating lipolysis might be a therapeutic approach to treat those metabolic diseases. In T2D patients, lipolysis inhibition might decrease fatty acid flux from hypertrophic adipose tissue, which contributes to insulin resistance and glucose intolerance (Grabner *et al.*, 2021). In case of obese patients, some might have impaired catecholamine-lipolysis in SCF (Langin *et al.*, 2005; Rydén *et al.*, 2022). Furthermore, anti-obesity drugs, beside other actions, may enhance lipolysis (Müller *et al.*, 2022; Wen *et al.*, 2022). However, lipolysis studies in mice are controversial (Langin *et al.*, 2005; Grabner *et al.*, 2021). In adipose tissue, lipolysis involves the hydrolysis of TGs by the consecutive action of ATGL (adipose triglyceride lipase), HSL and MGL (monoacylglycerol lipase). Intracellularly, lipolysis releases fatty acids from lipid droplets into the cytoplasm and, later, into the circulation. Then, peripheral tissues use the free fatty acids as substrate for β-oxidation or ATP production (Nielsen *et al.*, 2014; Grabner *et al.*, 2021). Although ATGL plays an important role in this process, we focused on HSL, which catalyses the rate-limiting step in humans and is associated with dyslipidaemia, hepatic steatosis and T2D (Langin *et al.*, 2005; Grabner *et al.*, 2021). We observed an increasing trend in the expression of active phosphorylated HSL (Ser563 and Ser660) in HFD-fed mice supplemented with L-serine in PGF and SCF. These changes were not statistically significant, however we could not directly rule out that lipolysis in WAT did not contribute at all to the decrease in body weight regain. We should note that fasting is a condition leading to a negative energy balance that requires mobilization of energy stores (Nielsen *et al.*, 2014). Thus, we could also expect an overall increase in lipolysis in all groups. Hence, fasting might blunt lipolysis in adipose tissue in L-serine supplemented mice. In order to evaluate whether L-serine would promote lipolysis as a direct effect on WAT, perigonadal fad pads were incubated with this amino acid. Compared to isoproterenol, a β-adrenergic receptor agonist that promotes lipolysis, L-serine exposure did not increase or promote (together with

isoproterenol) lipolysis. These findings showed that L-serine *per se* did not have a direct lipolytic effect in PGF.

In contrast to WAT, which stores energy, BAT function is to dissipate energy as heat as well as to maintain body temperature in the cold. Thus, promoting BAT activity represents also an approach to treat obesity and other metabolic diseases. BAT thermogenesis is not only activated by the cold, but also by food intake (Saito, 2013; Saito *et al.*, 2020; Onogi and Ussar, 2022). Diet-induced thermogenesis is an adaptive increase in EE after eating aiming to maintain energy balance (Saito *et al.*, 2020). However, fasting impacts substrate availability and promotes glucagon (Onogi and Ussar, 2022), ghrelin and corticosterone secretion (Jensen *et al.*, 2013). Glucagon can activate BAT (Beaudry *et al.*, 2019; Onogi and Ussar, 2022), however mice after 7 h of fasting reduced their body temperature and even become torpid (Brown and Staples, 2010; Jensen *et al.*, 2013). In our fasted mice, a decrease in BAT weight with L-serine supplementation was observed in CD, but in HFD-fed mice also BAT tended to be lighter. In line with these results, lipid droplets in BAT with L-serine supplementation were smaller for both CD and HFD-fed mice. In order to understand these changes in BAT as well as body weight regain in HFD after repeated fasting and changes in liver metabolism, we reproduced our experiment in parallel to a random fed group.

5.1.3. L-serine supplementation does not affect glucose tolerance, but alters liver metabolism in random fed and fasted mice

Body weight regain did not change in CD or HFD-fed random fed mice supplemented with L-serine as we observed in our previous study (López-Gonzales *et al.*, 2022). Although body weight regain was not statistical significant in fasted mice, it decreased in HFD-fed mice supplemented with L-serine in line with our previous results. Mice lose 16% of their weight after overnight fasting (Jensen *et al.*, 2013). Indeed, when compared the random fed with the fasted mice, we observed a clear impact of fasting on the body weight, but it did not impact glucose tolerance.

As we expected, liver weight of fasted mice decreased compared to random fed mice. Several studies reveal how fasting decreases the weight of organs such as the liver, kidney, spleen and thymus, in contrast to the brain and testicles (in male mammals) whose weights are preserved (Longo and Mattson, 2014; Weindruch, Walford and Guthrie, 2018). Differences in weight observed in liver of random fed mice with L-serine supplementation were absent in fasted mice. This event can be explained by the fact that the liver is the main glucose reservoir organ. The

liver stores glucose in the form of glycogen and it is the first source of glucose during fasting (Longo and Mattson, 2014). After overnight fasting in mice, we can expect complete hepatic glycogen depletion. While using up the glucose reservoir during fasting, insulin levels drop, deactivating PI3K-Akt/GSK pathway. Thus, Foxo translocates to the nucleus promoting the transcription of *G6Pase* and *Pepck* genes and, so, activating gluconeogenesis (Barthel, Schmoll and Unterman, 2005; Greer and Brunet, 2005; Han *et al.*, 2016). Gluconeogenesis starts with PC action in the mitochondria, converting pyruvate in oxaloacetate. Then, the latter is converted to phosphonenolpyruvate by Pepck. After some consecutive reactions, glucose-6-phosohate is finally converted to D-glucose by G6Pase (Han *et al.*, 2016). In random fed mice, glucose is obtained from the food; therefore, we may assume that gluconeogenesis is slightly active or not active. Interestingly, L-serine supplementation in CD-fed mice promoted the expression of *Foxo1* and *Pepck*, whereas it downregulated *G6Pase* expression. Potential explanations for this event might be: (1) gluconeogenesis is promoted by L-serine in CD-fed mice at transcriptional level through *Foxo1* and *Pepck*, but glucose availability downregulates *G6Pase* expression; which leads to no changes in glucose production and glucose levels. (2) same as (1), but at translational level, both Pepck and G6Pase expression increased leading to glucose production. Then, *G6Pase* downregulation could mean a compensatory effect for the glucose surplus. However, the contribution is so small that cannot be detected by measuring randomly blood glucose levels. (3) L-serine excess is partly metabolized to pyruvate, providing a substrate and so, promoting gluconeogenesis. In fasted mice, glucose must be produced due to the lack of food. Thus, we can assume that gluconeogenesis is activated. Although in fasted CD and HFD control mice there was an overall *Pepck* upregulation, we detected a downregulation in CD-fed mice supplemented with L-serine. These findings are the opposite to what we observed in random fed mice.

Once the glycogen levels in the liver are depleted during fasting, energy is obtained from free fatty acids, fat-derived glycerol, fat-derived ketone bodies and amino acids (Longo and Mattson, 2014). While the diet had an impact on the liver metabolome after fasting, L-serine supplementation did not. Here, we detected glycogen content after overnight fasting. Interestingly, after one-week L-serine supplementation, we already observed a trend in increasing glycogen content in CD-fed mice, as shown previously in this thesis at eight-week L-serine supplementation. Although, L-serine supplementation affected glycogen content of random fed mice liver in an inverse trend (López-Gonzales *et al.*, 2022). Taken together, these findings reveal that L-serine has an impact on liver glycogen mobilization.

Energy imbalance leads to the development of obesity and metabolic diseases. Thus, restoring energy balance is the main goal to prevent and treat them. Energy balance might be reached by either decreasing energy intake or increasing EE (Blüher, 2019; Ludwig *et al.*, 2022). On the one hand, intermittent fasting, period fasting, caloric restriction and diet restrictions represent some of the strategies to decrease food intake (Longo and Mattson, 2014; Li *et al.*, 2017). On the other hand, increase in physical exercise and cold exposure are approaches to promote increase in EE (Blüher, 2019; Gaesser and Angadi, 2021). Hence, we analyzed the energy metabolism of our mice to understand whether changes in energy balance caused the decrease in body weight regain. Energy balance was reached in all groups of CD-fed mice, since they did not show significant changes in body weight. In random fed mice supplemented with L-serine, balance was reached by decreasing energy expenditure, whereas in fasted mice was by increasing EE. In line with these results, CD-fed mice metabolism adapted their substrate utilization during fasting as well as the amount of food. Metabolic flexibility of CD-fed regardless L-serine supplementation was maintained during cold exposure and thermoneutrality. Even though the interpretation of the results was complex, we observed that HFD-fed mice lost the energy balance seen in CD-fed mice. Furthermore, activity or substrate utilization in these mice did not change.

The ARC of the hypothalamus plays an essential role in the regulation of food intake through the melanocortin system. This system consists of AgRP/NPY and POMC neurons. Activation of these specific neuronal populations leads to promotion of hunger, AgRP/NPY neurons, or satiety, POMC neurons. These neurons are characterized by the expression of NPY and POMC neuropeptides, respectively (Krashes, Lowell and Garfield, 2016; Roh, Song and Kim, 2016). As well as other amino acids, L-serine can cross the blood-brain barrier (Kasai *et al.*, 2011; Cutruzzol *et al.*, 2021; Ye *et al.*, 2021). However, L-serine can also be synthesized *de novo* by astrocytes, providing a substrate to produce D-serine (NMDAR co-agonist) (Neame *et al.*, 2019; Cutruzzol *et al.*, 2021). In this regard, measuring these peptides confirmed the impact on food intake of fasting, particularly clear in CD-fed mice, but not of L-serine supplementation.

5.1.4. L-serine supplementation activates BAT thermogenesis after overnight fasting

The activation of BAT thermogenesis aims to dissipate the energy excess by heat production in the mitochondria. This process involves UCP1, a protein that shuttles protons from the intermembrane space to the mitochondrial matrix and so, uncouples production of ATP with the metabolism of glucose and fatty acids (Saito, 2013; Betz and Enerbäck, 2018; Saito *et al.*, 2020). Fasting decreased BAT weight, however L-serine supplementation did not. While L-serine tended

to upregulate *Pgc1α* (transcription factor that stimulates mitochondrial biogenesis (Kang and Ji, 2012)) and *Prdm16* (transcriptional coregulatory involved in function and determination of brown and beige adipocytes (Chi and Cohen, 2016)) in CD fasted mice, did not change *Ucp1* gene expression. Nevertheless, L-serine supplementation increased expression of UCP1 protein in CD-fed mice, suggesting that, in line with results in EE, it increased BAT thermogenesis.

Changes in energy balance are sensed by AMPK in many tissues. Activation of AMPK occurs upon alterations in cellular AMP/ATP ratio. This activation results in the modulation of metabolism leading to catabolism promotion to stimulate ATP production and anabolism inhibition to decrease ATP consumption (Cantó *et al.*, 2009; Herzig and Shaw, 2018; Belli and Yaman, 2020). For instance, in skeletal muscle, after exercise, AMPK regulates EE through de-acetylation and activation of PGC1α as well as activation of SIRT1 (Cantó *et al.*, 2009). Moreover, both AMPK and PGC1α activation are necessary for the increase in mitochondrial biogenesis due to energy deprivation (Cantó and Auwerx, 2009). In the liver, AMPK activation limits the expression of genes involved in gluconeogenesis: *G6Pase* and *Pepck*. However, hepatic AMPK is not essential for hepatic gluconeogenesis inhibition (Day, Ford and Steinberg, 2017). Nevertheless, the activation of hepatic AMPK leads to phosphorylation of acetyl-CoA carboxylase (ACC), which controls lipid synthesis and fatty acid oxidation, important for preventing NAFLD (Fullerton *et al.*, 2013; Day, Ford and Steinberg, 2017). Metformin, a drug used for controlling glucose levels in T2D, activates AMPK decreasing hepatic glucose production and improving liver sensitivity. However, these effects are not mediated by hepatic AMPK. Studies in rats showed that intestinal (duodenal) AMPK is the responsible for the decrease in hepatic glucose production by metformin, which is the result of exciting neuronal circuits signaling to the brain, through GLP-1 receptor and protein kinase A (PKA) communication (Duca *et al.*, 2015; Smith and Steinberg, 2015; Day, Ford and Steinberg, 2017). AMPK expression in the hypothalamus plays an opposite role as in the other tissues here described. Activation of hypothalamic AMPK results in body weight gain by regulating food intake, insulin sensitivity, BAT thermogenesis and WAT browning (Wen *et al.*, 2022). Moreover, there is evidence showing that inhibition of AMPK in neurons of the ARC and VMN of the hypothalamus led to a decrease in body weight and activation of BAT thermogenesis (Liu, Xu and Hu, 2020; Milbank *et al.*, 2021; Wen *et al.*, 2022). In WAT, activation of AMPK occurs due to an increase in lipolysis, as an energy-sparing mechanism (Macpherson *et al.*, 2016). Nevertheless, it is also necessary to maintain basal lipolysis (S. Kim *et al.*, 2016). Furthermore, AMPK activation is essential for browning of adipocytes by maintaining PCG1α basal levels (Wan *et al.*, 2014; Day, Ford and Steinberg, 2017) and increasing PRDM16 activity (Chi and Cohen,

2016; Day, Ford and Steinberg, 2017). Additionally, chronic activation of AMPK in obese mice improved glucose tolerance, protected them from body weight gain and WAT expansion (Wu *et al.*, 2018). However, adipose tissue-specific AMPK knockout in mice did not affect glucose metabolism under a CD (Choi *et al.*, 2019). In BAT, AMPK is not only important for maintaining its metabolic function, but also for its development. AMPK knockout in BAT resulted in reduction of PRDM16 expression and reduced cold tolerance (Yang *et al.*, 2016); whereas AMPK hyperactivation led to increased UCP1 expression and increased cold tolerance as well as increased mitochondrial biogenesis and PCG1α activation (Zhang *et al.*, 2015; Yan *et al.*, 2016). Interestingly, activation of intestinal (E. Zhang *et al.*, 2022) and skeletal muscle (Kim, Kim and Seong, 2022) AMPK and inhibition of hypothalamic AMPK promoted BAT thermogenesis (Milbank *et al.*, 2021). Therefore, BAT thermogenesis may be influenced by BAT AMPK activity as well as AMPK activity from other tissues. Because of all AMPK metabolic functions involving energy homeostasis, it is considered a target for the treatment of obesity and other metabolic diseases (Day, Ford and Steinberg, 2017; Herzig and Shaw, 2018). In fact, many pharmacological agents base their mechanism of action on directly or indirectly activating AMPK to treat metabolic syndrome, cancer and other diseases (J. Kim *et al.*, 2016; Herzig and Shaw, 2018). Serine supplementation in HFD-fed mice activated liver AMPK and modulated glutathione synthesis-related gene expression, protecting them from diet-induced oxidative stress (Zhou, He, Zuo, Zhang, Wan, Long, *et al.*, 2018). However, we did not observe any changes in liver AMPKα phosphorylation (data not shown). Moreover, serine supplementation protected mice from intestinal inflammation by increasing phosphorylation of intestinal AMPK (Zhou, Zhang, *et al.*, 2017) and improved microbiota functions in inflamed gut (Kitamoto *et al.*, 2020). Unfortunately, we do not know whether intestinal AMPK activity changed in our mice upon HFD and/or L-serine supplementation or if any potential changes in intestinal AMPK could have affected BAT thermogenesis. Neither could we rule out whether inhibition of AMPK in the hypothalamus contributed to the phenotype observed in these mice. Nevertheless, we observed increased phosphorylation of BAT AMPKα in CD-fed mice supplemented with L-serine both *ad libitum* and after fasting. Therefore, this suggests that L-serine supplementation modulates BAT thermogenesis through AMPKα activity in mice leading to a decrease in body weight gain after repeated fasting; however, this might not be the only event contributing. Fasting is an enormous metabolic challenge, which also activates AMPK in many tissues (Day, Ford and Steinberg, 2017; Belli and Yaman, 2020), but also in the hypothalamus having an opposite role. Moreover, hypothalamic AMPK activity is increased upon HFD leading to an increase in food intake (Wang and Cheng, 2018). Interestingly, chronic L-serine supplementation (24 months) was shown to

reduce food intake, body weight gain and decrease oxidative stress in the hypothalamus (Zhou, Zhang, *et al.*, 2018). Thus, studying the effect of L-serine on the hypothalamus of HFD-fed mice could provide compelling insights.

5.1.5. L-serine supplementation activates primary brown adipocytes

BAT is an organ rich in mitochondria, which are the organelles responsible for its thermogenic capacity (van der Vaart, Boon and Houtkooper, 2021). AMPK in brown adipocytes regulates of mitochondria homeostasis through the activation of mitochondrial biogenesis, mitochondrial fission and mitochondrial fusion (Mottillo *et al.*, 2016; Day, Ford and Steinberg, 2017; Wang and Cheng, 2018; van der Vaart, Boon and Houtkooper, 2021). Moreover, it is essential for BAT mitochondria quality (Mottillo *et al.*, 2016). Therefore, AMPK mitochondrial health regulation is essential for BAT activity. *In vitro* studies have shown that serine is crucial for mitochondrial metabolism (Gao *et al.*, 2018) and its supplementation prevents mitochondrial damage (Kim *et al.*, 2019). We observed that with L-serine exposure not only phosphorylation of AMPK increased in primary brown adipocytes after 10 min of, but also maximal mitochondrial respiration. Taken together, these findings suggest that L-serine increases mitochondrial activity in primary brown adipocytes.

In conclusion, L-serine supplementation together with fasting might improve the HFD-metabolic alterations and prevented mice from becoming obese, partly by increasing BAT thermogenesis. However, we cannot rule out another mechanism underlying this effect on energy balance. Taken altogether, L-serine supplementation represents a safe alternative and thereby help tackle one of the major problems of current obesity therapies.

5.2. Metabolic effects of NMDAR knockout in PVN neurons of Grin1$^{flox/flox}$ mice
5.2.1. PVN-NMDAR knockout validation of AAV-injected Grin1$^{flox/flox}$ mice

Validating the NMDAR knockout was the most important step before studying the role of NMDARs in the PVN of Grin1$^{flox/flox}$ mice. By doing so, we would ensure that any changes in phenotype and whole-body metabolism were a consequence of the loss of these receptors in the PVN of the knockout mice. Our results on the NMDAR currents recordings in GFP-expressing neurons of GFP (control) and Cre mice not only demonstrated that both GFP-Cre and GFP control AAV vectors infected neurons, but also that the GFP-Cre AAV vector efficiently deleted the NMDARs in those PVN neurons of Grin1$^{flox/flox}$ mice. Nevertheless, each mouse brain was analyzed to whether the GFP-expressing neurons were PVN neurons. In order to do that, we studied the PVN-

containing brain slices of all mice. On the PVN-containing slices, we observed that PVN neurons were efficiently targeted by the viruses. However, GFP expression was not homogenous in all mice. There was some variability in the total number of GFP-expressing neurons and the number GFP-expressing neurons between hemispheres. One should bear in mind that NMDAR currents recordings were performed two weeks after injection, while the analysis of the PVN brain slices was carried out at the end of each experiment (12 weeks) which is 14 weeks post-injection. Within this window of time, changes in fluorescence intensity might have happened. Stereotaxic injections with AAV vectors require small volumes of virus, reduce off-targeted regions and achieve regional expression, but the surgeries are invasive and there is a potential damage in the targeted area (Haery *et al.*, 2019). Nevertheless, evidence shows that AAV techniques are safe for neurons and that GFP expression is robust and stable over time (Chamberlin *et al.*, 1998; Haery *et al.*, 2019) and so it was for our mice.

Combining GFP immunostaining with *in situ* hybridization for GRIN1 helped us to visualize the GRIN1 loss of the GFP-expressing neurons injected with the GFP-Cre AAV vector. There was a decrease in GRIN1 signal in those GFP-expressing neurons of the GFP-Cre-AVV-injected mice. However, there was still some GRIN1 signal, which was difficult to discern whether it was from the GFP-expressing neurons, non-GFP-expressing neurons or part of the background signal. In summary, we could validate the NMDAR knockout by identifying the loss of NMDAR currents and GRIN1 signal in GFP-expressing neurons in the PVN of Grin1$^{flox/flox}$ mice.

5.2.2. Grin1^{PVN-KO} mice did not show phenotypic differences compared to control mice

Over the 12 weeks of the experiment, both Grin1^{PVN-KO} and control mice showed similar body weight as well as glucose levels in blood. In line with body weight, body composition showed no differences between groups. All these findings indicated that deletion of PVN-NMDARs did not trigger metabolic effects resulting in changes in body weight and/or composition and blood glucose levels in mice.

Glucose tolerance and insulin levels were thus not affected by the deletion of PVN-NMDARs. A study previously mentioned on chronic D-serine supplementation suggested that hypothalamic NMDARs may regulate insulin secretion via sympathetic stimulation. In this study, PVN neuronal activity was also altered by supplementation with the NMDAR co-agonist D-serine. Furthermore, they showed that supplementation with a low concentration of D-serine (0.1%) could improve insulin secretion (Suwandhi *et al.*, 2018). Thus, by supplementing our mice with 0.1% D-serine,

we expected to observe differences in insulin secretion in the control mice. However, not only there were no changes in insulin secretion in the control mice, but also no changes in the Grin1^{PVN-KO} mice after two weeks of 0.1% D-serine supplementation. Moreover, insulin secretion did not change in Grin1^{PVN-KO} mice after an oral glucose bolus compared to control. There might be several possible explanations for our observations: (1) NMDARs only in a specific neuronal population in the PVN are involved in the regulation of insulin secretion in the pancreas; (2) NMDARs in other hypothalamic nuclei, not the PVN, are responsible for insulin secretion regulation. (3) PVN-NMDARs might be involved in the insulin secretion regulation but loss of action after NMDAR deletion is compensated by other parts brain-pancreas axis. Regarding the first point, the AAV vector used targeted neurons indiscriminately; however, different neuronal populations with different functions have been identified in the PVN. For instance, melanocortin-4-receptor-expressing neurons (PVN^{MCR4}) involved in satiety (Fenselau *et al.*, 2017) and PVN corticotrophin-releasing hormone neurons (PVN^{CRH}), which regulate stress responses (Yuan *et al.*, 2019). Also, oxytocin PVN neurons (PVN^{OXT}), which have shown to suppress insulin secretion by acting on β-cells (Papazoglou *et al.*, 2022) and, in turn, are regulated by central insulin (Zhang *et al.*, 2018). For the second and third point, one must consider that PVN is a hub connecting different hypothalamic nuclei and its neuronal activity might be influenced by the activity of nuclei that innervate it (Jennifer W. Hill, 2012). Pseudorabies neuronal tracing studies have shown that both parasympathetic and sympathetic nerves innervate pancreatic islets. These nerves emanate in other nuclei in the hypothalamus, such as ARC, VMN and LH, but link with PVN as well (Rosario *et al.*, 2016; Faber *et al.*, 2020). Interestingly, in the D-serine study, neuronal activities of ARC, VMN and LH were also altered (Suwandhi *et al.*, 2018). Nevertheless, further investigations are needed to elucidate the exact role or contribution of hypothalamic NMDARs to the regulation of insulin secretion.

5.2.3. Grin1^{PVN-KO} mice had lower EE at room temperature and decreased their food intake during cold exposure

At room temperature, Grin1^{PVN-KO} mice showed a lower EE compared to control, while the other parameters such as RER, locomotor activity and food and water intake did not change. Under cold exposure, Grin1^{PVN-KO} mice could adapt their EE, but they did not eat during 4 h of exposure. Regarding BAT, room and cold temperatures led to opposite effects. While there was a decrease in weight with no changes in UCP1 expression at room temperature, there were no changes in weight but an increase in UCP1 expression at 4 °C. Nevertheless, with the data available on our Grin1^{PVN-KO} mouse model, it is still difficult to elucidate why the different temperatures resulted in

these distinct events. Energy homeostasis is maintained by the balance between EE and energy intake (Tran *et al.*, 2022). In addition, BAT thermogenesis is an important component in energy homeostasis regulation as well as body temperature, especially at low temperatures. Skin thermoreceptors and changes in core temperature trigger alterations in sympathetic outflow to BAT through a complex thermoregulatory neural network (Morrison, Madden and Tupone, 2014; Yang and Ruan, 2015). Moreover, diet and feeding also contribute to BAT thermogenesis regulation as well (Morrison, Madden and Tupone, 2014). There are several hypothalamic nuclei involved in BAT thermogenesis regulation such as POA, DMN, ARC, VMN and PVN that, in turn, regulate energy homeostasis (Labbé *et al.*, 2015; Yang and Ruan, 2015). In the case of PVN, results are controversial. While injection of NMDA in the PVN inhibited cold-evoked BAT activity (Madden and Morrison, 2009), stimulation with glutamate activated BAT thermogenesis (Amir, 1990). Neuronal populations within the PVN have also shown to possess different roles regarding the activation of BAT. On the one hand, some PVN neurons promoted BAT activity. For instance, two different studies showed that the ablation of PVN^{OXT} neurons decreases BAT and core temperature under cold exposure, suggesting that this neuronal population plays an important role in cold-stress response (Kasahara *et al.*, 2007; Xi *et al.*, 2017). BAT thermogenesis is induced after treatment with melanotan II (MC4R agonist) on PVN^{MC4R} neurons (Song *et al.*, 2008). Furthermore, ablation of Sim1 (essential transcription factor for PVN neurons development) reduced EE and BAT temperature (Balthasar *et al.*, 2005). On the other hand, other neuronal populations in the PVN inhibit BAT activity. Stimulation of glutamatergic anteroventral and periventricular portions of medial preoptic area (apMPOA), which project to the ARC and PVN, decreased food intake, inhibited BAT thermogenesis and increased heat dissipation. Furthermore, ablation of apMPOA-recipient PVN neurons increased food intake at high (35 °C), room and low temperature (10 °C), with no differences in rectal temperature. Thus, suggesting that this PVN neuronal population regulates feeding behavior and BAT thermogenesis upon changes in temperature (Qian *et al.*, 2022). NPY is neuropeptide that stimulates food intake and reduces EE. A study on NPY effects found that arcuate nucleus NPY-expressing (ARC^{NPY}) neurons regulated PVN tyrosine hydroxylase-expressing (PVNTH) neurons suppression of sympathetic activity of BAT. Thus, NPY signaling to PVNTH neurons decreased BAT thermogenesis and temperature as well as UCP1 expression (Shi *et al.*, 2013).

Based on our findings, we postulate that NMDARs in the PVN have a direct or indirect role in the regulation of energy homeostasis and that their role changes depending on ambient temperature.

However, further investigations are required to address the neuronal populations in the PVN or in other hypothalamic nuclei involved and the impact of temperature.

6. Conclusions and future perspectives

The prevalence of obesity and T2D are exponentially rising because of the unlimited access to high-calorie with low-nutritional value food, low physical activity as well as social, environmental and genetic factors. Current therapeutic approaches have not succeeded in preventing or treating these diseases in many cases. Indeed, it is not surprising owing to the complexity of their etiology and the factors involved in their development. Precision or personalized medicine might be key to find the best solution for each individual. Hence, it is essential to explore and investigate all potential mechanisms not only involved in the development of these diseases but also those mechanisms that might help to prevent or attenuate them. Unbalanced energy homeostasis leads to development of metabolic diseases such as obesity and T2D. Therefore, studying the different components of energy homeostasis (EE, food intake and BAT thermogenesis) can help us find alternative strategies to return to balance and so, to metabolic health. In this regard, the first aim of this thesis was to elucidate the metabolic effects of L-serine in mice. L-serine is a safe and accessible dietary supplement associated with many beneficial metabolic effects. Here, we discovered that supplementation with L-serine together with overnight fasting decreases body weigh regain in CD but significantly in HFD-fed mice while no other metabolic parameters were affected. This decrease in body weight regain was due to an activation of BAT thermogenesis. Moreover, we observed that L-serine supplementation also activated the metabolism of brown adipocytes and promoted maximal mitochondrial respiration. Although we analysed the liver in detail, L-serine effects on this tissue are not fully elucidated. Further experiments should be carried out to discern the role of L-serine in hepatic glucose metabolism, specifically its contributions to gluconeogenesis in *ad libitum* mice and glycogen metabolism. Moreover, owing to its safety and accessibility, L-serine is a good candidate to be tested in obese and pre-diabetic humans. Based on the utilization of L-serine as treatment in neurological diseases, additional assessment of L-serine effects (with or without fasting) in the CNS may provide very valuable insights. In fact, L-serine enantiomer, D-serine exerts its function through NMDARs in both the CNS and pancreas. D-serine co-activation of NMDARs in the CNS and pancreas was the basis of our second aim, in which we addressed the potential role of NMDARs in the regulation of insulin secretion as well as whole-body metabolism by specific knockout in the PVN of the hypothalamus of Grin1$^{flox/flox}$ mice. Although we encountered some challenges in the validation of the knockout, we demonstrated that NMDARs were deleted in GFP-expressing neurons of AAV-GFP-Cre-injected Grin1$^{flox/flox}$ mice by the loss of NMDAR currents and GRIN1 expression. We did not observe any changes in insulin secretion in the Grin1^{PVN-KO} mice. However, we could not rule out

that NMDARs regulate pancreatic insulin secretion in a specific neuronal population in the PVN or elsewhere in the hypothalamus. Future research should investigate NMDARs role in insulin secretion regulation in other hypothalamic nuclei such as ARC, VMN and LH as well as in specific neuronal populations in the PVN. Nevertheless, the striking findings in the Grin1^{PVN-KO} mice were the changes in EE, food intake and BAT thermogenesis at different ambient temperatures. At room temperature, they decreased their EE and BAT weight, whereas, at cold temperature, energy expenditure increased to control levels, decreased their food intake and increased BAT thermogenesis. Further research should focus on identifying the neuronal populations in the PVN involved and discerning the contribution of the ambient temperature.

Taken together, the findings presented in this thesis show two different mechanisms that are involved in the regulation of energy homeostasis through EE and BAT activity modulation. Our data on L-serine supplementation provides a potential approach to tackle obesity and T2D, while our results on the role of PVN-NMDARs contribute to and might be a precedent for future studies on hypothalamic control of energy homeostasis.

7. References

Acuna-hidalgo, R. *et al.* (2014) 'Neu-Laxova Syndrome Is a Heterogeneous Metabolic Disorder Caused by Defects in Enzymes of the L-Serine Biosynthesis Pathway', *The American Journal of Human Genetics.* The American Society of Human Genetics, 95, pp. 285–293. doi: 10.1016/j.ajhg.2014.07.012.

Adell, A. (2020) 'Brain NMDA receptors in schizophrenia and depression', *Biomolecules*, 10(6), pp. 1–27. doi: 10.3390/biom10060947.

Amir, S. (1990) 'Stimulation of the paraventricular nucleus with glutamate activates interscapular brown adipose tissue thermogenesis in rats', *Brain Research*, 508(1), pp. 152–155. doi: 10.1016/0006-8993(90)91129-5.

Arimura, Emi Ushika Miharu, Horiuchi, M. (2021) 'Higher Branched-chain Amino Acids and Lower Serine Exist in the Plasma of Nondiabetic Mice : A Comparison Between High- and Low-protein Diet Conditions', *In vivo*, 35, pp. 1555–1560. doi: 10.21873/invivo.12410.

Arslanian, S. *et al.* (2018) 'Evaluation and management of youth-onset type 2 diabetes: A position statement by the American diabetes association', *Diabetes Care*, 41(12), pp. 2648–2668. doi: 10.2337/dci18-0052.

Ashley, E. A. (2016) 'Towards precision medicine', *Nature Reviews Genetics*, 17(9), pp. 507–522. doi: 10.1038/nrg.2016.86.

Aslan, H. *et al.* (2002) 'Prenatal diagnosis of Neu-Laxova syndrome : a case report', *BMC Pregnancy and Childbirth*, 4(Figure 3), pp. 2000–2003.

Athanasaki, A. *et al.* (2022) 'Type 2 Diabetes Mellitus as a Risk Factor for Alzheimer's Disease: Review and Meta-Analysis', *Biomedicines*, 10(4). doi: 10.3390/biomedicines10040778.

Bach, E. C., Halmos, K. C. and Smith, B. N. (2015) 'Enhanced NMDA receptor-mediated modulation of excitatory neurotransmission in the dorsal vagal complex of streptozotocin-treated, chronically hyperglycemic mice', *PLoS ONE*, 10(3), pp. 1–21. doi: 10.1371/journal.pone.0121022.

Balthasar, N. *et al.* (2005) 'Divergence of melanocortin pathways in the control of food intake and energy expenditure', *Cell*, 123(3), pp. 493–505. doi: 10.1016/j.cell.2005.08.035.

Barthel, A., Schmoll, D. and Unterman, T. G. (2005) 'FoxO proteins in insulin action and metabolism', 16(4). doi: 10.1016/j.tem.2005.03.010.

Batchuluun, B., Pinkosky, S. L. and Steinberg, G. R. (2022) 'Lipogenesis inhibitors: therapeutic opportunities and challenges', *Nature Reviews Drug Discovery.* Springer US, 21(4), pp. 283–305. doi: 10.1038/s41573-021-00367-2.

Batterham, R. L. (2022) 'Weight stigma in healthcare settings is detrimental to health and must be eradicated', *Nature Reviews Endocrinology.* Springer US, 18(7), pp. 387–388. doi: 10.1038/s41574-022-00686-3.

Beaudry, J. L. *et al.* (2019) 'The brown adipose tissue glucagon receptor is functional but not essential for control of energy homeostasis in mice', *Molecular Metabolism*. Elsevier GmbH, 22(February), pp. 37–48. doi: 10.1016/j.molmet.2019.01.011.

Belli, İ. and Yaman, M. (2020) 'The Role of AMPK in the Regulation of Appetite and Energy Homeostasis: Role of AMPK in Appetite', *International Journal of Innovative Research and Reviews*, 4(1), pp. 25–31.

Benarroch, E. E. (2018) 'Glutamatergic synaptic plasticity and dysfunction in Alzheimer disease: Emerging mechanisms', *Neurology*, 91(3), pp. 125–132. doi: 10.1212/WNL.0000000000005807.

Betz, M. J. and Enerbäck, S. (2018) 'Targeting thermogenesis in brown fat and muscle to treat obesity and metabolic disease', *Nature Reviews Endocrinology*. Nature Publishing Group, 14(2), pp. 77–87. doi: 10.1038/nrendo.2017.132.

Blüher, M. (2019) 'Obesity : global epidemiology and pathogenesis'. Springer US, 15(May). doi: 10.1038/s41574-019-0176-8.

Boslem, E., Meikle, P. J. and Biden, T. J. (2012) 'Roles of ceramide and sphingolipids in pancreatic b-cell function and dysfunction', (June), pp. 177–187.

Brehm, B. J. and D'Alessio, D. A. (2008) 'Weight loss and metabolic benefits with diets of varying fat and carbohydrate content: Separating the wheat from the chaff', *Nature Clinical Practice Endocrinology and Metabolism*, 4(3), pp. 140–146. doi: 10.1038/ncpendmet0730.

Breslow, D. K. and Weissman, J. S. (2010) 'Membranes in Balance: Mechanisms of Sphingolipid Homeostasis', *Molecular Cell*, 40(2), pp. 267–279. doi: 10.1016/j.molcel.2010.10.005.

Brown, J. C. L. and Staples, J. F. (2010) 'Mitochondrial metabolism during fasting-induced daily torpor in mice', *Biochimica et Biophysica Acta - Bioenergetics*. Elsevier B.V., 1797(4), pp. 476–486. doi: 10.1016/j.bbabio.2010.01.009.

Brychta, R. J. and Chen, K. Y. (2017) 'Cold-induced thermogenesis in humans', *European Journal of Clinical Nutrition*. Nature Publishing Group, 71(3), pp. 345–352. doi: 10.1038/ejcn.2016.223.

Cantó, C. *et al.* (2009) 'AMPK regulates energy expenditure by modulating NAD + metabolism and SIRT1 activity', *Nature*, 458(7241), pp. 1056–1060. doi: 10.1038/nature07813.

Cantó, C. and Auwerx, J. (2009) 'PGC-1α, SIRT1 and AMPK, an energy sensing network that controls energy expenditure', *Current Opinion in Lipidology*, 20(2), pp. 98–105. doi: 10.1097/MOL.0b013e328328d0a4.

Cavalieri, R. *et al.* (2022) 'Activating ligands of Uncoupling protein 1 identified by rapid membrane protein thermostability shift analysis', *Molecular Metabolism*. The Authors, 62(June), p. 101526. doi: 10.1016/j.molmet.2022.101526.

Chamberlin, N. L. *et al.* (1998) 'Recombinant adeno-associated virus vector: use for transgene expression and anterograde tract tracing in the CNS', *Brain Res*, 793(1–2), pp. 169–175.

Chen, R. *et al.* (2020) 'Serine administration as a novel prophylactic approach to reduce the severity of acute pancreatitis during diabetes in mice', *Diabetologia*, 63(9), pp. 1885–1899. doi: 10.1007/s00125-020-05156-x.

Cheng, H. *et al.* (2021) 'Dietary compounds regulating the mammal peripheral circadian rhythms and modulating metabolic outcomes', *Journal of Functional Foods*. Elsevier Ltd, 78, p. 104370. doi: 10.1016/j.jff.2021.104370.

Cheng, L. *et al.* (2021) 'Brown and beige adipose tissue: a novel therapeutic strategy for obesity and type 2 diabetes mellitus', *Adipocyte*. Taylor & Francis, 10(1), pp. 48–65. doi: 10.1080/21623945.2020.1870060.

Cheng, M. *et al.* (2022) 'Prevalence of hyperhomocysteinemia (HHcy) and its major determinants among hypertensive patients over 35 years of age', *European Journal of Clinical Nutrition*. Springer US, 76(4), pp. 616–623. doi: 10.1038/s41430-021-00983-6.

Cheung, B. M. Y., Cheung, T. T. and Samaranayake, N. R. (2013) 'Safety of antiobesity drugs', *Therapeutic Advances in Drug Safety*, 4(4), pp. 171–181. doi: 10.1177/2042098613489721.

Chi, J. and Cohen, P. (2016) 'The multifaceted roles of PRDM16: Adipose biology and beyond', *Trends in Endocrinology and Metabolism*. Elsevier Ltd, 27(1), pp. 11–23. doi: 10.1016/j.tem.2015.11.005.

Choi, R. H. *et al.* (2019) 'Adipose tissue-specific knockout of AMPKα1/α2 results in normal AICAR tolerance and glucose metabolism', *Biochemical and Biophysical Research Communications*, 519(3), pp. 633–638. doi: 10.1016/j.bbrc.2019.09.049.

Chow, A. *et al.* (2022) 'Trends in the Utilization of Intragastric Balloons: a 5-Year Analysis of the MBSAQIP Registry', *Obesity Surgery*. Springer US, 32(5), pp. 1649–1657. doi: 10.1007/s11695-022-06005-z.

ClinicalTrials.gov (2016) *Serine Supplementation for Obese Subjects With Fatty Liver Disease. NCT02599038*. Available at: https://beta.clinicaltrials.gov/study/NCT02599038?patient=L-serine&locStr=&distance=0&page=2&tab=results (Accessed: 22 July 2022).

ClinicalTrials.gov (2017) *Phase IIa L-serine Trial for eAD (LSPI-2). NCT03062449*. Available at: https://beta.clinicaltrials.gov/study/NCT03062449?patient=L-serine alzheimer&locStr=&distance=0 (Accessed: 11 July 2022).

ClinicalTrials.gov (2019) *Serine and Fenofibrate Study in Patients With MacTel Type 2 (SAFE). NCT04907084*. Available at: https://beta.clinicaltrials.gov/study/NCT04907084?patient=L-serine&locStr=&distance=0&page=3 (Accessed: 25 July 2022).

ClinicalTrials.gov (2020) *Tolerability and Efficaty of L-serine in Patients With GRIN-related Encephalopathy. NCT04646447*. Available at: https://beta.clinicaltrials.gov/study/NCT04646447?patient=NCT04646447&locStr=&distance=0 (Accessed: 13 June 2022).

ClinicalTrials.gov (2021) *D-serine Supplementation for Depression. NCT04721249*. Available at:

https://beta.clinicaltrials.gov/study/NCT04721249?patient=L-serine&locStr=&distance=0&page=2 (Accessed: 12 July 2022).

ClinicalTrials.gov (2022) *D-serine AudRem: R33 Phase. NCT05046353*. Available at: https://beta.clinicaltrials.gov/study/NCT05046353?patient=L-serine&locStr=&distance=0 (Accessed: 12 July 2022).

Colombarolli Stivaleti, M., Oliveira, J. De and Cordás, T. A. (2022) 'Craving for carbs : food craving and disordered eating in low - carb dieters and its association with intermittent fastingli, Maíra Stivaleti Oliveira, Jô'. Springer International Publishing, (0123456789).

Van Der Crabben, S. N. *et al.* (2013) 'An update on serine deficiency disorders', *Journal of Inherited Metabolic Disease*, 36(4), pp. 613–619. doi: 10.1007/s10545-013-9592-4.

Curioni, C. C. and Lourenço, P. M. (2005) 'Long-term weight loss after diet and exercise: A systematic review', *International Journal of Obesity*, 29(10), pp. 1168–1174. doi: 10.1038/sj.ijo.0803015.

Cutruzzol, F. *et al.* (2021) 'The Emerging Role of Amino Acids of the Brain Microenvironment in the Process of Metastasis Formation'.

David L. Nelson, M. M. C. (2008) *Lehninger Principles of Biochemistry*. 6th edn.

Davis, D. A. *et al.* (2020) 'L -Serine Reduces Spinal Cord Pathology in a Vervet Model of Preclinical ALS / MND', *J Neuropatholo Exp Neurol*, 79(4), pp. 393–406. doi: 10.1093/jnen/nlaa002.

Day, E. A., Ford, R. J. and Steinberg, G. R. (2017) 'AMPK as a Therapeutic Target for Treating Metabolic Diseases', *Trends in Endocrinology and Metabolism*. Elsevier Ltd, 28(8), pp. 545–560. doi: 10.1016/j.tem.2017.05.004.

Dietrich, M. O. and Horvath, T. L. (2013) 'Hypothalamic control of energy balance : insights into the role of synaptic plasticity'. Elsevier Ltd, 36(2), pp. 65–73.

Docherty, N. G. and le Roux, C. W. (2020) 'Bariatric surgery for the treatment of chronic kidney disease in obesity and type 2 diabetes mellitus', *Nature Reviews Nephrology*. Springer US, 16(12), pp. 709–720. doi: 10.1038/s41581-020-0323-4.

Domaszewski, P. *et al.* (2022) 'Effect of a six-week times restricted eating intervention on the body composition in early elderly men with overweight', *Scientific Reports*. Nature Publishing Group UK, 12(1), pp. 1–6. doi: 10.1038/s41598-022-13904-9.

Duca, F. A. *et al.* (2015) 'Metformin activates a duodenal Ampk-dependent pathway to lower hepatic glucose production in rats', *Nature Medicine*, 21(5), pp. 506–511. doi: 10.1038/nm.3787.

Due, A. *et al.* (2008) 'Comparison of 3 ad libitum diets for weight-loss maintenance, risk of cardiovascular disease, and diabetes: A 6-mo randomized, controlled trial', *American Journal of Clinical Nutrition*, 88(5), pp. 1232–1241. doi: 10.3945/ajcn.2007.25695.

Dunlop, R. A., Powell, J. T., *et al.* (2018) 'L -Serine-Mediated Neuroprotection Includes the Upregulation of the ER Stress Chaperone Protein Disulfide Isomerase (PDI)', *Neurotox Res*. Neurotoxicity Research, 33, pp. 113–122. doi: 10.1007/s12640-017-9817-7.

Dunlop, R. A., Powell, J., *et al.* (2018) 'Mechanisms of L -Serine Neuroprotection in vitro Include ER Proteostasis Regulation', *Neurotox REs*. Neurotoxicity Research, (33), pp. 123–132.

Dunlop, R. A. and Carney, J. M. (2021) 'Mechanisms of L -Serine-Mediated Neuroprotection Include Selective Activation of Lysosomal Cathepsins B and L', *Neurotoxicity Research*. Neurotoxicity Research, 39, pp. 17–26.

Edelstein, A. *et al.* (2010) 'Computer control of microscopes using manager', *Current Protocols in Molecular Biology*, (SUPPL. 92), pp. 1–17. doi: 10.1002/0471142727.mb1420s92.

Eichler, F. S. *et al.* (2009) 'Overexpression of the Wild-Type SPT1 Subunit Lowers Desoxysphingolipid Levels and Rescues the Phenotype of HSAN1', *The Journal of Neuroscience*, 29(46), pp. 14646–14651. doi: 10.1523/JNEUROSCI.2536-09.2009.

El-hattab, A. W. (2016) 'Serine biosynthesis and transport defects', *Molecular Genetics and Metabolism*. Elsevier Inc. doi: 10.1016/j.ymgme.2016.04.010.

Esaki, K. *et al.* (2015) 'L-serine deficiency elicits intracellular accumulation of cytotoxic deoxysphingolipids and lipid body formation', *Journal of Biological Chemistry*, 290(23), pp. 14595–14609. doi: 10.1074/jbc.M114.603860.

Faber, C. L. *et al.* (2020) 'CNS control of the endocrine pancreas', *Diabetologia*. Diabetologia, 63(10), pp. 2086–2094. doi: 10.1007/s00125-020-05204-6.

Fenselau, H. *et al.* (2017) 'A rapidly acting glutamatergic ARC→PVH satiety circuit postsynaptically regulated by α-MSH', *Nature Neuroscience*, 20(1), pp. 42–51. doi: 10.1038/nn.4442.

Field, B. C., Gordillo, R. and Scherer, P. E. (2020) 'The Role of Ceramides in Diabetes and Cardiovascular Disease Regulation of Ceramides by Adipokines', *Frontiers in Endocrinology*, 11(October), pp. 1–14. doi: 10.3389/fendo.2020.569250.

Food Policy and Food Science Service, Nutrition Division, F. (1981) *AMINO-ACID CONTENT OF FOODS AND BIOLOGICAL DATA ON PROTEINS*. Available at: https://www.fao.org/3/AC854T/AC854T00.htm#TOC.

Forman, H. J. (2021) 'Targeting oxidative stress in disease : promise and limitations of antioxidant therapy', *Nature Reviews Drug Discovery*. Springer US, 20(September). doi: 10.1038/s41573-021-00233-1.

Fridman, V. *et al.* (2019) 'Randomized trial of l -serine in patients with hereditary sensory and autonomic neuropathy type 1', *Neurology*, 92(4), pp. E359–E370. doi: 10.1212/WNL.0000000000006811.

Fullerton, M. D. *et al.* (2013) 'Single phosphorylation sites in Acc1 and Acc2 regulate lipid

homeostasis and the insulin-sensitizing effects of metformin', *Nature Medicine*. Nature Publishing Group, 19(12), pp. 1649–1654. doi: 10.1038/nm.3372.

Furman, D. *et al.* (2019) 'Chronic inflammation in the etiology of disease across the life span', *Nature Medicine*. Springer US, 25(12), pp. 1822–1832. doi: 10.1038/s41591-019-0675-0.

Gaesser, G. A. and Angadi, S. S. (2021) 'Obesity treatment: Weight loss versus increasing fitness and physical activity for reducing health risks', *iScience*. Elsevier Inc., 24(10), p. 102995. doi: 10.1016/j.isci.2021.102995.

Gangwisch, J. E. *et al.* (2005) 'Inadequate sleep as a risk factor for obesity: Analyses of the NHANES I', *Sleep*, 28(10), pp. 1289–1296. doi: 10.1093/sleep/28.10.1289.

Gao, X. *et al.* (2018) 'Serine Availability Influences Mitochondrial Dynamics and Function through Lipid Metabolism', *Cell Reports*. ElsevierCompany., 22(13), pp. 3507–3520. doi: 10.1016/j.celrep.2018.03.017.

Garofalo, K. *et al.* (2011) 'Oral L-serine supplementation reduces production of neurotoxic deoxysphingolipids in mice and humans with hereditary sensory autonomic neuropathy type 1', *Journal of Clinical Investigation*, 121(12), pp. 4735–4745. doi: 10.1172/JCI57549.

Garrigue, N. De *et al.* (2020) 'Grant Report on d-Serine Augmentation of Neuroplasticity- Based Auditory Learning in Schizophrenia', *J Psychiatr Brain Sci*, 5(4), pp. 1–34.

Gelfin, E. *et al.* (2012) 'D-serine adjuvant treatment alleviates behavioural and motor symptoms in Parkinson's disease', *International Journal of Neuropsychopharmacology*, 15(4), pp. 543–549. doi: 10.1017/S1461145711001015.

Gimble, J. M. *et al.* (2011) 'Prospective influences of circadian clocks in adipose tissue and metabolism', *Nature Reviews Endocrinology*. Nature Publishing Group, 7(2), pp. 98–107. doi: 10.1038/nrendo.2010.214.

Gomez, G. and Stanford, F. C. (2018) 'US health policy and prescription drug coverage of FDA-approved medications for the treatment of obesity', *International Journal of Obesity*. Nature Publishing Group, 42(3), pp. 495–500. doi: 10.1038/ijo.2017.287.

Grabner, G. F. *et al.* (2021) 'Lipolysis: cellular mechanisms for lipid mobilization from fat stores', *Nature Metabolism*. Springer US, 3(11), pp. 1445–1465. doi: 10.1038/s42255-021-00493-6.

Greer, E. L. and Brunet, A. (2005) 'FOXO transcription factors at the interface between longevity and tumor suppression', pp. 7410–7425. doi: 10.1038/sj.onc.1209086.

Gunther, S. H. *et al.* (2020) 'Serum acylcarnitines and amino acids and risk of type 2 diabetes in a multiethnic Asian population', *BMJ Open Diabetes Research & Care*, 8, pp. 1–12. doi: 10.1136/bmjdrc-2020-001315.

Gurgul-Convey, E. (2020) 'Sphingolipids in Type 1 Diabetes: Focus on Beta-Cells', *Cells*, 9(8). doi: 10.3390/cells9081835.

Haery, L. *et al.* (2019) 'Adeno-Associated Virus Technologies and Methods for Targeted Neuronal Manipulation', *Frontiers in Neuroanatomy*, 13(November), pp. 1–16. doi: 10.3389/fnana.2019.00093.

Hagopian, K., Ramsey, J. J. and Weindruch, R. (2005) 'Serine utilization in mouse liver: Influence of caloric restriction and aging', *FEBS Letters*, 579(9), pp. 2009–2013. doi: 10.1016/j.febslet.2005.02.062.

Han, H. S. *et al.* (2016) 'Regulation of glucose metabolism from a liver-centric perspective', *Experimental and Molecular Medicine*. Nature Publishing Group, 48(3), pp. 1–10. doi: 10.1038/emm.2015.122.

Hannun, Y. A. and Obeid, L. M. (2018) 'Sphingolipids and their metabolism in physiology and disease', *Nature Reviews Molecular Cell Biology*, 19(3), pp. 175–191. doi: 10.1038/nrm.2017.107.

Hansen, K. B. *et al.* (2017) *NMDA receptors in the central nervous system*, *Methods in Molecular Biology*. doi: 10.1007/978-1-4939-7321-7_1.

Hardiman, O. *et al.* (2017) 'Amyotrophic lateral sclerosis', *Nature Publishing Group*. Macmillan Publishers Limited, 3, pp. 1–18. doi: 10.1038/nrdp.2017.71.

Heijboer, A. C. *et al.* (2005) 'Sixteen hours of fasting differentially affects hepatic and muscle insulin sensitivity in mice', *Journal of Lipid Research*, 46(3), pp. 582–588. doi: 10.1194/jlr.M400440-JLR200.

Heresco-levy, U. *et al.* (2005) 'D-serine Efficacy as Add-on Pharmacotherapy to Risperidone and Olanzapine for Treatment-Refractory Schizophrenia', *Biological Psichiatry*, 57, pp. 577–585. doi: 10.1016/j.biopsych.2004.12.037.

Herzig, S. and Shaw, R. J. (2018) 'AMPK: Guardian of metabolism and mitochondrial homeostasis', *Nature Reviews Molecular Cell Biology*. Nature Publishing Group, 19(2), pp. 121–135. doi: 10.1038/nrm.2017.95.

Hesaka, A. *et al.* (2019) 'Dynamics of D-serine reflected the recovery course of a patient with rapidly progressive glomerulonephritis', *CEN case reports*. Springer Singapore, 8(4), pp. 297–300. doi: 10.1007/s13730-019-00411-6.

Hesaka, A. *et al.* (2021) 'd-Serine Mediates Cellular Proliferation for Kidney Remodeling', *Kidney360*, 2(10), pp. 1611–1624. doi: 10.34067/kid.0000832021.

Hill, Jennifer W. (2012) 'PVN pathways controlling energy homeostasis', *Indian Journal of Endocrinology and Metabolism*, 16(9), p. 627. doi: 10.4103/2230-8210.105581.

Hill, Jennifer W (2012) 'Review Article PVN pathways controlling energy homeostasis', 16, pp. 627–636. doi: 10.4103/2230-8210.105581.

Hinney, A., Körner, A. and Fischer-Posovszky, P. (2022) 'The promise of new anti-obesity therapies arising from knowledge of genetic obesity traits', *Nature Reviews Endocrinology*.

Springer US, 18(10), pp. 623–637. doi: 10.1038/s41574-022-00716-0.

Holm, L. J. *et al.* (2018) 'L-serine supplementation lowers diabetes incidence and improves blood glucose homeostasis in NOD mice', *PLoS ONE*, 13(3), pp. 1–11. doi: 10.1371/journal.pone.0194414.

Holm, L. J. and Buschard, K. (2019) 'L-serine: a neglected amino acid with a potential therapeutic role in diabetes', *Apmis*, 127(10), pp. 655–659. doi: 10.1111/apm.12987.

Hotamisligil, G. S. (2006) 'Inflammation and Metabolic disorders', *Insight Review - Nature*. doi: doi:10.1038/nature05485.

Huang, X. T. *et al.* (2021) 'Activation of N-methyl-D-aspartate receptor regulates insulin sensitivity and lipid metabolism', *Theranostics*, 11(5), pp. 2247–2262. doi: 10.7150/thno.51666.

Hurtado, M. D. and Acosta, A. (2021) 'Precision Medicine and obeisty', *Gastroenterol Clin North Am.*, 50(1), pp. 127–139. doi: doi:10.1016/j.gtc.2020.10.005.

Isenmann, E., Dissemond, J. and Geisler, S. (2021) 'The effects of a macronutrient-based diet and time-restricted feeding (16:8) on body composition in physically active individuals—a 14-week randomised controlled trial', *Nutrients*, 13(9). doi: 10.3390/nu13093122.

Ito, Y. *et al.* (2014) 'Effects of L-serine ingestion on human sleep', pp. 3–7.

Iwasaki, Y; Ikeda, K; Shiojima, T; Kinoshita, M. (1992) 'Increased plasma concentrations of aspartate , glutamate and glycine in Parkinson ' s disease', *Neurosicence Letters*, 145, pp. 175–177.

Jebeile, H. *et al.* (2021) 'Eating disorder risk in adolescents with obesity', (August 2020), pp. 1–10. doi: 10.1111/obr.13173.

Jensen, T. L. *et al.* (2013) 'Fasting of mice: A review', *Laboratory Animals*, 47(4), pp. 225–240. doi: 10.1177/0023677213501659.

Kalhan, S. C. and Hanson, R. W. (2012) 'Resurgence of serine: An often neglected but indispensable amino acid', *Journal of Biological Chemistry*, 287(24), pp. 19786–19791. doi: 10.1074/jbc.R112.357194.

Kang, C. and Ji, L. L. (2012) 'Role of PGC-1α signaling in skeletal muscle health and disease', *Annals of the New York Academy of Sciences*, 1271(1), pp. 110–117. doi: 10.1111/j.1749-6632.2012.06738.x.

Kantrowitz, J. T. *et al.* (2016) 'Neurophysiological mechanisms of cortical plasticity impairments in schizophrenia and modulation by the NMDA receptor agonist', *Brain*, 139, pp. 3281–3295. doi: 10.1093/brain/aww262.

Kasahara, Y. *et al.* (2007) 'Impaired thermoregulatory ability of oxytocin-deficient mice during cold-exposure', *Bioscience, Biotechnology and Biochemistry*, 71(12), pp. 3122–3126. doi: 10.1271/bbb.70498.

Kasai, Y. *et al.* (2011) 'Transport systems of serin at the brain barriers and in brain parenchymal cells', *Journal of Neurochemistry*, (118), pp. 304–313. doi: 10.1111/j.1471-4159.2011.07313.x.

Kersten, S. (2001) 'Mechanisms of nutritional and hormonal regulation of lipogenesis', *EMBO Reports*, 2(4), pp. 282–286. doi: 10.1093/embo-reports/kve071.

Kim, H. J., Kim, Y. J. and Seong, J. K. (2022) 'AMP-activated protein kinase activation in skeletal muscle modulates exercise-induced uncoupled protein 1 expression in brown adipocyte in mouse model', *Journal of Physiology*, 600(10), pp. 2359–2376. doi: 10.1113/JP282999.

Kim, J. *et al.* (2016) 'AMPK activators: Mechanisms of action and physiological activities', *Experimental and Molecular Medicine*. Nature Publishing Group, 48(4), pp. 1–12. doi: 10.1038/emm.2016.16.

Kim, K. Y. *et al.* (2019) 'L-Serine protects mouse hippocampal neuronal HT22 cells against oxidative stress-mediated mitochondrial damage and apoptotic cell death', *Free Radical Biology and Medicine*. Elsevier B.V., 141(July), pp. 447–460. doi: 10.1016/j.freeradbiomed.2019.07.018.

Kim, S. *et al.* (2016) 'AMPK Phosphorylates desnutrin/ATGL and Hormone Sensitive Lipase To Regulate Lipolysis and Fatty Acid Oxidation within', *Molecular and cellular biology*, 36(14), pp. 1961–1976. doi: 10.1128/MCB.00244-16.Address.

Kimura, T., Hesaka, A. and Isaka, Y. (2020) 'd-Amino acids and kidney diseases', *Clinical and Experimental Nephrology*. Springer Singapore, 24(5), pp. 404–410. doi: 10.1007/s10157-020-01862-3.

Kitamoto, S. *et al.* (2020) 'Dietary l-serine confers a competitive fitness advantage to Enterobacteriaceae in the inflamed gut', *Nature Microbiology*. Springer US, 5(1), pp. 116–125. doi: 10.1038/s41564-019-0591-6.

Knopman, D. S. *et al.* (2021) 'Alzheimer disease', *Nature Reviews Disease Primers*, 7(1), pp. 1–21. doi: 10.1038/s41572-021-00269-y.

Kohlmeier, M. (2015) 'Amino acids and nitrogen compounds', in *Nutrient Metabolism*. Second. Academic Press, pp. 265–477. doi: 10.1016/B978-0-12-387784-0.00008-0.

de Koning, T. J. (2006) 'Treatment with amino acids in serine deficiency disorders', *Journal of Inherited Metabolic Disease*, 29(2–3), pp. 347–351. doi: 10.1007/s10545-006-0269-0.

De Koning, T. J. *et al.* (2003) 'L-serine in disease and development', *Biochemical Journal*, 371(3), pp. 653–661. doi: 10.1042/BJ20021785.

De Koning TJ, Duran, M, Dorland L, Gooskens R, Van Schaftingen E, Jaeken J, Blau N, Berger R, P.-T. B. (1998) 'Beneficial effects of L-serine and glycine in the management of seizures in 3-Phosphoglycerate Dehydrogenase Deficiency', *Annals of Neurology*, 44(2261–265).

Kono, M. *et al.* (2019) 'Interneuronal NMDA receptors regulate long-term depression and motor learning in the cerebellum', *Journal of Physiology*, 597(3), pp. 903–920. doi: 10.1113/JP276794.

Korenfeld, N. *et al.* (2021) 'Fasting Hormones Synergistically Induce Amino Acid Catabolism Genes to Promote Gluconeogenesis', *Cmgh*. Elsevier Inc, 12(3), pp. 1021–1036. doi: 10.1016/j.jcmgh.2021.04.017.

Krashes, M. J., Lowell, B. B. and Garfield, A. S. (2016) 'Melanocortin-4 receptor – regulated energy homeostasis', 19(2). doi: 10.1038/nn.4202.

Krause, A. J. *et al.* (2017) 'The sleep-deprived human brain', *Nature Reviews Neuroscience*. Nature Publishing Group, 18(7), pp. 404–418. doi: 10.1038/nrn.2017.55.

Labbé, S. M. *et al.* (2015) 'Hypothalamic control of brown adipose tissue thermogenesis', *Frontiers in Systems Neuroscience*, 9(November), pp. 1–13. doi: 10.3389/fnsys.2015.00150.

Lacerda, D. R. *et al.* (2019) 'Role of adipose tissue inflammation in fat pad loss induced by fasting in lean and mildly obese mice', *Journal of Nutritional Biochemistry*, 72. doi: 10.1016/j.jnutbio.2019.06.006.

Langin, D. *et al.* (2005) 'Adipocyte Lipases and Defect of Lipolysis in Human Obesity', *Diabetes*, 54(November).

Larsen, T. M. *et al.* (2010) 'Diets with High or Low Protein Content and Glycemic Index for Weight-Loss Maintenance', *New England Journal of Medicine*, 363(22), pp. 2102–2113. doi: 10.1056/nejmoa1007137.

Lau, C. G. and Zukin, R. S. (2007) 'NMDA receptor trafficking in synaptic plasticity and neuropsychiatric disorders', *Nature Reviews Neuroscience*, 8(6), pp. 413–426. doi: 10.1038/nrn2153.

Levine, T. D. *et al.* (2017) 'Phase I clinical trial of safety of L-serine for ALS patients', *Myotrophic Lateral Sclerosis and Frontotemporal Degeneration*, 18. doi: 10.1080/21678421.2016.1221971.

Lewitt, P. A., Lu, M. and Auinger, P. (2017) 'Metabolomic biomarkers as strong correlates of Parkinson disease progression', *Neurology*, 88.

Li, G. *et al.* (2017) 'Intermittent Fasting Promotes White Adipose Browning and Decreases Obesity by Shaping the Gut Microbiota', *Cell Metabolism*. Elsevier, 26(4), pp. 672-685.e4. doi: 10.1016/j.cmet.2017.08.019.

Liu, H., Xu, Y. and Hu, F. (2020) 'AMPK in the Ventromedial Nucleus of the Hypothalamus: A Key Regulator for Thermogenesis', *Frontiers in Endocrinology*, 11(September), pp. 1–13. doi: 10.3389/fendo.2020.578830.

Logan, R. W. and McClung, C. A. (2019) 'Rhythms of life: circadian disruption and brain disorders across the lifespan', *Nature Reviews Neuroscience*. Springer US, 20(1), pp. 49–65. doi: 10.1038/s41583-018-0088-y.

Longo, V. D. and Mattson, M. P. (2014) 'Review Fasting : Molecular Mechanisms and Clinical Applications', *Cell Metabolism*. Elsevier Inc., 19(2), pp. 181–192. doi: 10.1016/j.cmet.2013.12.008.

Loos, R. J. F. and Yeo, G. S. H. (2022) 'The genetics of obesity: from discovery to biology', *Nature Reviews Genetics*. Springer US, 23(2), pp. 120–133. doi: 10.1038/s41576-021-00414-z.

López-Gonzales, E. *et al.* (2022) 'L-Serine Supplementation Blunts Fasting-Induced Weight Regain by Increasing Brown Fat Thermogenesis', *Nutrients*, 14(9). doi: 10.3390/nu14091922.

Louise, S. *et al.* (2019) 'Impaired serine metabolism complements LRRK2-G2019S pathogenicity in PD patients', *Parkinsonism and Related Disorders*. Elsevier, 67(September), pp. 48–55. doi: 10.1016/j.parkreldis.2019.09.018.

Lu, S. C. (2009) 'Regulation of glutathione synthesis', *Molecular Aspects of Medicine*. Elsevier Ltd, 30(1–2), pp. 42–59. doi: 10.1016/j.mam.2008.05.005.

Ludwig, D. S. *et al.* (2022) 'Competing paradigms of obisity pathogenesis: energy balance versus carbohydrate-insulin models', (July). doi: ; https://doi.org/10.1038/s41430-022-01179-2.

Macpherson, R. E. K. *et al.* (2016) 'Reduced ATGL-mediated lipolysis attenuates β-adrenergic-induced AMPK signaling, but not the induction of PKA-targeted genes, in adipocytes and adipose tissue', *American Journal of Physiology - Cell Physiology*, 311(2), pp. C269–C276. doi: 10.1152/ajpcell.00126.2016.

Madden, C. J. and Morrison, S. F. (2009) 'Neurons in the paraventricular nucleus of the hypothalamus inhibit sympathetic outflow to brown adipose tissue', *American Journal of Physiology - Regulatory Integrative and Comparative Physiology*, 296(3), pp. 831–843. doi: 10.1152/ajpregu.91007.2008.

Magkos, F., Hjorth, M. F. and Astrup, A. (2020) 'Diet and exercise in the prevention and treatment of type 2 diabetes mellitus', *Nature Reviews Endocrinology*. Springer US, 16(10), pp. 545–555. doi: 10.1038/s41574-020-0381-5.

Magliano, D. J. *et al.* (2020) 'Young-onset type 2 diabetes mellitus — implications for morbidity and mortality', *Nature Reviews Endocrinology*. Springer US, 16(6), pp. 321–331. doi: 10.1038/s41574-020-0334-z.

Malik, V. S. and Hu, F. B. (2007) 'Popular weight-loss diets: From evidence to practice', *Nature Clinical Practice Cardiovascular Medicine*, 4(1), pp. 34–41. doi: 10.1038/ncpcardio0726.

Marquard, J. *et al.* (2015) 'Characterization of pancreatic NMDA receptors as possible drug targets for diabetes treatment', 21(4). doi: 10.1038/nm.3822.

Martinez, J. A. *et al.* (2014) 'Personalized weight loss strategies - The role of macronutrient distribution', *Nature Reviews Endocrinology*. Nature Publishing Group, 10(12), pp. 749–760. doi: 10.1038/nrendo.2014.175.

Mathieu, C. (2021) 'One hundred years of insulin therapy', *Nature Reviews Endocrinology*. Springer US, 0123456789. doi: 10.1038/s41574-021-00542-w.

Maugard, M. *et al.* (2021) 'L-Serine links metabolism with neurotransmission', *Progress in Neurobiology*, 197(August). doi: 10.1016/j.pneurobio.2020.101896.

McNeill, B. T., Suchacki, K. J. and Stimson, R. H. (2021) 'Human brown adipose tissue as a therapeutic target: Warming up or cooling down?', *European Journal of Endocrinology*, 184(6), pp. R243–R259. doi: 10.1530/EJE-20-1439.

Meiser, J. *et al.* (2016) 'Serine one-carbon catabolism with formate overflow', *Science Advances*, 2(10). doi: 10.1126/sciadv.1601273.

Mielnik, C. A. *et al.* (2021) 'Consequences of NMDA receptor de fi ciency can be rescued in the adult brain', *Molecular Psychiatry*. Springer US, pp. 2929–2942. doi: 10.1038/s41380-020-00859-4.

Milan Holecek (2022) 'Serine Metabolism in Health and Disease and as a Conditionally Essential Amino Acid', (7). doi: https://doi.org/10.3390/nu14091987.

Milbank, E. *et al.* (2021) 'Small extracellular vesicle-mediated targeting of hypothalamic AMPKα1 corrects obesity through BAT activation', *Nature Metabolism*. Springer US, 3(10), pp. 1415–1431. doi: 10.1038/s42255-021-00467-8.

Moffatt, B. A. and Ashihara, H. (2002) 'Purine and Pyrimidine Nucleotide Synthesis and Metabolism', *The Arabidopsis Book*, 1(May), p. e0018. doi: 10.1199/tab.0018.

Mohammadpour, S. *et al.* (2020) 'Effects of glucomannan supplementation on weight loss in overweight and obese adults: A systematic review and meta-analysis of randomized controlled trials', *Obesity Medicine*. Obesity Surgery, 19, pp. 2743–2753. doi: 10.1016/j.obmed.2020.100276.

Morrison, S. F., Madden, C. J. and Tupone, D. (2014) 'Central neural regulation of brown adipose tissue thermogenesis and energy expenditure', *Cell Metabolism*. Elsevier Inc., 19(5), pp. 741–756. doi: 10.1016/j.cmet.2014.02.007.

Mottillo, E. P. *et al.* (2016) 'Lack of Adipocyte AMPK Exacerbates Insulin Resistance and Hepatic Steatosis through Brown and Beige Adipose Tissue Function', *Cell Metabolism*. Elsevier Inc., 24(1), pp. 118–129. doi: 10.1016/j.cmet.2016.06.006.

Müller, T. D. *et al.* (2022) 'Anti-obesity drug discovery: advances and challenges', *Nature Reviews Drug Discovery*. Springer US, 21(3), pp. 201–223. doi: 10.1038/s41573-021-00337-8.

Murtas, G. *et al.* (2020) 'L - serine synthesis via the phosphorylated pathway in humans', *Cellular and Molecular Life Sciences*. Springer International Publishing, 77, pp. 5131–5148.

Mwinyi, J. *et al.* (2017) 'Plasma 1-deoxysphingolipids are early predictors of incident type 2 diabetes mellitus', *PLoS ONE*, 12(5). doi: 10.1371/journal.pone.0175776.

Nagamachi, S. *et al.* (2018) 'Dietary L-serine modifies free amino acid composition of maternal milk and lowers the body weight of the offspring in mice', *Journal of Veterinary Medical Science*, 80(2), pp. 235–241. doi: 10.1292/jvms.17-0577.

Nakamura, Y. and Nakamura, K. (2018) 'Central regulation of brown adipose tissue thermogenesis and energy homeostasis dependent on food availability'. Pflügers Archiv -

European Journal of Physiology, pp. 823–837.

National Institutes of Health. Office of Dietary Supplements. (2022) *Dietary supplements for Weight loss- fact sheet for Health Professionals*. doi: 10.1016/s1042-0991(15)30331-5.

Neame, S. *et al.* (2019) 'The NMDA receptor activation by D -serine and glycine is controlled by an astrocytic Phgdh-dependent serine shuttle'. doi: 10.1073/pnas.1909458116.

Newgard, C. B. *et al.* (2009) 'A Branched-Chain Amino Acid-Related Metabolic Signature that Differentiates Obese and Lean Humans and Contributes to Insulin Resistance', *Cell Metabolism*. Elsevier Ltd, 9(4), pp. 311–326. doi: 10.1016/j.cmet.2009.02.002.

Newman, A. C. and Maddocks, O. D. K. (2017) 'Serine and Functional Metabolites in Cancer', *Trends in Cell Biology*. Elsevier Ltd, 27(9), pp. 645–657. doi: 10.1016/j.tcb.2017.05.001.

Newsholme, P. *et al.* (2011) *Amino Acid Metabolism*. Second Edi, *Comprehensive Biotechnology, Second Edition*. Second Edi. Elsevier B.V. doi: 10.1016/B978-0-08-088504-9.00002-7.

Nielsen, T. S. *et al.* (2014) 'Dissecting adipose tissue lipolysis: Molecular regulation and implications for metabolic disease', *Journal of Molecular Endocrinology*, 52(3). doi: 10.1530/JME-13-0277.

Nouwen, A. *et al.* (2010) 'Type 2 diabetes mellitus as a risk factor for the onset of depression: A systematic review and meta-analysis', *Diabetologia*, 53(12), pp. 2480–2486. doi: 10.1007/s00125-010-1874-x.

Nowosad, K. and Sujka, M. (2021) 'Effect of Various Types of Intermittent Fasting (IF) on Weight Loss and Improvement of Diabetic Parameters in Human', *Current Nutrition Reports*. Current Nutrition Reports, 10(2), pp. 146–154. doi: 10.1007/s13668-021-00353-5.

Obici, S., Feng, Z., *et al.* (2002) 'Decreasing hypothalamic insulin receptors causes hyperphagia and insulin resistance in rats', *Nature Neuroscience*, 5(6), pp. 566–572. doi: 10.1038/nn861.

Obici, S., Zhang, B. B., *et al.* (2002) 'Hypothalamic insulin signaling is required for inhibition of glucose production', *Nature Medicine*, 8(12), pp. 1376–1382. doi: 10.1038/nm798.

Okada, A. *et al.* (2017) 'D-serine, a novel uremic toxin, induces senescence in human renal tubular cells via GCN2 activation', *Scientific Reports*. Springer US, 7(1), pp. 1–13. doi: 10.1038/s41598-017-11049-8.

Okekunle, A. P. *et al.* (2019) 'Higher intakes of energy-adjusted dietary amino acids are inversely associated with obesity risk', *Amino Acids*. Springer Vienna, 51(3), pp. 373–382. doi: 10.1007/s00726-018-2672-x.

Olivares, D. *et al.* (2012) 'N-Methyl D-Aspartate (NMDA) Receptor Antagonists and Memantine Treatment for Alzheimer's Disease, Vascular Dementia and Parkinson's Disease HHS Public Access', *Curr Alzheimer Res*, 9(6), pp. 746–758.

Olthof, M. R. *et al.* (2006) 'Acute Effect of Folic Acid, Betaine, and Serine Supplements on Flow-

Mediated Dilation after Methionine Loading: A Randomized Trial', *PLoS Clinical Trials*, 1(1), p. e4. doi: 10.1371/journal.pctr.0010004.

Onogi, Y. and Ussar, S. (2022) 'Regulatory networks determining substrate utilization in brown adipocytes', *Trends in Endocrinology and Metabolism*. Elsevier Ltd, 33(7), pp. 493–506. doi: 10.1016/j.tem.2022.04.001.

Ostendorf, D. M. *et al.* (2022) 'Comparison of weight loss induced by daily caloric restriction versus intermittent fasting (DRIFT) in individuals with obesity: study protocol for a 52-week randomized clinical trial', *Trials*. BioMed Central, 23(1), pp. 1–19. doi: 10.1186/s13063-022-06523-2.

Othman, A., Bianchi, R., *et al.* (2015) 'Lowering Plasma 1-Deoxysphingolipids Improves Neuropathy in Diabetic Rats', 64(March), pp. 1035–1045. doi: 10.2337/db14-1325.

Othman, A., Saely, C. H., *et al.* (2015) 'Plasma 1-deoxysphingolipids are predictive biomarkers for type 2 diabetes mellitus', *BMJ Open Diabetes Research & Care*, 3, pp. 1–9. doi: 10.1136/bmjdrc-2014-000073.

Ouchi, N. *et al.* (2011) 'Adipokines in inflammation and metabolic disease', *Nature Reviews Immunology*. Nature Publishing Group, 11(2), pp. 85–97. doi: 10.1038/nri2921.

Papazoglou, I. *et al.* (2022) 'A distinct hypothalamus-to-β cell circuit modulates insulin secretion', *Cell Metabolism*. Elsevier Inc., 34(2), pp. 285-298.e7. doi: 10.1016/j.cmet.2021.12.020.

Parker, S. J. and Metallo, C. M. (2016) 'Chasing One-Carbon Units to Understand the Role of Serine in Epigenetics', *Molecular Cell*. Elsevier Inc., 61(2), pp. 185–186. doi: 10.1016/j.molcel.2016.01.006.

Penno, A. *et al.* (2010) 'Hereditary Sensory Neuropathy Type 1 Is Caused by the Accumulation of Two Neurotoxic Sphingolipids * □', *Jornal of Biological Chemistry*, 285(15), pp. 11178–11187. doi: 10.1074/jbc.M109.092973.

Pérez-Otaño, I., Larsen, R. S. and Wesseling, J. F. (2016) 'Emerging roles of GluN3-containing NMDA receptors in the CNS', *Nature Reviews Neuroscience*. Nature Publishing Group, 17(10), pp. 623–635. doi: 10.1038/nrn.2016.92.

Perreault, L., Skyler, J. S. and Rosenstock, J. (2021) 'Novel therapies with precision mechanisms for type 2 diabetes mellitus', *Nature Reviews Endocrinology*. Springer US, 17(6), pp. 364–377. doi: 10.1038/s41574-021-00489-y.

Pocal, A. *et al.* (2005) 'Hypothalamic KATP channels control hepatic glucose production', *Nature*, 434(7036), pp. 1026–1031. doi: 10.1038/nature03439.

Pomares-Millan, H. *et al.* (2022) 'Estimating the Direct Effect between Dietary Macronutrients and Cardiometabolic Disease, Accounting for Mediation by Adiposity and Physical Activity', *Nutrients*, 14(6). doi: 10.3390/nu14061218.

Potter, G. D. M. *et al.* (2016) 'Nutrition and the circadian system', pp. 434–442. doi:

10.1017/S0007114516002117.

Poulsen, S. K. *et al.* (2014) 'Health effect of the new nordic diet in adults with increased waist circumference: A 6-mo randomized controlled trial', *American Journal of Clinical Nutrition*, 99(1), pp. 35–45. doi: 10.3945/ajcn.113.069393.

Puigserver, P. (2018) *Signaling Transduction and Metabolomics*. Seventh Ed, *Hematology: Basic Principles and Practice*. Seventh Ed. Elsevier Inc. doi: 10.1016/B978-0-323-35762-3.00007-X.

Qian, S. *et al.* (2022) 'A temperature-regulated circuit for feeding behavior', *Nature Communications*. Springer US, 13(1). doi: 10.1038/s41467-022-31917-w.

Qin, C., Li, J. and Tang, K. (2018) 'The paraventricular nucleus of the hypothalamus: Development, function, and human diseases', *Endocrinology*, 159(9), pp. 3458–3472. doi: 10.1210/en.2018-00453.

Roden, M. and Shulman, G. I. (2019) 'The integrative biology of type 2 diabetes', *Nature*. Springer US, 576(7785), pp. 51–60. doi: 10.1038/s41586-019-1797-8.

Roh, E., Song, D. K. and Kim, M. (2016) 'Emerging role of the brain in the homeostatic regulation of energy and glucose metabolism'. Nature Publishing Group, (December 2015). doi: 10.1038/emm.2016.4.

Rosario, W. *et al.* (2016) 'The brain-to-pancreatic islet neuronal map reveals differential glucose regulation from distinct hypothalamic regions', *Diabetes*, 65(9), pp. 2711–2723. doi: 10.2337/db15-0629.

Rubino, F. *et al.* (2020) 'Joint international consensus statement for ending stigma of obesity', *Nature Medicine*. Springer US, 26(4), pp. 485–497. doi: 10.1038/s41591-020-0803-x.

Rydén, M. *et al.* (2022) 'Lipolysis defect in people with obesity who undergo metabolic surgery', *Journal of Internal Medicine*, pp. 667–678. doi: 10.1111/joim.13527.

Saito, M. (2013) 'Brown adipose tissue as a regulator of energy expenditure and body fat in humans', *Diabetes and Metabolism Journal*, 37(1), pp. 22–29. doi: 10.4093/dmj.2013.37.1.22.

Saito, M. *et al.* (2020) 'Brown Adipose Tissue, Diet-Induced Thermogenesis, and Thermogenic Food Ingredients: From Mice to Men', *Frontiers in Endocrinology*, 11(April). doi: 10.3389/fendo.2020.00222.

Sanderson, S. M. *et al.* (2019) 'Methionine metabolism in health and cancer : a nexus of diet and precision medicine', *Nature Reviews Cancer*. Springer US, 19(November), pp. 625–637. doi: 10.1038/s41568-019-0187-8.

Sarin, H. V. *et al.* (2019) 'Substantial fat mass loss reduces low-grade inflammation and induces positive alteration in cardiometabolic factors in normal-weight individuals', *Scientific Reports*. Springer US, 9(1), pp. 1–14. doi: 10.1038/s41598-019-40107-6.

Schneeberger, M., Gomis, R. and Claret, M. (2014) 'Hypothalamic and brainstem neuronal

circuits controlling homeostatic energy balance', *Journal of Endocrinology*, 220. doi: 10.1530/JOE-13-0398.

Schoettl, T., Fischer, I. P. and Ussar, S. (2018) 'Heterogeneity of adipose tissue in development and metabolic function', *Journal of Experimental Biology*, 121. doi: 10.1242/jeb.162958.

Scholz, O., Welters, A. and Lammert, E. (2017) 'Role of NMDA Receptors in Pancreatic Islets', pp. 121–134. doi: 10.1007/978-3-319-49795-2.

Shaheen, R. *et al.* (2014) 'Neu-laxova syndrome, an inborn error of serine metabolism, is caused by mutations in PHGDH', *American Journal of Human Genetics*. The American Society of Human Genetics, 94(6), pp. 898–904. doi: 10.1016/j.ajhg.2014.04.015.

Shi, Y. C. *et al.* (2013) 'Arcuate NPY controls sympathetic output and BAT function via a relay of tyrosine hydroxylase neurons in the PVN', *Cell Metabolism*. Elsevier, 17(2), pp. 236–248. doi: 10.1016/j.cmet.2013.01.006.

Sim, W.-C. *et al.* (2015) 'L-Serine Supplementation Attenuates Alcoholic Fatty Liver by Enhancing Homocysteine Metabolism in Mice and Rats', *The Journal of Nutrition*, 145(2), pp. 260–267. doi: 10.3945/jn.114.199711.

Simonson, M., Boirie, Y. and Guillet, C. (2020) 'Protein, amino acids and obesity treatment', *Reviews in Endocrine and Metabolic Disorders*. Reviews in Endocrine and Metabolic Disorders, 21(3), pp. 341–353. doi: 10.1007/s11154-020-09574-5.

Smith, B. K. and Steinberg, G. R. (2015) 'Duodenal energy sensing regulates hepatic glucose output', *Nature Medicine*. Nature Publishing Group, 21(5), pp. 428–429. doi: 10.1038/nm.3859.

Solinas, G., Borén, J. and Dulloo, A. G. (2015) 'De novo lipogenesis in metabolic homeostasis: More friend than foe?', *Molecular Metabolism*. Elsevier GmbH, 4(5), pp. 367–377. doi: 10.1016/j.molmet.2015.03.004.

Song, C. K. *et al.* (2008) 'Melanocortin-4 receptor mRNA expressed in sympathetic outflow neurons to brown adipose tissue: Neuroanatomical and functional evidence', *American Journal of Physiology - Regulatory Integrative and Comparative Physiology*, 295(2). doi: 10.1152/ajpregu.00174.2008.

Soto, D. *et al.* (2019) 'dietary supplementation is associated with clinical improvement of loss-of-function GRIN2B -related pediatric encephalopathy', pp. 1–16.

Spires-Jones, T. L. and Hyman, B. T. (2014) 'The Intersection of Amyloid Beta and Tau at Synapses in Alzheimer's Disease', *Neuron*. Elsevier Inc., 82(4), pp. 756–771. doi: 10.1016/j.neuron.2014.05.004.

Stenvers, D. J. *et al.* (2019) 'Circadian clocks and insulin resistance', *Nature Reviews Endocrinology*. Springer US, 15(2), pp. 75–89. doi: 10.1038/s41574-018-0122-1.

Šterk, M. *et al.* (2021) 'NMDA receptor inhibition increases, synchronizes, and stabilizes the collective pancreatic beta cell activity: Insights through multilayer network analysis', *PLoS*

Computational Biology, 17(5), pp. 1–29. doi: 10.1371/journal.pcbi.1009002.

Straczkowski, M. *et al.* (2004) 'Relationship between Insulin Sensitivity and Sphingomyelin Signaling Pathway in Human Skeletal Muscle', *Diabetes*, 53(5), pp. 1215–1221. doi: 10.2337/diabetes.53.5.1215.

Suchacki, K. J. and Stimson, R. H. (2021) 'Nutritional regulation of human brown adipose tissue', *Nutrients*, 13(6). doi: 10.3390/nu13061748.

Summers, S. A. and Nelson, D. H. (2005) 'A role for sphingolipids in producing the common features of type 2 diabetes, metabolic syndrome X, and Cushing's syndrome', *Diabetes*, 54(3), pp. 591–602. doi: 10.2337/diabetes.54.3.591.

Suwandhi, L. *et al.* (2018) 'Chronic D-serine supplementation impairs insulin secretion', *Molecular Metabolism*. Elsevier GmbH, 16, pp. 191–202. doi: 10.1016/j.molmet.2018.07.002.

Tajima, N. *et al.* (2022) 'Development and characterization of functional antibodies targeting NMDA receptors', *Nature Communications*. Springer US, 19(923), pp. 1–16. doi: 10.1038/s41467-022-28559-3.

Takahashi, H. *et al.* (2015) 'Pharmacologically targeted NMDA receptor antagonism by NitroMemantine for cerebrovascular disease', *Scientific Reports*. Nature Publishing Group, 5(March), pp. 1–15. doi: 10.1038/srep14781.

Tang, H. N. *et al.* (2017) 'Plasticity of adipose tissue in response to fasting and refeeding in male mice', *Nutrition and Metabolism*. Nutrition & Metabolism, 14(1), pp. 1–14. doi: 10.1186/s12986-016-0159-x.

Thakur, A. K., Tyagi, S. and Shekhar, N. (2019) 'Comorbid brain disorders associated with diabetes: therapeutic potentials of prebiotics, probiotics and herbal drugs', *Translational Medicine Communications*. Translational Medicine Communications, 4(1), pp. 1–13. doi: 10.1186/s41231-019-0043-6.

The Jackson Laboratory (2022) *The Jackson Laboratory. Grin1 flox mice. B6.129S4-Grin1tm2Stl/J. Strain details*. Available at: https://www.jax.org/strain/005246 (Accessed: 27 October 2022).

Thorens, B. (2010) 'Central control of glucose homeostasis: the brain -endocrine pancreas axis', *Diabetes and Metabolism*. Elsevier, 36(SUPPL. 3), pp. S45–S49. doi: 10.1016/S1262-3636(10)70466-3.

Tomic, D., Shaw, J. E. and Magliano, D. J. (2022) 'The burden and risks of emerging complications of diabetes mellitus', *Nature Reviews Endocrinology*. Springer US, 18(9), pp. 525–539. doi: 10.1038/s41574-022-00690-7.

Tran, L. T. *et al.* (2022) 'Hypothalamic control of energy expenditure and thermogenesis', *Experimental and Molecular Medicine*. Springer US, 54(4), pp. 358–369. doi: 10.1038/s12276-022-00741-z.

Turpin-Nolan, S. M. and Brüning, J. C. (2020) 'The role of ceramides in metabolic disorders: when size and localization matters', *Nature Reviews Endocrinology*. Springer US, 16(April). doi: 10.1038/s41574-020-0320-5.

U.S. Food and Drug Administration (2022) *CFR - Code of Federal Regulations Title 21.* Available at: https://www.accessdata.fda.gov/scripts/cdrh/cfdocs/cfCFR/CFRSearch.cfm?fr=170.3&SearchTerm=170.3 (Accessed: 22 July 2022).

U.S.A. Food & Drug Adminsitration (2022) *Tainted Weight Loss Products.* Available at: https://www.fda.gov/drugs/medication-health-fraud/tainted-weight-loss-products (Accessed: 21 July 2022).

Umemura, G. S. *et al.* (2021) 'Sleep deprivation affects gait control', *Scientific Reports*. Nature Publishing Group UK, 11(1), pp. 1–11. doi: 10.1038/s41598-021-00705-9.

van der Vaart, J. I., Boon, M. R. and Houtkooper, R. H. (2021) 'The role of ampk signaling in brown adipose tissue activation', *Cells*, 10(5). doi: 10.3390/cells10051122.

Vance, J. E. (2015) 'Phospholipid Synthesis and Transport in Mammalian Cells', *Traffic*, 16(1), pp. 1–18. doi: 10.1111/tra.12230.

Vangipurapu, J. *et al.* (2019) 'Nine amino acids are associated with decreased insulin secretion and elevated glucose levels in a 7.4-year follow-up study of 5,181 Finnish men', *Diabetes*, 68(6), pp. 1353–1358. doi: 10.2337/db18-1076.

Vanle, B. (2018) 'NMDA antagonists for treating the non- motor symptoms in Parkinson ' s disease', *Translational Psychiatry*. Springer US. doi: 10.1038/s41398-018-0162-2.

Varady, K. A. *et al.* (2022) 'Clinical application of intermittent fasting for weight loss: progress and future directions', *Nature Reviews Endocrinology*. Springer US, 18(5), pp. 309–321. doi: 10.1038/s41574-022-00638-x.

Verhoef, P. *et al.* (2004) 'Dietary serine and cystine attenuate the homocysteine-raising effect of dietary methionine: A randomized crossover trial in humans', *American Journal of Clinical Nutrition*, 80(3), pp. 674–679. doi: 10.1093/ajcn/80.3.674.

Wan, Z. *et al.* (2014) 'Evidence for the role of AMPK in regulating PGC-1 alpha expression and mitochondrial proteins in mouse epididymal adipose tissue', *Obesity*, pp. 730–738. doi: 10.1002/oby.20605.

Wang, B. and Cheng, K. K. Y. (2018) 'Hypothalamic AMPK as a mediator of hormonal regulation of energy balance', *International Journal of Molecular Sciences*, 19(11). doi: 10.3390/ijms19113552.

Wang, W. *et al.* (2013) 'Glycine metabolism in animals and humans: Implications for nutrition and health', *Amino Acids*, 45(3), pp. 463–477. doi: 10.1007/s00726-013-1493-1.

Wang, W. *et al.* (2021) 'Targeting Pyrimidine Metabolism in the Era of Precision Cancer Medicine',

Frontiers in Oncology, 11(May), pp. 1–17. doi: 10.3389/fonc.2021.684961.

Weindruch, R., Walford, R. O. Y. L. and Guthrie, F. A. (2018) 'The Retardation of Aging in Mice by Dietary Restriction : Longevity , Cancer , Immunity and Lifetime Energy Intake1', (March).

Welters, A. *et al.* (2017) 'NMDAR antagonists for the treatment of diabetes mellitus—Current status and future directions', *Diabetes, Obesity and Metabolism*, 19, pp. 95–106. doi: 10.1111/dom.13017.

Wen, X. *et al.* (2022) 'Signaling pathways in obesity: mechanisms and therapeutic interventions', *Signal Transduction and Targeted Therapy*. Springer US, 7(1). doi: 10.1038/s41392-022-01149-x.

Wernstedt Asterholm, I. *et al.* (2014) 'Adipocyte inflammation is essential for healthy adipose tissue expansion and remodeling', *Cell Metabolism*. Elsevier Inc., 20(1), pp. 103–118. doi: 10.1016/j.cmet.2014.05.005.

Whitehead, A. *et al.* (2021) 'Brown and beige adipose tissue regulate systemic metabolism through a metabolite interorgan signaling axis', *Nature Communications*, 12(1), pp. 1–21. doi: 10.1038/s41467-021-22272-3.

Whittle, A., Relat-Pardo, J. and Vidal-Puig, A. (2013) 'Pharmacological strategies for targeting BAT thermogenesis', *Trends in Pharmacological Sciences*. Elsevier Ltd, 34(6), pp. 347–355. doi: 10.1016/j.tips.2013.04.004.

Wimberley, T. *et al.* (2022) 'Temporally ordered associations between type 2 diabetes and brain disorders – a Danish register-based cohort study', *BMC Psychiatry*. BioMed Central, 22(1), pp. 1–12. doi: 10.1186/s12888-022-04163-z.

Wollheim, C. B. and Maechler, P. (2015) 'Beta cell glutamate receptor antagonists: Novel oral antidiabetic drugs?', *Nature Medicine*. Nature Publishing Group, 21(4), pp. 310–311. doi: 10.1038/nm.3835.

Wolosker, H. and Balu, D. T. (2020) 'd-Serine as the gatekeeper of NMDA receptor activity: implications for the pharmacologic management of anxiety disorders', *Translational Psychiatry*. Springer US, 10(1). doi: 10.1038/s41398-020-00870-x.

Wu, L. *et al.* (2018) 'AMP-Activated Protein Kinase (AMPK) regulates energy metabolism through modulating thermogenesis in adipose tissue', *Frontiers in Physiology*, 9(FEB), pp. 1–23. doi: 10.3389/fphys.2018.00122.

Wu, Y. K. and Berry, D. C. (2018) 'Impact of weight stigma on physiological and psychological health outcomes for overweight and obese adults: A systematic review', *Journal of Advanced Nursing*, 74(5), pp. 1030–1042. doi: 10.1111/jan.13511.

Wu, Z. and Tam, W. L. (2021) 'A new foe in folate metabolism', *Nature Metabolism*. Springer US, 3(11), pp. 1436–1438. doi: 10.1038/s42255-021-00474-9.

Xi, D. *et al.* (2017) 'Ablation of oxytocin neurons causes a deficit in cold stress response', *Journal*

of the Endocrine Society, 1(8), pp. 1041–1055. doi: 10.1210/js.2017-00136.

Xiangwei, W., Jiang, Y. and Yuan, H. (2018) 'De novo mutations and rare variants occurring in NMDA receptors', *Current Opinion in Psychology*. Elsevier Ltd, 2, pp. 27–35. doi: 10.1016/j.cophys.2017.12.013.

Xiao, F. and Guo, F. (2022) 'Impacts of essential amino acids on energy balance', *Molecular Metabolism*. The Authors, 57(November 2021), p. 101393. doi: 10.1016/j.molmet.2021.101393.

Xu, R. *et al.* (2020) 'Gender- and age-related differences in homocysteine concentration: a cross-sectional study of the general population of China', *Scientific Reports*. Nature Publishing Group UK, 10(1), pp. 1–11. doi: 10.1038/s41598-020-74596-7.

Xue, H. H. *et al.* (1999) 'Flux of the L-serine metabolism in rat liver: The predominant contribution of serine dehydratase', *Journal of Biological Chemistry*. Â© 1999 ASBMB. Currently published by Elsevier Inc; originally published by American Society for Biochemistry and Molecular Biology., 274(23), pp. 16020–16027. doi: 10.1074/jbc.274.23.16020.

Yan, M. *et al.* (2016) 'Chronic AMPK activation via loss of FLCN induces functional beige adipose tissue through PGC-1α/ERRα', *Genes and Development*, 30(9), pp. 1034–1046. doi: 10.1101/gad.281410.116.

Yang, M. and Vousden, K. H. (2016) 'Serine and one-carbon metabolism in cancer', *Nature Reviews Cancer*. Nature Publishing Group, 16(10), pp. 650–662. doi: 10.1038/nrc.2016.81.

Yang, Q. *et al.* (2016) 'AMPK/α-Ketoglutarate Axis Dynamically Mediates DNA Demethylation in the Prdm16 Promoter and Brown Adipogenesis', *Cell Metabolism*. Elsevier Inc., 24(4), pp. 542–554. doi: 10.1016/j.cmet.2016.08.010.

Yang, X. and Ruan, H. Bin (2015) 'Neuronal Control of Adaptive Thermogenesis', *Frontiers in Endocrinology*, 6(September), pp. 1–9. doi: 10.3389/fendo.2015.00149.

Yasuo, S. *et al.* (2017) 'L -Serine Enhances Light-Induced Circadian Phase Resetting in Mice and Humans', pp. 2347–2355. doi: 10.3945/jn.117.255380.

Ye, L. *et al.* (2021) 'L-Serine , an Endogenous Amino Acid , Is a Potential Neuroprotective Agent for Neurological Disease and Injury', 14(September), pp. 1–9. doi: 10.3389/fnmol.2021.726665.

Yin, J. *et al.* (2018) 'Potential Mechanisms Connecting Purine Metabolism and Cancer Therapy', *Frontiers in Immunology*, 9(July), pp. 1–8. doi: 10.3389/fimmu.2018.01697.

Yuan, Y. *et al.* (2019) 'Reward Inhibits Paraventricular CRH Neurons to Relieve Stress', *Current Biology*. Elsevier Ltd., 29(7), pp. 1243-1251.e4. doi: 10.1016/j.cub.2019.02.048.

Yun, H. *et al.* (2020) 'Associations among circulating sphingolipids, β-cell function, and risk of developing type 2 diabetes: A population-based cohort study in China', *PLoS Medicine*, 17(12), pp. 1–19. doi: 10.1371/journal.pmed.1003451.

Zarou, M. M. (2021) 'Folate metabolism : a re-emerging therapeutic target in haematological

cancers', *Leukemia*. Springer US, pp. 1539–1551. doi: 10.1038/s41375-021-01189-2.

Zhang, B. *et al.* (2018) 'Central insulin action induces activation of paraventricular oxytocin neurons to release oxytocin into circulation', *Scientific Reports*. Springer US, 8(1), pp. 1–5. doi: 10.1038/s41598-018-28816-w.

Zhang, E. *et al.* (2022) 'Intestinal AMPK modulation of microbiota mediates crosstalk with brown fat to control thermogenesis', *Nature Communications*. Springer US, 13(1), pp. 1–10. doi: 10.1038/s41467-022-28743-5.

Zhang, H. *et al.* (2015) 'MicroRNA-455 regulates brown adipogenesis via a novel HIF1an-AMPK-PGC1 signaling network.pdf', *EMBO Reports*, 16, pp. 1378–1393. doi: DOI 10.15252/embr.201540837.

Zhang, W. *et al.* (2022) 'Targeting NMDA receptors in neuropsychiatric disorders by drug screening on human neurons derived from pluripotent stem cells', *Translational Psychiatry*. Springer US, 12(1), pp. 1–11. doi: 10.1038/s41398-022-02010-z.

Zhou, X., He, L., *et al.* (2017) 'Serine alleviates oxidative stress via supporting glutathione synthesis and methionine cycle in mice', 201700262, pp. 1–13. doi: 10.1002/mnfr.201700262.

Zhou, X., Zhang, Y., *et al.* (2017) 'Serine prevents LPS-induced intestinal inflammation and barrier damage via p53-dependent glutathione synthesis and AMPK activation', *Journal of Functional Foods*. Elsevier, 39(September), pp. 225–232. doi: 10.1016/j.jff.2017.10.026.

Zhou, X., Zhang, H., *et al.* (2018) 'Long-term L-Serine administration reduces food intake and improves oxidative stress and Sirt1/NFκB signaling in the hypothalamus of aging mice', *Frontiers in Endocrinology*, 9(AUG). doi: 10.3389/fendo.2018.00476.

Zhou, X., He, L., Zuo, S., Zhang, Y., Wan, D. and Long, C. (2018) 'Serine prevented high-fat diet-induced oxidative stress by activating AMPK and epigenetically modulating the expression of glutathione synthesis- related genes', *BBA - Molecular Basis of Disease*. Elsevier, 1864(2), pp. 488–498. doi: 10.1016/j.bbadis.2017.11.009.

Zhou, X., He, L., Zuo, S., Zhang, Y., Wan, D., Long, C., *et al.* (2018) 'Serine prevented high-fat diet-induced oxidative stress by activating AMPK and epigenetically modulating the expression of glutathione synthesis-related genes', *Biochimica et Biophysica Acta - Molecular Basis of Disease*. Elsevier, 1864(2), pp. 488–498. doi: 10.1016/j.bbadis.2017.11.009.

Zisapel, N. (2018) 'New perspectives on the role of melatonin in human sleep, circadian rhythms and their regulation', *British Journal of Pharmacology*, 175(16), pp. 3190–3199. doi: 10.1111/bph.14116.

Zitomer, N. C. *et al.* (2009) 'Ceramide Synthase Inhibition by Fumonisin B 1 Causes Accumulation of 1-Deoxysphinganine A NOVEL CATEGORY OF BIOACTIVE 1-DEOXYSPHINGOID BASES AND 1-DEOXYDIHYDROCERAMIDES BIOSYNTHESIZED BY MAMMALIAN CELL LINES', *Journal of Biological Chemistry*. Â© 2009 ASBMB. Currently published by Elsevier Inc; originally published by American Society for Biochemistry and Molecular Biology., 284(8), pp. 4786–4795. doi: 10.1074/jbc.M808798200.

VI. Acknowledgements

Caminante, son tus huellas el camino y nada más;
Caminante, no hay camino, se hace camino al andar.
Al andar se hace camino, y al volver la vista atrás
se ve la senda que nunca se ha de volver a pisar.
Caminante no hay camino sino estelas en la mar.

Antonio Machado

I would like to start with this great piece from one of the best poets of the Spanish literature that says: *Traveler, there is no road, you make your own path as you walk*. It has been a great inspiration for me and helped me to get where I am today.

Utrecht. They have been always there for me, regardless the distance or the circumstances. I feel so glad and grateful to have them.

I have learnt so much, far more than I expected. Not only about science, but also about myself. I tried my best to do my bit in science and I hope that this serves as an inspiration for others. I am looking forward to sharing all of that during my professional career as well as continuing to learn and take up new challenges. Thank you all for being part of this step on my way.

VII. Appendices

Table 2. Consumables

Material	Provider
24-well Seahorse plate	Seahorse
384 well qPCR plates	Bio-Rad
96-well plates for assays (transparent)	Greiner bio-one
Bottle-top filter 150ml	Fisher Scientific
Cell culture plates 6, 24 and 96-well	Sarstedt
Cell strainer (100 µm)	Corning
Combitips (0.1, 1, 5, 10 ml)	Eppendorf
Cover glass	Menzel-Gläser, Epredia
Cryostatt blades	Leica
Empty cassette for gel (12,26)	Bio-rad
Filter tips (200, 1000 µl)	Biozym, Kisker Biotech
Histology cassettes	Simport Scientific Inc
Microscope slide (SuperFrost plus)	Thermo Fisher, Epredia
Microtome blades	Thermo Fisher
Needles	Braun
Pipette (5,10,25 ml)	Greiner bio-one
Pipette Tips (10, 200, 1000 µl)	Byozim
PVDF membrane (0,45µm)	Thermo Scientific
Reagent reservoir	Santa Cruz Biotechnology
Sample cap with snap cup (brain)	BrandTech
Syringes	Th. Geyer, Braun
Tubes (1.5, 2, 5 ml)	Eppendorf
Tubes (15, 50 ml)	Falcon (Corning), Sarstedt
Tubes and tube lids (PCR)	Sarstedt
Tubes Microvette CB 300 (blood collection)	Sarstedt
Whatman Paper	NeoLab

Table 3. Chemicals

Chemical	Provider
0.9% NaCl	Fresenius Kabi
2-Deoxy-glucose	Alfa Aesar
3,3',5'-Triiodo-L-thyronine (T3)	Calbiochem (Sigma-Aldrich)
3-isobutyl-1-methylxantine (IBMX)	Sigma-Aldrich
4',6-Diamidino-2-phenyl-indoldihydrochlorid (DAPI)	Merck Millipore
Acrylamide 30% (Rotiphorese® Gel 30)	Carl Roth
Agarose	Sigma-Aldrich

Amonium persulphate (APS)	Serva
Antimycin	Sigma-Aldrich
Bovine serum albumin (BSA)	Carl Roth
BSA fatty acid-free	Sigma Aldrich
Chloroform	Carl Roth
Chromotrope II R (Eosin)	Alfa Aesar
Collagenase IV	Gibco (Thermo Fisher Scientific)
Dexamethasone	Sigma-Aldrich
Dithiothreitol (DTT)	VWR Life sciences
dNTPS	BioLabs
D-serine (S4250-25G)	Sigma-Aldrich
Dubelcco's Modified Eagle Medium (DMEM)	Life technologies (Thermo Fisher Scientific)
EDTA disodium salt dihydrate	Carl Roth
Ethanol (99 %)	Merck Millipore
FBS	Gibco (Thermo Fisher Scientific)
FCCP (carbonyl cyanide-p-trifluoromethoxyphenylhydrazone)	R&D Systems
Fluorescent mounting medium	Dako
Glucose 20%	B. Braun
Glucose 40% (GSIS)	B. Braun
Goat serum	Sigma-Aldrich
Hematoxylin (Meyer)	Merck
Human Insulin (cells)	Sigma-Aldrich
Immobilon Western Chemiluminiscent HRP Substrate	Merck Millipore
Indomethacin	Sigma-Aldrich
Isoproterenol	Sigma-Aldrich
Ketamine	Bremer Pharma
L-serine (84959-100G)	Sigma-Aldrich
M 2-deoxy-D-glucose	Alfa Aesar
Metacam (Meloxicam)	Boehringer Ingelheim
Methanol	Merck Millipore
NaCL	Carl Roth
NaOH	Carl Roth
Normocin	InvivoGen
NuPage LDS sample buffer	Life technologies (Thermo Fisher Scientific)
Oligomycin	Merck
Penicillin/streptomycin	Gibco (Thermo Fisher Scientific)
PFA	Sigma-Aldrich
Phosphatase inhibitor cocktail II	Sigma-Aldrich
Phosphatase inhibitor cocktail III	Sigma-Aldrich
Platinum greeen	Invitrogen (Thermo Fisher)
Protease inhibitor cocktail	Sigma-Aldrich
Qiazol	Qiagen

Rotenone	Sigma-Aldrich
Roti®-Histokitt II	Carl Roth
SDS	Carl Roth
SDS pellets	Carl Roth
Skim milk	Serva
Sodium pyruvate	Acros organics
Sodium pyruvate	Sigma-Aldrich
Temed	AppliChem
Tissue-Tek® O.C.T.™ compound	Serva
Tris	Carl Roth
TRIS Pufferan®	Carl Roth
Triton-X	Sigma-Aldrich
Trypsin 0.05% EDTA	Gibco (Thermo Fisher Scientific)
Tween 20	Santa Cruz Biotechnology
XF Assay Medium Modified (DMEM)	Seahorse. Agilent
Xylazine	Belo-Pharm
Xylol	Thermo Fisher Scientific
β-mercaptoethanol	Carl Roth/Sigma

Table 4. Genotyping settings for GRIN1$^{flox/flox}$ mice

PCR Settings	Temperature (°C)	Time	# of cycles
1 Denaturation (Melting)	94°C	2 min	1
2 Amplification (Melting, Annealing, Polymerization)	94°C	20 s	10
	65°C; -0.5°C per cycle	15 s	
	68°C	10 s	
2 Amplification (Melting, Annealing, Polymerization)	94°C	15 s	28
	60°C	15 s	
	72°C	10 s	
3 Polymerization	72°C	5 min	1
4 Cooling	12°C	∞	1

Table 5. qPCR primers

Gene	Forward	Reverse
Acaca	TGGGCGGGATGGTCTCTTT	AGTCGCAGAAGCAGCCCATT
CD68	TCACCTTGACCTGCTCTCTC	AGGCCAATGATGAGAGGCAG
Fasn	GAGGACACTCAAGTGGCTGA	GTGAGGTTGCTGTCGTCTGT
Foxo1	AAAGTGCGGGCGAAGTGTAT	AAAGTGCGGGCGAAGTGTAT
G6Pase	ACTGTGGGCATCAATCTCCTC	CGGGACAGACAGACGTTCAGC
Gys-2	CCAGCTTGACAAGTTCGACA	ATCAGGCTTCCTCTTCAGCA

IL-6	CCAATCTGGGGTTCAATCAGG	ACCCACTCGTTTGAGGACTG
Npy	ACCGGTGGTCTCTTCTCTCA	CTTGTTACCTAGCATCGTGGC
PC	GCAGGGCGGAGCTAACATC	GCAGGGCGGAGCTAACATC
Pepck	CTGCATAACGGTCTGGACTTC	CAGCAACTGCCCGTACTCC
Pgc1α	AGCCGTGACCACTGACAACGAG	GCTGCATGGTTCTGAGTGCTAAG
Pygl	TTGGAGAGGATTATGTGAAAGA	CTGGCTGATTGGGAGAAAAGAA
Pomc	GCGAGGCAAACAAGATTGG	GAGGCACTGAACATCTTTGTC
Prdm16	CCGCTGTGATGAGTGTGATG	GGACGATCATGTGTTGCTCC
Srebp1	GGAGCCATGGATTGCACATT	AGGAAGGCTTCCAGAGAGGA
Tbp	ACCCTTCACCAATGACTCCTATG	TGACTGCAGCAAATCGCTTGG
TNFα	CCCACGTCGTAGCAAACCA	GTCTTTGAGATCCATGCCGTTG
Ucp1	CTGCCAGGACAGTACCCAAG	TCAGCTGTTCAAAGCACACA

Table 6. SDS gels composition

10% Resolving gel		4% Stacking gel	
H_2O	4.1 ml	H_2O	3 ml
30% acrylamide	3.3 ml	30% acrylamide	750 µl
Tris-HCl 1.5 M pH 8.8	2.6 ml	Tris-HCl 0.5 M pH 6.8	1.3 ml
10% SDS	100 µl	10% SDS	50 µl
10% APS	50 µl	10% APS	25 µl
Temed	15 µl	Temed	10 µl

Table 7. Antibodies

Antibody	Host	Dilution	Provider	Reference number
AMPKα	rabbit	1:1000	Cell signaling	5831
Anti-rabbit IgG HRP	goat	1:5000	Cell signaling	7074S
Anti-rat Alexa Fluor 488	goat	1:500	Life Technologies	A21206
Recombinant Anti-GFP [3H9]	rat	1:500	Abcam	ab252881
HSL	rabbit	1:1000	Cell signaling	4107
Phospho-AMPKα (Thr172) (40h9)	rabbit	1:1000	Cell signaling	2535
Phospho-HSL ser563	rabbit	1:1000	Cell signaling	4139S
Phospho-HSL ser565	rabbit	1:1000	Cell signaling	4137
Phospho-HSL ser660	rabbit	1:1000	Thermo Fisher	PA5-64494
Ucp1	rabbit	1:1000	Cell signaling	14670
β-actin-HRP	mouse	1:1000	Santa Cruz Biotechnologies	sc-47778